UCRL-19142

c. 2

RECEIVED
LAWRENCE
RADIATION LABORATORY

MAR 17 1970

LIBRARY AND
DOCUMENTS SECTION

ELECTRON SPIN RESONANCE SPECTRA OF RADICALS IN SOLUTIONS

Chia-Tung Raymond Pao
(Ph.D. Thesis)

January 1970

AEC Contract No. W-7405-eng-48

TWO-WEEK LOAN COPY

This is a Library Circulating Copy which may be borrowed for two weeks. For a personal retention copy, call Tech. Info. Division, Ext. 5545

LAWRENCE RADIATION LABORATORY
UNIVERSITY of CALIFORNIA BERKELEY

UCRL-19142

DISCLAIMER

This document was prepared as an account of work sponsored by the United States Government. While this document is believed to contain correct information, neither the United States Government nor any agency thereof, nor the Regents of the University of California, nor any of their employees, makes any warranty, express or implied, or assumes any legal responsibility for the accuracy, completeness, or usefulness of any information, apparatus, product, or process disclosed, or represents that its use would not infringe privately owned rights. Reference herein to any specific commercial product, process, or service by its trade name, trademark, manufacturer, or otherwise, does not necessarily constitute or imply its endorsement, recommendation, or favoring by the United States Government or any agency thereof, or the Regents of the University of California. The views and opinions of authors expressed herein do not necessarily state or reflect those of the United States Government or any agency thereof or the Regents of the University of California.

TABLE OF CONTENTS

ABSTRACT

I. INTRODUCTION ---------- 1

II. THEORY ---------- 4

A. Theory of Hyperfine Coupling ---------- 4

B. Hyperfine Interaction in Sigma Radicals ---------- 7

C. Indirect Exchange Couplings ---------- 9

D. Hyperfine Interaction of an Electron with Nuclei Other Than H ---------- 13

E. Alpha Proton Hyperfine Coupling Constants in Olefins ---------- 15

F. Hyperfine Coupling in Beta Protons ---------- 16

G. Hyperconjugation Mechanism of the Hyperfine Couplings ---------- 18

H. Molecular Orbital Theory of Spin Properties of Conjugated Systems ---------- 22

1. HMO Method ---------- 22

2. Restricted Hartree-Fock Method ---------- 24

3. Spin Densities Calculated by Perturbation Method In MO Theory ---------- 26

4. Unrestricted Hartree-Fock Method ---------- 27

5. INDO Computational Method ---------- 33

III. EXPERIMENTAL TECHNIQUES AND DISCUSSIONS ---------- 39

A. Generation of Radical Ions ---------- 39

B. Modifications in the Spectrometer ---------- 41

1. Microwave Bridge ---------- 41

2. Phase Sensitive Detector ---------- 42

3. NMR Tracking System ---------- 43

4. Digital Data Acquisition System ---------- 44

5. Computer Programs for Data Handling ---------- 45

IV. RESULTS AND DISCUSSIONS ---------- 48

A. 1.3.5-cuclooctatriene---------- 48

B. Di-deutero-1,3,5-cyclooctatriene----------52

C. Carbon-13 Satellites in Cyclooctatetraene---------- 63

D. P-cyano-pyridine-N-oxide---------- 65

E. Pyrazine---------- 69

F. 4,5-methlene-phenanthrene---------- 71

G. 1,4-phenylene diamine---------- 76

H. Aniline---------- 87

I. Radical Anion of Tetrasulfur Tetranitride---------- 92

APPENDIX

Molecular Orbital Calculation by INDO Approximation---------- 99

ACKNOWLEDGEMENTS----------104

REFERENCES----------105

FIGURE CAPTIONS----------112

FIGURES----------113

ELECTRON SPIN RESONANCE SPECTRA OF RADICALS IN SOLUTIONS

Chia-Tung Raymond Pao

Inorganic Materials Research Division, Lawrence Radiation Laboratory
and Department of Chemistry
University of California, Berkeley, California

ABSTRACT

Radical anions of various organic and inorganic compounds were generated by intra muros electrolytic reduction in liquid ammonia or other nonaqueous solvents. The RSR spectrometer was modified extensively with a new optional high/low power bridge network, a NMR field tracking system, and a digital data acquisition system. A least squares curve fitting technique was used to assign the ESR parameters for most of the spectra. Since this technique requires a good line shape for each hyperfine component, the limiting factors in the application of the least square fitting technique are the dispersive component of the ESR signals, the NMR tracking error, and the line width variations. This least squares fitting technique can be useful in accurately assigning complicated ESR spectra. We have also successfully applied it to the problem of the satellite signals of the low natural abundance isotopes in the presence of strong hyperfine signals.

Huckel, McLachlan, and Intermediate Neglect of Differential Overlap (INDO) approximation molecular obrital calculations have been performed for the various radical systems. The INDO calculation gives a fairly good result for the planar aromatic radicals, but gives only fair or even poor agreement for the nonplanar ones. Our results indicate the sensitivity of the INDO approximation towards geometrical factors. Hence, the INDO calculations can be used to predict the geometrical configurations of the radical species.

The radical anion of 1,3,5-cylooctatriene gives a complicated but well resolved ESR spectrum. The nonplanar equilibrium configuration of the eight-membered ring was determined from the spectrum. The hyperconjugation of the endo methylene protons was proven to be very important.

The 4,5 methylene phenanthrene radical anion was observed. The assigned proton coupling constants are much larger than the corresponding constants in the radical anion of unsubstituted phenanthrene. A large spin polarization parameter for the methylene-substituted radical was proposed. This indicates that the geometrical structure of the radical is somewhat different from that of the unsubstituted species. The spin polarization parameter for the methylene protons is found to be about -3 Gauss.

The radical anions of aniline and p-phenylene diamine were also generated in liquid ammonia. Their spectra were assigned by computer simulation techniques. The observed NH_2 splitting parameters are only consistent with geometrical structures in which the NH_2 groups and benzene rings are not coplanar.

The tetrasulfur tetranitride anion radical was generated by electrolytic reduction in tetrahydrofuran at -30 C. The least squares adjusted curve fitting method gives an excellent fit between the experimental and theoretical spectra. A Jahn-Teller distortion of this D_2 radical species is proposed. However, no S-33 signal was observed using our present data reduction system.

I. INTRODUCTION

The important characteristics of ESR spectra or radicals in solution are the coupling constants, line widths, and g factors. The anisotropy of the g factors and coupling constants are averaged out due to motional modulation or tumbling of the radicals in solutions. Only the isotropic nature of the unpaired electron and of the magnetic nuclei contribute significant information. In an isotropic spectrum line width variations are sensitive to the dynamic processes of rate effects occuring during the measurement.

Numerous techniques have been developed to generate radicals in solutions and the very high sensitivity of ESR spectrometers allows chemists to study small amounts of transient metastable radicals. ESR is a unique and useful tool for the study of the kinetics and mechanisms of reactions involving radical species, and also for the investigation of the correlation of isotropic hyperfine coupling constants with the electronic structure of radicals.

A great variety of organic radicals have been subjected to examination by ESR. Significant advances have been made during the past fifteen years, and important conclusions relating to the theory of electronic structure and kinetics have been reached.

ESR studies have furnished a great deal of data about organic radicals which is essential in the development of the theories of molecular electronic structure. Experimental parameters obtained from radical species can also test the validity of the closed shell and the one electron approximations. ESR parameters, in addition, guide the theoretician in amending controversial theories and developing new approaches.

Theoretical calculations of molecular properties, especially spin properties, are still quite approximate. ab initio, MO calculations are available only for small molecules, although certain significant advances have occurred in semiempirical approaches. Several theoretical calculations have been performed to explain and predict hyperfine coupling constants. Semiempirical molecular orbital calculation with various approximations give reasonable agreement. Conjugation of the methyl and methylene groups with pi bonds in molecules is an old concept. However, the development of a unified picture of hyperconjugation has been plagued by apparent mutual inconsistencies in the ideas derived from several different areas. Despite the concentrated efforts to find a satisfactory quantum theoretical view, one must admit that the conflict between the proponents and opponents of this simple concept has not yet been settled satisfactorily. This thesis is partly an attempt to justify and interpret the hyperconjugation model for the methyl and methlene coupling constants, and to correlate this model to the neutral molecules.

Valence bond theory has never been widely used because of the tedious manipulations involved, although it sometimes gives interesting results. At present, painstaking efforts in valence bond formulation of conjugated systems are getting much attention in the literature.[13-15]

The limiting factor in the use of ESR is the sensitivity of the spectrometer. Hence, the technique used to produce radicals continuously in some suitable solvent medium must give a steady state concentration which exceeds the minimum detectable radical concentration of the ESR spectrometer. For a particular radical, this steady state concentration is determined by both the lifetime and the rate of generation of the radical.

ESR spectra of radical ions in solution can be completely described by the coupling constants, line widths, line shapes, and the g value of the radical. In general, all the hyperfine lines in a radical spectrum have the same g value and often the same line width as well as the same line shape; therefore, the existence of anomolous g values or variations in the line widths or line shapes can yield additional information on the molecular rate processes in the system.

Previously, the technique used to analyze ESR spectra was rather limited: The initial assignment of hyperfine splittings was done by inspection. These assignments were often be checked through either stick diagrams or more sophisticated computer simulated spectra. The information obtained in this way from spectra is somewhat limited, owing to the possible existence of a low signal to noise ratio of the complex overlapping of lines. The subsequent development of the digital data acquisition and averaging techniques soon overcome this limitation, but only during the past decade have computer techniques advanced sufficiently to make their application to ESR a practical method of resolving complicated spectra. The use of these methods enables spectroscopists to obtain information from the previously inaccessible weak signals. Lately, the least squares curve fitting technique has been applied to the assignment of spectra. ESR parameters can be accurately determined through the use of this technique. This method together with the computer smoothing program, not only can obtain the information that a time averaging computer can, but also can extract information about unresolved weak lines which are actually buried completely underneath the predominate lines. This thesis also applies the least squares adjusted fitting technique to ESR spectroscopy.

II. THEORY

A. Theory of Hyperfine Coupling

Hyperfine coupling is a magnetic interaction between electron and nucleus which is described by a spin Hamiltonian (1). Since the interaction is generally very weak, this spin Hamiltonian can be treated as a peturbation of the spin independent Hamiltonian. The spin dependent Hamiltonian operator may be divided into the sum of two terms: H_{se}, an electronic term including the electronic Zeeman interactions and the interaction of electron spins with each other, and H_{sn}, a nuclear term involving the nuclear interaction with magnetic field, H, with other nuclei, and with electron spins.

$$H_{se} = \beta S \cdot \underline{g} \cdot H + S \cdot \underline{D} \cdot S \qquad (1)$$

$$H_{sn} = S \cdot \underline{T} \cdot I + I \cdot \underline{Q} \cdot I - I \cdot \underline{U} \cdot H \qquad (2)$$

The tensor operators $\underline{g}$, $\underline{D}$, $\underline{T}$, $\underline{Q}$, and $\underline{U}$ depend on the electronic properties of the paramagnetic species and their environments.

The significant terms of radicals ESR in a liquid of low viscosity are the Zeeman term and the contact term, $AI \cdot S$, which is the diagonal elements of the matrix $S \cdot T \cdot I$. Various derivations of the contact term have been reported, by using relativistic[2] or classical and semi-classical nonrelativistic treatments.[3-5]

There is a simple way to get some insight into this contact interaction: The nucleus is regarded as a uniformly magnetized sphere with a magnetic field $\bar{B}$ inside the sphere, whereas it acts like a magnetic dipole outside the sphere. This dipole interacts with the outside electron in a classical dipole-dipole interaction. The energy of the electron side the nucleus is similar to the classical interaction of the magnetic field $\bar{B}$ and a

magnetic bar with magnetic moment $\bar{\mu}$:

$$E = -\bar{\mu}\cdot\bar{B} = g\beta|\psi(0)|^2 \tau \; \bar{S}\cdot\bar{B} \tag{3}$$

where τ is the volume of the nucleus, $|\psi(0)|^2\tau$ is the probability that the odd electron is inside the nucleus and $\bar{S}$ is an electron spin operator. Classical magnetism requires that the magnetic intensity $\bar{H}$ inside a magnetized sphere is equal to $-4\pi\bar{M}/3$. $\bar{M}$ is the nuclear magnetization and can be expressed in terms of nuclear spin $\bar{I}$ and nuclear g factor g_n:

$$M = \frac{\gamma_N \hbar I}{\tau} = \frac{g_N \beta_N \bar{I}}{\tau} \quad . \tag{4}$$

Therefore, the magnetic field B inside the nucleus is:

$$\bar{B} = \bar{H} + 4\pi\bar{M} = \frac{8}{3}\pi\bar{M} = \frac{8}{3}\pi \; g_N\beta_N \; \bar{I}/\tau \tag{5}$$

and contact interaction energy for an electron and a nucleus is:

$$E = \frac{8\pi}{3} \; g_N\beta_N g\beta \; |\psi(0)|^2 \; \bar{S}\cdot\bar{I} \quad . \tag{6}$$

The coupling constant A is defined as:

$$A = \frac{8\pi}{3} \; g_N\beta_N g\beta \; \delta(\bar{r}) \tag{7}$$

where $\delta(\bar{r}) = \delta(\bar{r}_e - \bar{r}_N)$ is the three dimensional Dirac delta function.

In a many electron system the contact interaction should involve all the electrons and all the nuclei in the radical. The Hamiltonian now has the form:

$$\mathcal{H} = \frac{8\pi}{3} g_N\beta_N g\beta \sum_{K=1}^{N} \delta(\bar{r}_K)\bar{S}_K \cdot \bar{I} \tag{8}$$

where N is the total number of electrons in the radical. When the expression isaveraged over the ground state wave function ψ_0 , the term can be expressed as:

$$\mathcal{H} = \sum_i A_i \bar{I}_i \cdot \bar{S} \tag{9}$$

where

$$A_i = 4/3\pi g\beta\ g_{N_i}\ \beta_N \quad \frac{\langle \psi_0 \mid \sum_k S(\gamma_k)\ Skz \mid \psi_0 \rangle}{S_z} \tag{10}$$

$$= 4/3\pi g\beta\ g_{N_i}\ \beta_N\ \rho\ (\gamma_{N_i})$$

S_{kz} is the z component of the k-th electron spin operator.

S_z is the z component of the total spin operator.

The summation of all electrons in the system may give a hyperfine splittings due to negative spin density. It is obvious that the contact interaction is proportional to the difference between the alpha and beta spin probabilities, $\rho\ (\gamma_{N_i})$, at the nucleus i, and also to the magnitudes of the magnetogyric ratio and nuclear spin of that nucleus.

The electronic energy of a doublet radical in strong magnetic field H is the sum of the Zeeman and contact interaction energies:

$$g\beta\ H\ M_s + \sum_i A_i M_s M_{I_i} \tag{11}$$

An ESR transition between an electron spin of -1/2 state and one of the +1/2 state results from a perturbation due to the H_1 field of the microwave frequency ν_1. The energy change during the transition is:

$$h\nu_1 = g\beta\ H + \sum_i A_i\ M_i \tag{12}$$

when ν_1 is fixed and the magnetic field is weeped, the position of each individual absorption line can be deduced as:

$$H_i = \frac{h\nu_i}{g\beta} - \sum \frac{A_i}{g\beta}\ M_{I_i} = \sum_i A_i'\ M_{I_i} \tag{13}$$

where A_i' is in the magnetic field units, and Ho is the center of the spectrum. A typical hyperfine pattern versus magnetic field sweep is shown in Fig. 1.

In a well resolved ESR spectrum the total number of absorption lines is related to the number of distinguishable types of nuclei, m, and to the number of equivalent nuclei of one type N_i by the relation:

$$\text{Number of possible Lines} = \prod_{i=1}^{m} (2N_i I_i + 1)$$

The magnetic field position of an ESR spectrum is determined by its g factor. The g factor gives valuable information in the study of crystals and the transition metal ions, but it gives very little information about organic radicals. Because of the large separation of the energy levels and the small λ value for light atoms, the deviation of the organic radical g factor from the free electron g factor is small unless the radical contains heavier atoms. In this work little attention will be paid to the g value because of this relatively small deviation.

B. Hyperfine Interaction in Sigma Radicals

Most of the organic radicals studied by ESR are pi radicals with the unpaired electron occupying a p-orbital. The stability of these radicals is increased by delocalization of the unpaired electron into pi molecular orbitals.

In some transient radicals or in radicals trapped into some suitable matrix the unpaired electron may be stable enough to locate itself in a particular p orbital without delocalization.

Radicals with the unpaired electron localized in an orbital of sigma symmetry have been observed recently.[6-12] Many distinctive facts of sigma radicals have been reported: The beta protons of sigma radicals have different hyperfine splittings at the cis and the trans positions due to the preferential transmission of the spin density along the sigma bonds of the entire system. The beta and gamma proton coupling constants have a

large angular dependence, and the coupling is strongest when the sigma bond system is planar; In substituted aromatic radicals the ortho proton coupling constants is not affected by a substituent at the para position.

The essential theoretical difficulties are the use of the proper and meaningful sigma orbital wave functions explicitly in the calculation, hence, sigma radicals have received relatively little theoretical attention, and their modes of interaction are not well understood. Valence bond,[13-15] extend Huckel[14,16] and modified hyperconjugation method[15] have all achieved some success. CNDO/2 and UHF methods have been used in the calculation of sigma radicals[17] with high accuracy. For those well localized sigma radicals, a simple proportionality relationship is reasonable in dealing with the CH_i bond function. The coupling constant for i-th proton is:

$$A_i = Q_i \rho_i \tag{14}$$

where Q_i = 508, 26G, for proton, ρ_i is dimensionless and is the spin density in an orbital $\psi(r_i)$ at hydrogen atom i. ρ_i is related to the unpaired electron density or spin density at the nucleus, $\rho(r_i)$, by the relation: $\rho(r_i) = \rho_i \, |\psi(r_i)|^2$ (15)

Spin densities at the nearest neighbor bonds may contribute to the proton hyperfine couplings in those radicals where the odd electron is not so well localized. The coupling constant is related to the spin densities by the formula: $A_i = Q_i \rho_i + D\rho_i^c$ where ρ_i^c is the spin density at the carbon atom to which i=th proton is bonded. D contains exchange integrals involving other bonds. The values of Q_i and D can be found from the least-squares fit of the experimental coupling constants and the calculated spin densities of the known sigma radicals:

$$Q_i = 309.10 \text{ gauss}, \quad D = 12.91 \text{ gauss}.$$

C. Indirect Exchange Couplings

The sigma-pi electron separability is not a satisfactory approximation for explaining pi radical ESR spectra. The contact term requires a non-vanishing odd electron probability distribution at a nucleus; however the pi electron approximation predicts that the unpaired electron wave function should possess a nodal plane at the proton position in an aromatic planar radical. Neglecting the one or multicenter interaction between a sigma and a pi electron causes a serious deficiency in the theoretical evaluation of molecular spin properties.

Sigma-pi exchange coupling can be treated as a perturbation in most molecular orbital[19,20] or valence bond[18,21] treatments. This exchange perturbation is spin unsymmetric; hence, there is an unpaired electron density at the aromatic proton nucleus.

A linear relation was found[18] between the proton hyperfine coupling constant A_H and the spin density of the odd electron at the adjacent carbon p-orbital, ρ_π:

$$A_H = Q\,\rho_\pi \tag{16}$$

A general expression for the spin density at atom c is:

$$\rho_c = \frac{\sum_\mu \Delta(\mu)\, S_{\mu z}}{\sum_\mu S_{\mu z}} \tag{17}$$

where atomic delta function $\Delta c(\mu)$ is zero unless the electron is in a p_z orbital centered on atom c.

The proportionality factor Q measures the attenuation of the hyperfine interaction from that of a free H atom A_H°, as spin polarization occurs along a CH fragment.

$$Q = fA_H^\circ \tag{18}$$

Q is constant within 10%, and its values is approximately 23-25 gauss.

The experimental attenuation factor for aromatic radicals is f=0.05. From a perturbation treatment the spin attenuation factor for an unpaired carbon atom electron which is exchange polarized along a C-H fragment is: $f = -K_{\pi,tr}/z\bar{\Delta}E$ where $K_{\pi,tr}$ is the atomic exchange integral. The numerator, $\bar{\Delta}E$, is the average electronic excitation energy from the bonding orbital Σ to the antibonding orbital Σ^*. It is generally believed that the variation in Q may be caused by either the change in hybridization or the change in excess charge density. The exchange integral changes when the hybridization is no longer pure trigonal sp^2. Valence bond calculations give a factor of two variation in Q, but no detailed study of hybridization effects has been made using the MO approach. The effect of excess charge on Q is a rather interesting proposal and has recently received a lot of attention. It is worthwhile to further discuss this effect in a later section.

Q is roughly constant for almost all aromatic radical anions. The calculated unpaired electron spin density at each ring carbon, therefore, is directly related to the assigned proton coupling constants.

The spectral width is related to the coupling constants, hence to the Q value and spin densities in the following ways:

$$\begin{aligned} \text{width} &= \sum_r |Ar| \\ &= -Q\left[\sum_r |\rho_r| - \sum_{r'} |\rho_{r'}|\right] \end{aligned} \tag{19}$$

where subscript r is used to represent all carbon atoms in the radical and subscript r' is used to represent only those carbon atoms without adjacent protons. For a system with total spin S where no negative spin density exists:

$$\Sigma \ |\rho_r| = 2S = 1 .$$

Therefore, the width becomes $-Q\ (1 - \sum_{r} |\rho_{r'}|)$. According to this relation, the spectral width may be less than the Q value because of the loss of hyperfine splitting due to the spin density at carbon atoms without adjacent protons. However, if there is a significant amount of negative spin density, $\Sigma\ |\rho_r| > 1$, the total spread in the hyperfine splitting may no exceed the Q value, if the negative spin density contribution is large enough, $(\sum_{r}(\rho_r) - \sum_{r'} |\rho_{r'}|) > 1$.

It is known that on each carbon atom of aromatic radical ions there is a nonzero excess charge density besides nonzero spin density. Relatively few cation radicals have been observed in ESR; however, from the known data the proton hyperfine coupling constants in cation radicals are larger than those in anion radicals.[22]

The valence bond method provides a direct approach in explaining this difference in cation and anion radicals.[23] On the other hand, the naive Huckel MO treatment or the more refined Hartree-Fock treatments based on the pairing theorem predict equal spin densities in cation and anion radicals. Moreover, MO theory requires sigma electron orbitals to be unaffected by the + or - charge on a C atom; a variation of the sigma-pi polarization parameter Q with excess charge is suggested[24] to get around the molecular orbital deficiency.

It is suggested that Q depends on the hybrid orbital and so on the bond angles in the conjugated molecules. Experimental evidence implies that the variation of Q with bond angle is not pronounced.

In the configuration interaction treatment two excited doublet states are mixed into the ground state wave function. The resulting spin

polarization parameter consists of a spin density term and an excess charge term:

$$A_i^{\pm} = (Q_o \pm K\epsilon_i)\ \rho_i \qquad (20)$$

where Q_o and K are constants.

ϵ_i is the excess charge at atom i; it is equal to the difference between a unit charge and the total pi electron density at the i-th atom.

Alternatively, the nearest neighbor overlap term is introduced[26] instead of the excess charge term.

$$A_i = Q_o\ c_{ki}^2 + Q_1 \sum_j c_{kj}\ c_{ki} \qquad (21)$$

where c_{ki}, c_{kj} are the coefficients of the 2p atomic orbitals of carbon atom i, j in the k-th MO wave function of the unpaired electron. Recently, it has been shown that this relation imples a Q dependence only on various radicals, and not on different carbon position within the same radical.[27]

Much attention has been paid to the excess charge term, and the nearest-neighbor term.[25,27-32] Huckel MO[31] and unrestricted Hatree-Fock[33] calculations favor the excess charge term, while a restricted Hatree-Fock perturbation calculation[25] concludes that neither of the two above modified relations is better than the McConnell relation. This conclusion has been challenged: Current Huckel MO treatment and a statistical analysis of the available experimental proton coupling constants from even-alternat hydrocarbon ions[27] demonstrate the necessity of the extra term and show the choice of the excess charge term seems to be more favorable.

In any event, although the mechanism of this controversial effect remains uncertain, an additional term must be retained. A comparison of the Hyperfine splitting of the radical anions and cations requires that

both Q and ρ variation should contribute significantly to the difference in coupling constants.

D. Hyperfine Interaction of an Electron with Nuclei Other than H

The spin of magnetic nuclei other than potons can be coupled with the unpaired electron spin to give hyperfine splittings. The interpretation of the splittings is quite complicated, because of the coupling constants depend on the spin density on the atom itself and also on the spin densities on the adjacent atoms.

The magnetic nucleus obtains unpaired spin distribution in its s orbitals and yields hyperfine splittings through two mechanisms: A direct mechanism results from the exchange polarization between the unpaired electron in a p orbital and the 2s valence electrons and/or 1s inner shell electrons. In addition, an indirect mechanism is caused by sigma bond polarization due to the unpaired electron distribution at adjacent atoms. This interpretation for the C-13 hyperfine splittings is expressed in the form:[34]

$$A^c = (S^c + \sum_{i=1}^{3} Q^c_{cx_i})\, \rho^\pi_i \qquad (22)$$

where S^c and Q's are, respectively, the sigma-pi interaction parameters for 1s and 2s electrons with the odd electron. The sigma-pi interaction parameters depend on the bond length, type of hybridization, and the nature of the bonding atoms. The superscript is the atom at which the splittings occur. The subscript CX_i means the spin polarization of the CX_i bond due to the unpaired electron at the C atom. Pi electron spin densities on adjacent atoms are included explicity to account for the variation of the spin polarization with different bonds and also to

account for the possibility that the sigma electron spin density at opposite ends of a bond may not have the same magnitude, that is $|Q^c_{cx}| \neq |Q^c_{xc}|$. Hence, the explanation of hyperfine splittings requires a knowledge of the sigma-pi interaction parameters and the pi electron spin density at each atom.

Carbon-13 isotope hyperfine couplings are extremely sensitive to the pi electron spin densities and to the accuracy of the sigma-pi interaction parameters. Furthermore, in a nonplanar radical fragment the unpaired electron occupies a hybrid orbital which has s-orbital character. The sigma-pi parameters are susceptible to the extent of this hybridization. Hence, the variation in hybridization can cause additional complications in the interpretation of the spectra.

Many experimental efforts have been made to determine nitrogen spin polarization parameters. The three parameters can be evaluated from the known coupling constants and the spin densities from three or more spectra. The coupling constants are obtained from the experimental spectrum, and the spin densities are yielded by either valence bond or molecular orbital calculations. In this method the determination relies upon the accurate theoretical evaluation of the spin densities; therefore the obtained parameters are even less accurate than those from approximate quantum mechanical calculations.

A refined determination[35] based only on experimental data should give more reliable parameters, if the choice of data has been made carefully. Spectra of pyridine, pyrazine and pyrimidine radical anions have been used for an entirely experimental evaluation. The necessary assumption is that each of three nitrogen coupling parameters in these three radicals are identical. It is a reasonable assumption that the

nitrogen bond angles and hybridization are unchanged in this series.

When a deuterium atom is substituted for a hydrogen atom in a radical, the magnitude of the deuterium coupling constant is expected to be reduced from the unsubstituted proton coupling constant by a factor of the magnetogyric ratio of D to H. This ratio is 1/6.514. In general, one would not expect the isotropic substitution to alter the spin density distribution, but in some cases, the isotopic substitution does cause a slight change in the spin density. This effect may have many different causes in different radicals. Persumably, deuterium has some position inductive effect and withdraws more electron density from the conjugated fragment.[36] Deuterium substitution may also result in a lifting of the orbital degeneracy of the ground state,[37] the substitution will cause further separation in energy and reduce the effectiveness of the mixing between the low lying excited state and the ground state.[38] The perturbation of the C-H stretching vibration[39] or of the out of plane vibration[40] may be expected from D substitution in the radicals characterized by strong vibronic interactions.[41]

E. Alpha Proton Hyperfine Coupling Constants In Olefins

The alpha proton is defined conventionally as the proton which is attached to a sp^2 hybrid carbon atom. The hyperfine interaction of this proton is similar to that of the aromatic proton. The exchange polarization mechanism is the only important interactior which causes the contact interaction on the alpha proton. It is believed that the relation in Eq. 16 is equally applicable to the olefin alpha proton.

F. Hyperfine Coupling in Beta Protons

A beta proton in aromatic or olefinic radicals is a proton on either a methyl or methylene group attached to an alpha carbon atom. The isotropic hyperfine coupling of the beta proton is a direct measurement of the spin density present on the aliphatic proton. Aliphatic protons do not lie in the pi electron nodal plane. However, the spin polarization mechanism alone will no longer satisfactorily explain the hyperfine splittings. The hyperconjugation mechanism[9,42-48] is believed to be very important. It arises when the unpaired pi electron overlaps directly with the alkyl proton through the conjugation effect.[49,50]

Spin polarization of alkyl-substituted benzene or olefin radicals arises exclusively through sigma-pi electron exchange coupling. In alkyl-substituted radicals the exchange interaction can present itself through two mechanisms:[46] a direct exchange polarization and an indirect polarization. The direct process arises from the exchange polarization of the odd electron directly with the C-H bond electrons of the alkyl group. The indirect process originates from two consecutive exchange interactions: exchange coupling first through the sp^2C - Sp^3C bond and then the alkyl CH bond. Owing to the different polarization steps, the direct mechanism will causes a negative spin density, whereas the indirect process will give a positive spin density at the alkyl beta proton. A theoretical estimation of the direct exchange parameter using C-C-H radical fragment gives -1.76 gauss through the first order perturbation term and +0.83 gauss from the second order term. This estimation seems to be valid for alkyl group protons lying inside and also outside of the odd electron nodal plane.

The overall hyperfine splitting from the spin polarization mechanism is

$$A_{CH_3} = 0.9\rho^c \tag{23}$$

where ρ^c is the spin density at the alpha carbon.

A experimental evaluation of this overall spin polarization parameter is reported for the cycloheptatriene radical anion.[51] The molecule is expected to be in its tub conformation with methylene protons attached on C_7. From MO symmetry consideration and neglecting electron correlation, the odd electron wave function has a nodal plane across C_7 along the reflection symmetric plane. No significant hyperconjugation contributes to the methylene proton splitting because of this node. The total methylene hyperfine splitting in this radical is the sum of a small hyperconjugation contribution and a relatively large spin polarization contribution. From this radical anion spectrum and a Coulson and Crawford type hyperconjugation calculation, the hyperconjugation portion of the splitting is 0.38 gauss, which leaves 1.78 gauss as the spin polarization contribution to the hyperfine splitting. The sigma-pi interaction parameter obtained from this experiment has a value of -2.78 gauss, which seems to agree with the calculated value for the C-C-H fragment.

Many workers have notices the relation of beta proton coupling constants to the dihedral angle between the alpha-carbon $2p_z$ orbital and the plane containing the beta-proton C-H bond.[52-57] The splittings are roughly proportional to the square of the cosine of the dihedral angle:

$$A^H = Q^H_{CCH}\ \rho_\pi\ \cos^2\theta \tag{24}$$

Where Q^H_{CCH} is a constant characterizing the C-C-H system. The estimation of Q^H_{CCH} is difficult because of the uncertainty of the spin polarization contribution and difficulty in evaluating the spin density ρ_π. A generally acceptable value is Q^H_{CCH} = 50 gauss.

Another empirical formula to account for both spin polarization and hyperconjugation effect is often used:

$$A^H_\beta = B_1 + B_2 \cos^2 \theta \qquad (25)$$

where B_1 = 4 gauss, B_2 = 50 gauss.

This equation can be applied to explain the internal rotation of a methyl group in a radical. When the rotation about the C_α - C_β bond is rapdi compared with the ESR time of measurement. $A_{H\beta}$ is the average value for all possible conformations with their appropriate weighing factors. Accordingly, a rotational energy barrier can be calculated from the temperature dependence study of $A_{H\beta}$. The magnitude of the beta proton coupling constant yields information on the stereochemistry of the radical. Hence, conformation analysis is an important application of ESR technique to physical organic chemistry.[58]

G. Hyperconjugation Mechanism of the Hyperfine Coupling

ESR spectroscopy is rather important in the study of hyperconjugation, there were conflicting views regarding its significance. ESR studies provide unambiguous evidence that only with the inclusion of hyperconjugation can one well explain the beta proton hyperfine couplings. All alternative explainations of the coupling constants give less agreement with the experimental findings.

Any model which explains the beta proton splittings constant must account for the observed ESR facts: (1) The hyperfine coupling constants for beta protons are positive in sign and usually larger than those for alpha protons; (2) they depend upon the conformation of the alkyl group relative to the alpha carbon p_z orbital; and (3) the coupling varies with the charge on the radical ion, with the cation radical giving larger beta splittings than the anion.

Spin polarization is suitable for explaining alpha proton splittings. However, for beta protons the attenuation which is expected from exchange polarization is not observed along the alkyl chain. An alkyl substituent will result in several distinct effects.[59-64] Since the alkyl group is saturated and has four localized bonds, no electron delocalization should be anticipated either from or to the alkyl group. However, any calculation which is based on this assumption simply does not agree with the experimental results from spectroscopic thermodynamic or kinetic measurements.

An inductive model for the methyl substituent can be treated by a first order perturbation on Coulomb parameters of alternate system. Calculations show there is no first order effect on the orbital energy difference, however, the UV results show a bathchromic shift for a methyl substituted benzene.

In a pseudo atom model where three protons are treated as one atom H_3, the methyl group contributes two pi electrons to the conjugated system. The pseudo atom is described by three group orbitals which are formed from the symmetric combinations of three hydrogen 1s AO's: h_a, h_b, h_c. The LCAO gives three orthonomal group orbitals:[65]

$$\psi_1 = \frac{2h_a - h_b - h_c}{\sqrt{6 - 6\,S_h}} \qquad \psi_2 = \frac{h_b - h_c}{\sqrt{2 - 2\,S_h}}$$

$$\psi_3 = \frac{h_a + h_b + h_c}{\sqrt{3 + 6\,S_h}} \tag{26}$$

One group orbital, ψ_3 has sigma symmetry relative to the C-C sigma bond. The other two group orbitals, ψ_1 and ψ_2 have either a bonding or an antibonding pi symmetry relative to the sigma bond. The methyl group carbon can also be described in terms of two sp hybrid AO's and two 2p AO's. The resultant methyl group orbitals can be formed with the two sigma bond orbitals and two pi bond orbitals from carbon and the pseudo atom group orbitals with the appropriate symmetry. For the methyl group, two sigma bonding group orbitals are:

$$\frac{\psi_3 + \lambda_1}{\sqrt{1 + \lambda_1^2}} \times \frac{sp\sigma + \lambda_2\, sp^2\sigma^\pi}{\sqrt{1 + \lambda_2^2}}$$

while the two pi bonding group orbitals are:

$$\frac{\psi_1 + \psi_2}{\sqrt{2(1+Sch)}}\ ; \qquad \frac{\psi_2 + \psi_2}{\sqrt{2(1+Sch)}}$$

where the overlap integral $S_{ch} = \int \psi_{c1}\,\psi_1 d\tau = \int \psi_{c2}\,\psi_2\, d\tau$. According to symmetry, only one of these group orbitals can participate in the pi conjugation. Hence, the MO for the entire molecule is

$$\psi_I = \sum_r C_{Ir}\ \phi_r + C_{I,r+1}\ \phi_{r+1} + C_{I,r+2}\ \phi_{r+2} \tag{27}$$

This conjugation phenomenon between the pi system and a methyl group is known as hyperconjugation. It involves a non-bond proton resonance structure in a canonical structure.

The influences of methyl substitution on the aromatic compounds

numerous, although most of the influences on righ properties are quite weak. The changes in dipole moment, heat of formation, chemical reactivity, ionization energy, and spectroscopic properties can all be used for empirical adjustment of theoretical parameters.

Coulson and Crawford's method[50] has been applied to various radical systems. Using this approach, Levy[47] worked out formulas for the calculation of coupling constants for methyl and methylene groups.

Colpa and de Boer claim that the antibonding orbitals of the methyl or methylene group are important, since the neglect of these antibonding orbitals leads to an error in the value for the spin density at the beta protons. In Coulson and Crawford's framework the inclusion of antibonding orbitals means the importance of the following group orbitals:

$$\frac{\psi_1 - \psi_1}{\sqrt{2(1-S_{ch})}} \qquad \frac{\psi_2 - \psi_2}{\sqrt{2(1-S_{ch})}} \tag{28}$$

A unperturbed wave function utilizing linear combinations of bonding and antibonding group orbitals as well as the carbon P_z orbital in the conjugated fragment is adequate to describe hyperconjugation. In other words, hyperconjugation can be described in terms of a configuration interaction between the ground state configuration and singly excited configurations of the proper pi symmetry.

Although there is little doubt that the hyperconjugation effect exists in the radical and in the excited state of the alkyl substituted conjugated system, the present status of the hyperconjugation concept and its importance in the neutral organic molecule is still controversial. Huckel Molecular Orbital Theory may overemphasize the role of this concept, especially in the ground state. Symmetry arguments favor hyper-

conjugation, but the effects which Huckel MO theory ascribes to hyperconjugation may be just due to the suppressed electronic interaction. Only the accurate self-consistent-field calculation can estimate the importance of the hyperconjugation effect.

H. Molecular Orbital Theory of Spin Properties of Conjugated Systems

There are two markedly different approaches of utilizing the molecular orbital theory to calculate the electronic structure of molecules. The first, the ab initio calculation, gives a highly accurate and quantitative treatment of small molecules, while the second gives a semiempirical treatment of large molecules. The semiempirical method involves many crude approximations, which are sometimes unjustifiable.

In the semiempirical calculations, it is necessary to select emiempirical parameters carefully by fitting values of the numerical integrals to the known atomic spectroscopic data. Subsequently, the best values of these integrals are used for other similar calculations.

1. HMO Method

The naive Huckel Theory has enjoyed a well deserved popularity for its handy sigma-pi separation approximation, and for its useful conceptual framework for the study of planar unsaturated aromatic organic molecules. In the simply Huckel LCAO-MO method,[66-68] the pi electron repulsion terms are averaged and are not explicitly included in the one-electron effective Hamiltonian. Only effective Coulombic integrals, resonance integrals and sometimes overlap integrals are included. The highly simplified formalism of Huckel theory is capable of elucidating many chemical and physical properties of conjugated molecules, although the neglect of the electron-electron repulsion term causes difficulties in

properly accounting for spectroscopic properties.

The revised and extended calculations, which are based on the original work of Goeppert-Mayer and Sklar,[69] employ anti-symmetrized products of molecular orbitals. In these calculations, pi electron wave functions in determinantal form are used and all the energy integrals including electronic repulsion are retained.

A general SCF-LCAO-MO theory was developed by Roothaan.[70] Later, Roothaan's method was simplified and modified by introducing various semiempirical integrals and was applied to pi electron calculation by Pariser and Parr[71] and also by Pople.[72] Their pi electron calculations, which includes the approximation of Zero Differential Overlap (ZDO) were successful not only in planar molecules but also in some nonplanar molecules as well. Their methods are often referred to as the Generalized Huckel method or the SCF-like LCAO-MO method. These methods give some success in calculating the properties of conjugated molecules; nevertheless, many attempts have been made recently to extend calculations to include all valence electrons.

The spin density at atom j calculated from the Huckel MO without including overlap is:

$$\rho_J = |C_{IJ}|^2 \tag{29}$$

given that

$$\psi_I = \sum_J C_{IJ}\psi_J$$

where the odd electron occupies the i-th molecular orbital. No negative spin density is expected from this calculation, and the spin density is everywhere positive.

In order to include the overlap phenomenon, the coefficients of a given molecular orbital must be renormalized. The overlap integral can

be introduced into the Huckel MO calculation without excessively complicating the calculation. When the overlap integrals are retained, the pairing property of orbitals is no longer found; i.e. for every orbital of energy $\alpha + m_i\beta$ there is no longer found a corresponding orbital of energy $\alpha - m_i\beta$. The orbital coefficients c'_{ij} in this approximation can also be computed from the Huckel coefficients c_{ij} by the relation

$$c'_{ij} = \frac{c_{ij}}{(1-Sm_i)^{1/2}} .$$

The spin densities, which are calculated from both methods, are related to each other by a factor $(1-Sm_i)$. Nevertheless, the ratio of the spin densities among different atoms in the molecule is unchanged whether or not overlap is included.

Heteroatoms may be treated in the Huckel MO formulism by appropriate changes in the empirical parameters of the Coulombic, α_x, and resonance integrals, β_{cx}, to account for the different inductive and resonance effects. Some semiquantitative treatments and their heteroatom parameters are listed for convenience.[67]

2. Restricted Hartree Fock Method

The doublet state of any radical ion can be described by a Slater determinant formed from doubly occupied orbitals, plus a singly occupied orbital, ϕ_0.[73-75] The Restricted HF wave functions do not give any good account in the spin properties of conjugated systems. The spin density has the same form as that in Eq. 29, in HMO method. The Restricted HF approach predicts zero spin density on every alternate carbon atom of the odd-alternant radical system, as HMO approach does. Nevertheless, the configuration interaction mixes the ground state with other excited

states. The self-consistent condition requires that the first order variation of the total energy by zero, when an unoccupied orbital mixes into one of the occupied ones. The resultant wave function can be expressed as the ground state function $^2\psi_0$, plus a perturbed excited state function, $^2\psi_1' : {}^2\psi_0 + \lambda {}^2\psi_1'$.

To a first order approximation, the wave function can be decomposed into two determinants:

$$|\Phi_i + \frac{\lambda}{\sqrt{6}} \Phi_K \quad \Phi_i - \frac{\lambda}{\sqrt{6}} \Phi_K \quad \Phi_n| + \frac{2\lambda}{\sqrt{6}} |\Phi_i \Phi_K \Phi_n| \tag{30}$$

where the first, the spin polarized determinant,[76] contributes spin polarization in the first order. On the other hand, the second determinant differs from the ground state wave function by two spin orbitals and consequently has no first order contribution to one electron spin operators. In these determinants only three excitation schemes are being considered: First, the electron in a singly occupied orbital is excited into an empty orbital, $\Phi_n \rightarrow \Phi_K$ $(n+1 \leq K)$. Secondly, the electron in any occupied orbital is excited into an empty spin orbital, $\Phi_n \rightarrow \Phi_K$. Thirdly, that electron is excited into a singly occupied orbital, $\bar{\Phi}_i \rightarrow \bar{\Phi}_n$ $(1 \leq i \leq n)$.

The total spin density can be obtained by simply algebraically summing the contributions from the various spin orbitals of the first determinant:

$$\rho_r = \Phi_n^2(r) + \frac{4\lambda}{\sqrt{6}} \Phi_i(r) \Phi_K(r) + \ldots \tag{31}$$

This expression shows that the configuration interaction produces a first order change in the spin density. This change can be used to explain the negative spin densities and the sigma-pi polarized spin densities at the nuclei of planar hydrocarbon radicals. A similar expression can be obtained

if the orbitals are written as linear combinations of atomic orbitals:

$$\Phi_i = \sum_r C_{ir} \psi_r \tag{32}$$

$$\rho_r = c_{or}^2 + 2 \sum_{i=1}^{n} \sum_{K=n+2}^{2n+1} \frac{\langle oi|Ko\rangle}{E^{iK} - E_o} c_{ir} c_{Kr}$$

3. Spin Densities Calculated by Perturbation Method in MO Theory

Coulson and Longuet-Higgins have shown that it is possible to calculate certain changes in molecular properties by perturbation methods. The perturbation scheme has been successfully applied in calculating the spin properties of molecules.[77] McLachlan shows that the exchange field of the odd electron can be treated as a small perturbation acting on the electronic wave functions. The electrons of different spins moves in slightly different orbitals because of this exchange field perturbations.

In Hückel framework, the perturbation of this exchange field is equivalent to a small attraction acting preferentially on those electrons with the same spins as the odd electron. The effective Hamiltonian for these electrons, is no longer the same as that for those electrons possessing opposite spin to the odd electron; i.e. H_{eff} is now replaced by H_{eff} - (K-K'), where K, K' is the exchange integral between the odd electron and the electrons with the same or opposite spin respectively. Hence, the unpaired spin density is modified through changes in the Coulombic and resonance integrals. McLachlan shows that the spin density at atom j-th is now related to the coefficients of the wave functions, c_{ij}, in the following way:

$$\rho_J = c_{IJ}^2 - (1/2)\gamma \sum_r \pi_{rt} c_{rJ}^2 \tag{33}$$

where π_{rt} is the mutual polarizability of the two atom, r and s; and γ

is the electronic repulsion integral. An adjustable parameter λ can be introduced into the equation to replace γ:

$$\rho_J = c_{IJ}^2 + \lambda \sum_r (\beta\pi_{rJ})\, c_{rJ}^2 \qquad (34)$$

Spin density calculations based on the Extended HF wave functions instead of HMO can be evaluated from the above equation as well.

In the above equations the first order spin density is expressed in terms of mutual polarizability coefficients. The readily available polarizability coefficients make the spin density easy to be computed. Furthermore, the perturbation scheme gives better spin density results than the unrestricted HF without annihilation operations does.

4. Unrestricted Hatree-Fock Method

In the restricted Hartree-Fock method correlation of electrons with opposite spins is not allowed, nevertheless, there are two ways to overcome this difficulty: One is the configuration interaction method which has been discussed in the last section. It allows a small admixture of excited configurations through a small exchange perturbation. Althernatively, the unrestricted Hartree-Fock method[78,79] uses a single determinant with different orbitals for alpha and beta spins and leads to the same pi-electron spin distribution. An extended Hartree-Fock method involves an unrestricted procedure to set up a determinantal wave function and to apply the projection operator before using the variation method. The unrestricted Hartree-Fock method has been applied to radicals, ions, and triplet states of alternant molecular systems. The unrestricted HF method uses a single determinantal wave function, and has an extra degree of freedom in the doubly occupied orbitals, i.e. different orbitals for

different spins are used to treat the correlation between electron with different spin explicitly.

Although ψ_{UHF} is an eigenfunction of S_z satisfying

$$S_z \ \psi_{UHF} = 1/2(p-g) \ \psi_{UHF} \tag{35}$$

where p-q=1 for radical anion with one unpaired electron.

ψ_{UHF} is not a spin eigenstate of S^2:

$$\psi_{UHF} = c_o \psi_{2s+1} \ c_i \ \psi_{2s+3} + \ldots \tag{36}$$

where for radical anion or cation 2s+1 = 2. Certain molecular properties, such as charge density, can be derived from the unprojected wave function directly, whereas molecular parameters for spin properties must be selected from the pure spin state by the projection operator technique. The projection technique projects the pure spin state after annihilation of those contaminated spin states:

$$P\psi_{UHF} = \sum_{r=s+1}^{N/2} [s^2 - r(r+1)] \ \psi_{UHF} \tag{37}$$

It is known that the major component in the UHF wave function of a radical anion is a doublet, but the quartet is also important, whereas the relative weight of the sextet is negligible. In order to make ψ_{UHF} a pure doublet spin state, projection operators must be used. The quartet annihilation operator (S^2- 15/4), when applied to ψ_{UHF}, will remove the quartet component, whille (S^2 - 35/4) will remove the sextet. Technically, it is difficult to derive spin densities from MO theory after the application of projection operators to the wave function. Generally, the major contamination component is quartet spin state. It might be sufficiently accurate just to remove the quartet state for general purposes, and, therefore simplify the annihilation procedure considerably.

The new wave function after quartet annihilation of the 2s+3, quartet, spin eigenstate is:

$$A_{s+1}\,\psi_{UHF} = [S^2-(s+1)(s+2)]\,\psi_{UHF} \tag{38}$$

where

$$A_{s+1} = 1/2\ N\ (N-4)\ -1/2\ \sum_{ij} P^s_{ij} - (s+1)(s+2)$$

and the p^s_{ij} operator interchanges the spin of the i-th and j-th electron. The wave function after projection is no longer a single determinant but a sum of determinants. It will be closed to a pure spin state. It has been show that such a procedure may lead to small error when spin densities are calculated. Annihilation makes an important change in spin density calculations but little change in charge densities and energies.

Synder and Amos[79b] formed formulas for spin and charge densities. Their values for the spin properties agree with experimental values. Unrestricted bond order matrices for alpha spin, P, and beta spin, Q, are introduced. If the basis sets of the atomic orbitals for alpha and beta spins are $2p_z$ carbon atomic orbitals, then the diagonal elements of P-Q and P+Q matrices will be the pi spin densities and charge densities at the carbon atoms.

From the pairing theorem, there are relations between the bond order matrices for the positive and negative radicals for alternant molecules. Therefore, the computations become much simpler.

The spin densities calculated directly for ψ_{UHF} are not meaningful and annihilation must be made before correct spin densities can be computed. The calculated spin densities can be compared to experimental coupling constants through the McConnell relation. Spin densities after

annihilation generally agree with the experiment. Hence, this method is superior to the restricted Hartree-Fock method which predicts no negative spin density in radicals without admittance of the configuration interaction technique.

The above molecular orbital calculation can be extended from calculations involving just pi-electrons to those involving all the valence electrons.[80,83] The applicability of the MO calculation is hence greatly increased, because the method permits a full treatment of sigma- and pi-electrons in planar molecules, and because it also allows us to handle a great many molecules where sigma-pi separation is irrelevant.

Lately, Pople and his coworkers proposed various approximations based on the neglect of differential overlap integrals, and on the invariance oftransformation of the atomic orbital basis set. In their complete neglect of differential overlap approximation,[81] CNDO, the product of pairs of different atomic orbitals in the electron-interaction integrals are omitted completely. All of the remaining parameters are determined semiempirically. Many physical properties have been computed with this approximation. It has satisfactorily reproduced the bond angles, bond length, bending force, and even molecular geometry.

A refine method,[82] CNDO/2 in which certain atomic and penetration parameters are modified, allows the calculation to be successful in predicting electronic spectra and also gives improved ionization potentials. Nevertheless, this approximation gives unsatisfactory spin density results, even if the unrestricted Hartree-Fock orbitals are used in CNDO/2. The neglect of exchange integrals between the sigma- and pi-electrons makes it impossible to correlate any spin properties.

Both of these approximations reproduce the correct stereo-chemistry of molecular ground states. However, they are incapable of reproducing spin properties for the use of ESR or other molecular spectroscopies., since they can not resolve the degeneracy of many open shell configurations. These kinds of treatment are intermediate in complexity between the full LCAO-SCF calculations for pi-electrons and the very simple Huckel approach which does not handle electron interaction in any explicit manner.

Neglect of Diatomic Differential Overlaps NDDO,[81] is a more complicated approximation. In this approximation products or orbitals on different atoms are neglected in the electron repulsion integrals. In as much as this elegant theory requires the inclusion of all exchange integrals, where each of the two electrons under consideration has to be in the same center, it requires the calculation of a much larger number of two center integrals; The immediate application of this method is, therefore, limited to small molecules only.

Dixon suggested an EMZDO method,[84] a method modifying the zero differential overlap approximation by the inclusion of one center exchange integrals. Most of the approximations in CNDO are still preserved, but the theory is extended further to account for the electron correlation problem between electrons with the same spins. The EMZDO method mainly differs from the CNDO method in two features: First, the inclusion of one-center two-electron exchange integrals; and, secondly, the possible orbital dependence of one center Coulombic integrals. The closed shell and the open shell calculations within this EMZDO approximation give in most cases reproducible equilibrium valence angles in the ground state and excited states. Definite improvements have been made over CNDO and

CNDO/2 in the valence angle and dipole moment calculations. Without using too many empirical parameters in the calculations, this method overestimates transition energies, inversion barriers and configurational splittings. Dixon proposed a possible computational method for large molecules. Unfortunately, no spin properties have ever been mentioned in his original paper; hence a direct application to ESR is impossible.

An approximation which is intermediate in complexity between the CNDO and NDDO treatments has been proposed lately. The method is quite similar to Dixon's theory and is referred to as the Intermediate Neglect of Differential Overlap (INDO) approximation.[85,86] It neglects all of the differential overlap integrals except those which are one-center, but retains the invariance properties. The formalism of this method is like that of the usual unrestricted Hartree-Fock scheme, with the Lowdin projection operators annihilating the major contaiminating spin component. Such as method is particularly useful in applications to the spin properties of open shell systems.

Most of the INDO approximations parallel those of CNDO method. The general approximations in the Neglect of Differential Overlap methods are the following: First, in the computation of HF matrix elements, certain lessimportant electron repulsion integrals are neglected; for example, three and four-center electron repulsion integrals are all eliminated in order to substantially reduce the computation time and effort. Therefore, the calculations on large polyatomic molecules are feasible. Many two-center integrals are also eliminated, but Coulombic integrals are still retained so that polar and ionic effects can still be considered explicitly.

Secondly, invariance criteria for the rotation and the hybridization are taken into consideration, so that the approximate orbital wave function will have some of the same transformation properties as the wave function computed by ab initio calculation. The rotational invariance requires that the approximate methods of calculation are invariant to the rotation of local atomic coordinate systems; the hybridizational invariance requires that these methods are invariant to the hybridization of the atomic functions of any constituent atom.

Thirdly, only those electrons in the valence shell are treated explicitly; the inner-shell electrons are treated as a nonpolarizable core.

Fourthly, some quantities can be readily calculated with the above approximation methods but can also be easily determined from the experimental data on atomic systems; hence, calibrations of these methods by using the experimental data can help compensate for some errors produced by the approximations.

The advantage of these NDO approximations is that they are simple enough to handle calculations of moderately large polyatomic molecules without excessive computational effort. However, the wave functions used in these NDO approximations still possess the important physical properties of the molecule; their treatments of all the valence electrons are sufficiently general and explicit to give some physical insights into the nature of various interaction.

5. INDO Computational Method

The INDO approximation[87] describes the open shell molecular orbitals as two orthonormal sets of linear combinations of atomic orbitals:

$$\psi_i^\alpha = \sum_i c_{ri}^\alpha \phi \qquad \psi_i^\beta = \sum_i c_{ri}^\beta \phi_r \tag{39}$$

where the ϕ_r's are atomic orbitals centered on the component atoms of the molecule, and the coefficients c_{ri}^α and c_{ri}^β are the eigenvectors of the Hartree-Fock matrices.

The unrestricted LCAO-SCF molecular wave function for n electrons (p of which have alpha spin and q, beta spin) has the form:

$$\Psi = |\psi_1^\alpha(1)\alpha(1) \ldots \psi_p^\alpha(p)\alpha(p)\ \psi_1^\beta(p+1)\beta(p+1) \ldots \psi_n^\beta(n)\beta(n)| \tag{40}$$

These molecular orbitals are eigenfunctions of a Hamiltonian operator. In order to find two sets of coefficients that give the best values for the orbital energies, the linear variational method is used. Hence, the linear expansion coefficients should satisfy the matrix equations:

$$F^\alpha C^\alpha = SC^\alpha E^\alpha \qquad F^\beta C^\beta = SC^\beta E^\beta \tag{41}$$

where F^α, F^β are the Hartree-Fock Hamiltonian matrices, C^α and C^β are the matrices of the linear expansion coefficients, E^α and E^β are the diagonal matrices of orbital energies, and S is the overlap matrix.

In INDO calculations differential over lap is neglected in all multicenter inter-electron repulsion integrals but one-center atomic exchange integrals are retained. The overlap integrals are required for all pairs of the atomic orbital basis functions, where the atomic orbital wave functions consist of Slater-type orbitals for the valence shell:

$$\psi_a(r,\theta,\psi) = Na\gamma^{Na-1} \exp(-\xi_a r)\ Y_{\ell a,m}(\theta,\psi) \tag{42}$$

given that n_a, ℓ_a, and m are the principal, azimuthal and magnetic quantum numbers, respectively, and ξ_a is the orbital exponent. N is the radical normalization constant.

$Y_{\ell a,m}$ is normalized spherical harmonics. The overlap integrals, which are evaluated from these basis functions form the elements of an overlap matrix referred to the coordinate system of the molecular frame. The calculation picks pairs of atoms each time and computes all of the overlap integrals between the sets of atomic functions centered on the two atoms under consideration in the local atomic frame. Then the overlap integrals in this frame are transformed back to the molecular frame by orthogonal transformations.

Next, the Coulombic integrals are calculated using the approximations for the diagonal elements formed from - (I+A)/2 and the off-diagonal elements formed from $(\overset{\circ}{\beta}_A + \overset{\circ}{\beta}_B)\ S_{rs}/2$.

The initial Fock matrices, which are constructed under the zero-differential-overlap extended Huckel approximation, are then diagonalized, and two initial density matrices are constructed:

$$P^{\alpha}_{rs} = \sum_{i}^{P} c^{\alpha}_{ri}\ c^{\alpha}_{si} \qquad P^{\beta}_{rs} = \sum_{i}^{g} c^{\beta}_{ri}\ c^{\beta}_{si} \tag{43}$$

The Hamiltonian is then modified by five INDO approximations in the evaluation of the new Fock matrices. These approximations are:
(1). The overlap integrals, Srs, between any pair of orbitals are neglected, except that the one-center overlap integral is set equal to 1. (2) All ofthe two electron multi-center integrals, except that in the two-center integrals, the nonzero integrals, $\langle rr|ss\rangle$ and $\langle rs|rs\rangle$, can be further expanded in terms of the Slater-Condon parameters, F, G^1, and F^2, whose values are obtained from atomic spectroscopic data.

(3). Diagonal core-matrix elements are calculated by separating the interactions of the orbital (centered on atom A) into those with the core of atom A and with each of the cores of other atoms. The approximation is incorporated intothe equation as:

$$H_{rr}^{core} = U_{rr}^{core} - \Sigma \langle r|V_B|r\rangle \tag{44}$$

where U_{rr}^{core} is a one-center core integral and $\langle r|V_B|r\rangle$ is approximated by $Z_B F^0$. (4) Two-center core-matrix elements are taken as zero if ϕ_r and ϕ_s are centered on the same atom, whereas $H_{rs} = (\beta_A^0 + \beta_B^0)\ S_{rs}/2$ if ϕ_r and ϕ_s are centered on different atoms A and B. The β_A^0 and β_B^0 are treated as adjustible parameters. Under the above approximations, the Fock matrix in the INDO formulation with the s and p atomic orbitals as the basis functions should have the form:

$$\begin{aligned} F_{rs}^{\alpha} &= H_{rs}^{core} + \sum_{tu} [P_{rs}(tu|rs) - P_{rs}^{\alpha}\ (tr|us)] \\ F_{rs}^{\beta} &= H_{rr}^{core} + \sum_{tu} [P_{rs}\ (tu|rs) - P_{rs}^{\beta}\ (tr|us)] \end{aligned} \tag{46}$$

where

$$H_{rs}^{core} = U_{rs} - \sum_{B(\neq A)} (\gamma|r_B|s)$$

(5) One-center atomic exchange integrals are also expanded in terms of Slater-Condon parameters as those integrals in Approximation.[2]

After the initial matrices, F^{α} and F^{β} are diagonalized and the density matrices, P^{α} and P^{β}, are constructed, new Fock matrices can be formed from the density matrices using the above approximations. The iteration procedure is repeated until the electronic energy converges to certain tolerable limit. Then P_{rs}, the total charge density-bond order matrix, and the spin density matrix, $\mathbb{P}_{rs}$, are computed from the

charge density-bond order matrices for alpha and beta spin:

$$P_{rs} = P^{\alpha}_{rs} + P^{\beta}_{rs} \quad , \quad P_{rs} = P^{\alpha}_{rs} - P^{\beta}_{rs} \tag{47}$$

The expectation value of the spin density operator is:

$$\langle\psi|\rho\ (\bar{r}_N)|\psi\rangle = \sum_{rs} \rho_{rs}\ \phi\ (\bar{r}_N)\ \phi_s(\bar{r}_N) \tag{48}$$

and the isotropic hyperfine coupling constant, A, of the magnetic nucleus of a radical is related to the electronic wave function by Eq. 10.

The INDO open shell wave functions account for both the exchange polarization and the hyperconjugation delocalization of the unpaired electron in aliphatic radicals. The INDO computation shows that most of the unpaired spin density still remains localized in the carbon 2pz atomic orbital and that only a small amount of it contributes to the sigma system. The finite probability of the unpaired electron distribution at the sigma carbon or proton nuclei accounts for the isotropic hyperfine interaction. Therefore, the signs and magnitudes of the coupling constants can be deduced unambiguously. The INDO method handles sigma electrons explicitly in the calculation without introducing additional assumptions. In this LCAO-SCF-INDO treatment of all valence electrons, numerous isotropic hyperfine coupling constants for various nuclei are correlated with calculated spin densities. Also in alkyl substituted radicals the relative weights of the mechanisms of the beta hyperfine couplings can be determined by choosing a set of conformations. An extensive study of the hyperconjugation effect is possible within the approximation.

The INDO method seems to be useful in predicting spin densities and hyperfine coupling constants. It is a definite improvement over

CNDO because of its better accommodation of spin density and atomic term level splittings. With its moderate complexity and reasonable approximations, it is valuable for predicting and explaining ESR spectra. Much attention will be given to its further applications to ESR spectroscopy in the future.

III. EXPERIMENTAL TECHNIQUES

A. Generation of Radical Ions

Much attention has been given to radical chemistry since the establishment of the ESR technique. A radical anion or cation is a molecular species possessing a negative or positive charge as well as an odd electron. A relatively stable anion radical is formed if the molecule has a low-lying empty orbital which the captured electron may occupy. On the other hand, the cation radical is formed from the parent molecule by removing an electron from the highest occupied orbital. The annihilation interaction of a radical with surroudning species is sometimes rather rapid. In general a cation radical has greater reactivity than an anion radical does. Negative ions may be formed in solution by the attachment of solvated electrons to parent molecules. Radiolysis and photolysis methods of generating radical anions have been reported. Chemical reductions of suitable electron acceptors are also feasible; alkali and alkaline-earth metals are often used as the reducing agents. Alternatively, radical anions can be generated by an electron transfer process among radical anion and other neutral molecules. The disproportionations of dianions can also produce radical anions. Electrolytic reduction may be performed to form radical ions. Among all these techniques, the liquid ammonia-alkali metal system has the advantage to be a powerful reducing agent, whereas the potential of the electrolysis is controllable.

Liquid ammonia[88] is one of the important basic, ionizing solvents. It has a relatively high dielectric constant and dipole moment as well as high van der Waals forces. Because of its strong van der Waals forces, liquid ammonia is able to dissolve covalent substances and even some

ionic ones with highly polarizable ions; therefore most of the olefinic and aromatic hydrocarbons are slightly soluble in liquid ammonia. Particularly, it is an excellent solvent for certain organic ammonium salts; these salts are good supporting electrolytes in ammonia. Since electrolyte solutions can be produced from ammonia and a wide range of organic solutes, liquid ammonia is an excellent medium to conduct redox reactions for organic compounds.

Hexamethylphosphoramide is also a powerful aprotic solvent and is capable of dissolving alkali and alkaline earth metals to form blue solutions.[89] This solvent is easy to handle because of its highest boiling point, but it also suffers a big disadvantage in low temperature ESR because of its high freezing point and high viscosity.

It is known that blue solutions are formed at the cathode during the electrolysis of tetraalkyl ammonium salts in liquid ammonia. The blue solutions are believed to resemble the blue solutions of alkali metals in ammonia, which have been regarded as containing metal cations and solvated electrons. The tetraalkylammonium ions and solvated electrons, presumed on the same basis, are present in the solutions of ammonia and some tetraalkyl ammonium salt during electrolysis.

In the presence of the solvated electrons and some reactive compound in liquid ammonia, the radical anion may be generated. The electrolytically generated radical anions have been successfully detected by ESR.[90] Liquid ammonia is used in the most of this thesis work as the solvent because of its high purity and low freezing point, and also because of its inertness to radical anions and supporting electrolytes, and its own high reducing potential.

The excellence of continuous electrolysis and the advantages of liquid ammonia as the solvent permits us to carry our study of radical anions further by using electrolytic reduction of organic compounds in liquid ammonia.[91-93]

Radical ions in solution may undergo various reactions to annihilate themselves. Some of the typical radical anion reactions which may occur during the generation of radicals by electrolysis in liquid ammonia are: equilibrium between radicals and their parent molecules, radical anion disproportionation, dimerization of radical ions and initiation of addition polymerization, and electron transfer reaction between radical ions and their parent molecules. All of these reactions may affect the existence of a radical species and its steady-state concentration, relaxation time, line width and line shape.

B. Modifications in the Spectrometer

A conventional X-band 100 kHz spectrometer is used in this work. The spectrometer was constructed by Levy and McCain, and has been used by Levy[92] and Talcott[93] previously. Nevertheless, several modifications have been made to accomodate this work, and these are described in the following sections. The block diagram of the modified spectrometer is shown in Fig. 2.

1. Microwave bridge

The bridge network has been substantially modified. The microwaves generated from the LFE klystron oscillator are transmitted into the bridge network through an isolator and a HP X375A variable attenuator. The microwaves are then divided into two portions at the arms of the magic tee. One portion coming from the magic tee propagates through another

variable flap attenuator to the arm No. 1 of a three port circulator; the microwaves come out of arm No. 2 of the circulator, and are fed into the resonant cavity after passing through a directional coupler. The reflected microwaves from the cavity propagated backward to arm No. 2 of the circulator. This portion of the microwaves comes out of No. 3 arm of the circulator, and superimposes at the detector arm with the other portion of the microwaves which come from the magic tee and propagates through a HP X382A precision variable attenuator and a HP X885A waveguide phase shifter. The detector arm consists of a 10 dB directional coupler, an isolator, and a crystal holder. When the impedance of these two sections of the network are matched and the two protions of the RF are adjusted to be exactly 180° out of phase with each other, no microwaves will appear at the detector crystal. Usually, a proper mismatching of the impedance is necessary to give enough RF power for the crystal bias. With this microwave bridge configuration, the RF power incident on the resonant cavity may be varied without changing the detector bias. Hence, this bridge network can fully utilize the maximum sensitivity of the crystal and, yet, suppress the dispersion mode of the signal.

2. Phase sensitive detector

A PAR model 121 phase sensitive detector is used for demodulation of the 100 kHz Zeeman-modulated signal and amplification of the dc signal. This lock in amplifier gives a more stable output and better linearity (±0.1%) than the previously used amplifier. In the new setup, the output first derivative signals can be fed into either a y-t or a x-y recorder for recording an analog spectrum, and can also be set into a digital voltmeter for recording a digital spectrum.

3. NMR tracking system

The magnetic field can be measured through its interaction with other physical observables. In particular, the interactions of the magnetic field with nuclear magnetic moments, such as those of H^1 and Li^7, can be employed as field indicators. NMR gives accurate field readings and is able to be used over a wide range of magnetic fields. Proton magnetic resonance gives a strong signal in the 3 kG region; therefore, it is ideal for measuring the field in organic radical ESR experiments. In our experiments, a water sample probe has been used in the NMR magnetometer. A NMR signal can be produced during the sweeping of the field only if the proton resonance condition is satisfied. Therefore, the information obtained about the field is limited to several frequency readings during each scan of the magnetic field. Interpolation of the field is necessary in order to analyze the analog spectrum. This interpolation relies on the accuracies of the limited number of measurements and on the linearity of the field sweep. In order to remedy these short comings, a tracking system was built so that the proton signal can be locked-in at the resonance varies in accordance with the field variation; hence, the resonance is maintained during the complete period of the experiment. This system gives numerous and accurate field readings so that the above difficulties are overcome.

The NMR tracking system constructed in this laboratory. It consists of a fast loop tracking unit and a slow loop tracking unit. The NMR marginal oscillator unit with a copper-doped water sample probe is used as before. In the present setup, the fast loop can lock a NMR signal to the magnetic field within a range of 3 gauss; the slow-loop can track over a 50 gauss width. Both loops has a set of two high Q voltage variable

capacitors which are parallel-coupled to other LC circuits in the network. The biases on these varactors determine their effective capacitances. The NMR oscillation frequency is determined by the overall reactance of these lc networks. When the magnetic field is sweeping over the spectrum region and the NMR oscillator is locked-in to the field, the servo system compares a command signal and a feedback NMR signal; an error signal is produced, if there is any significant difference between the two signals. The modulated 200 Hz error signal is detected, demodulated, and amplified by a phase detector in the fast loop. Its output dc signal is then fed into both the slow loop section and the fast loop varactor bias network. The NMR frequency will change due to the fast loop's varactor bias change; on the other hand, the output from the fast loop phase detector will also drive a slow loop dc amplifier of a servomechanism, which in turn drives a 40 turn helipot in the voltage divider circuit. The change of the biases of the slow loop varactors shifts the oscillation frequency unitl no significant error signal remains in the whole servo system. This tracking system gives an automatic magnetic field indication in the form of a NMR frequency reading from the HP counter. The accuracy of the tracking system can be as good as 5 milligauss. In order to track a wide range with great accuracy, careful adjustments of the fast loop phase detector and slow loop dc amplifier are needed besides the proper tuning of the marginal oscillator's level and gain controls.

4. Digital data acquisition system

A Honeywell-EI Automatic Data Loggin System Model S6114 is attached to the spectrometer. The unit consists of a HP 5245L electronic counter, a Honeywell EI 630S digital multimeter, a Honeywell model 825 Output

Control unit and a Kennedy 1400 incremental magnetic tape recorder. This data acquisition system is designed to record integrated ESR dc voltages and NMR frequency measurements simultaneously at the rate of six measurements per second. The maximum resolution is 10 microvolts in the voltmeter and 10Hz/sec. in the HP counter. The output control unit takes the data on parallel lines from the digital voltmeter and the counter. When it receives print commands both from the voltmeter and from the counter, the output control serializes and converts the data into 7-level BCD codes. Each measurement makes up a 14 character word, and the data is recorded on the magnetic tape in records consisting of 80 words or less. The 1248 ABC codes of the data on the magnetic tape arecompatible with both IBM 1401 and CDC 6600 computers used in the Radiation Laboratory for general tape handling and computational purpose respectively.

5. Computer programs for data handling

The digital spectra recorded on the magnetic tape can be summed and averaged to improve the signal to noise ratio. A special summing and averaging Fortran program (SUMTAP) was written by A. Bauder for these purposes.[94] Moreover, a mathematical curve smoothing technique is also included in this program. The summing routine improves the S/N by the factor of the square root of the number of scans due to the incoherent nature of the noise. A least squares adjusted fitting program for ESR organic radical anion spectra has been written by A. Bauder.[94] This Fortran program (ORGRAD) is useful in the assignment of the ESR spectrum; the parameters, such as coupling constants, line width, and spectrum center, can be accurately determined. The extraction of C-13 or other isotopic information from the spectrum may also be feasible. This program requires

the input parameters in the spectrum center, intensity, line width, coupling constants, baseline shift, and baseline drift. It also needs the number of the different kinds of nuclei, their spin quantum number, and the equivalent number of each kind of nuclei. The program requires input data on the experimental digitized spectrum which can be produced from the SUMTAP program. ORGRAD constructs the theoretical spectrum from the input parameters with the assumption of a Lorentzian lineshape for each of the individual first derivative signals. The program subsequently adjusts these parameters by the least-square procedure procedes until the adjusted parameters give a theoretical spectrum which fits to the actual digital spectrum within the present limit. This process involves the inversion of a matrix of the order of the number of total ESR lines; therefore, the time consumption in the CDC 6600 central processes increases drastically as the number of magnetic nuclei in the radical species increases. The final adjusted fitting parameters can be plotted into the spectrum by Cal-Comp Plot or CRT Plot. A typical plot is presented in Fig. 3, where the theoretical spectrum is given by the solid curve and the experimental spectrum by the crosses; the difference of the two spectra is presented on the bottom of the plot with a magnification factor at the left hand corner.

The above modifications of the spectrometer were essential for the detection of ESR signals and the improvement of the spectral quality. The use of the circulator instead of the magic tee in the bridge increases the sensitivity of the spectrometer. The line shape distortion is minimized due to the high linearity of the phase detector. The dispersive signal can be easily reduced because of the ease in tuning the microwave bridge. The NMR tracking system gives accurate field readings during the

scanning of the spectrum. Further digital data handling techniques may be used along with the available, sophisticated computer programs.

IV. RESULTS AND DISCUSSIONS

A. 1,3,5-Cyclooctatriene

1,3,5-cyclooctatriene is not available commerically. This is presumably because of its instability to air oxidation and polymerization. It is prepared from cyclooctatetraene (COT) by zinc dust reduction in alcoholic potassium hydroxide at steam bath temperature.[100] COT obtained from J.T. Baker Co., or donated by Badische Anilin and Soda Fabrik A.G., has 0.1% hydroquinone as stabilizer. Filtration and vacuum distillation of COT immediately before use are necessary. The reduction of COT is carried out under a nitrogen atomsphere, and a few drops of alcoholic platinum chloride must be added before any noticeable reaction can occur. After a five hour reaction period with occasional stirring, the product is first cooled to room temperature. n-pentane is used for solvent extraction, and the solvent is evaporated under vacuum at room temperature with a rotary evaporator. Vacuum fractionation with a 10 inch column packed with glass helices gives cyclooctatrienes as the main constituents at 40 mm pressure and 60°C. The product is yellowish in color and contains 1,3,5-cyclootatriene and 1,3,6-cyclootatriene in addition to a small COT contamination. Further purification is necessary to separate the cyclooctatrienes from each other and from COT.

Varian Aerograph Model 90-P3 gas chromatograph (G.C.) is used with a Carbowax-20M 5' 3/8" column and a He flow rate of 40 ml/min. The column temperature is set to about 90°C, and the temperature of the injector and collector are set around 200°C. Several U-shaped glass tubing traps immersed in a dry ice-acetone bath are used for collecting of the different separated fractions. The retention time of each component depends

upon the flow rate, oven temperature, injection temperature, and collector temperature, and particularly upon the length of the column and its stationary phase. Careful selection of the conditions and the packing material will give good separation. Under the above G.C. operating conditions, it is essential to re-inject the collected sample into the G. C. for higher purity. Usually, the twice purified material will be suitable for ESR purposes.

1,3,5-cyclooctatriene is also prepared from 1,5-cyclooctadiene.[101] Research grade 1,5-cyclooctadiene from Aldrich Chemical Co. undergoes allyic bromination by refluxing with N-bromosuccimide and some benzoyl peroxide in carbon tetrachloride for three hours. The mixture is cooled and filtered, and the filtrare is then washed with dilute sodium carbonate solution and then with warm water. The carbon tetrachloride is evaporated, and the monobromocyclooctadiene separated out by vacuum distillation at 60°C and 1 mm pressure. Dehydrobromination of the monobromocyclooctadiene is performed in a t-butanol solution. Potassium metal is added to an excess amount of t-butanol to form potassium t-butoxide in the solution of t-butanol. The solution of monobromocyclooctadiene in t-butanol is then slowly added into the k t-butoxide solution at the reflux temperature. After two hours of refluxing, the mixture is cooled and filtered. Then the solvent is evaporated, and the mixture is distilled under vacuum. The distillate of 1,3,5-cyclooctatriene can be further purified by gas chromatography. This synthesis gives 1,3,5-cyclooctatriene free from the contamination of 1,3,6-isomer and COT. It is, therefore, good for ESR purposes, since any trace amount of COT may interfere with the generation of triene radicals because of the low reducing potential of COT and

and the high stability of its radical anion relative to the radical anions of the triene.

ESR experiment is carried out by transferring 10 mg of 1,3,5-cyclooctratriene into a precooled electrolytic cell under vacuum. This cell already contains tetramethylammonium iodide, which was placed in the cell before evacuation. Matheson reagent grade liquid ammonia is next transfered into the cell. The solution is well-mixed by rising the cell temperature slightly above the boiling point of the liquid ammonia. After subsequently cooling the system down to about -60°C, the cell resistence should be of the order of magnitude of 1 megohm.. If the conductance is much lower than this value, one should repeat the above mixing procedure to expel any possible gas bubbles within the cathode region of the cell. The electrolytic reduction of cyclooctatriene is carried out inside the ESR cavity under vacuum at -60°C. In order to search for the anion radical, the magnetic field is swept continuously near 3 kG and the electrolytic voltage is gradually increased after each scan until ESR signals start to appear. Readjustments of the electrolytic voltage and careful tuning of the spectrometer are necessary to obtain a well-resolved spectrum.

In order to get a spectrum with symmetric first derivative signals, the microwave bridge needs to be well-balanced by impedance and phase matchings, and the klystron frequency must be stabilized on the sample cavity. In this case, the dispersion signal is locked out, and only the absorption component will be observed. Unfortunately, in our present spectrograph, the reference cavity lock method is used; therefore, any deviation of the phase adjustment in the birdge network or resonant frequency change in the sample cavity may give a certain amount of the

dispersive component. The line shape and width may also be altered by improper choice of the modulation and normalized time constant[99] in the detection circuit. In the recorder presentation of the spectrum, line shape distortion is not a serious problem, whereas sensitivity may be important; so selection of a normalized filter time constant about equal to the peak-to-peak line width gives the best sensitivity for the spectrum. Alternatively a digital spectrum may be taken for data reduction. In this case, an undistorted line shape and the best reproducibility are highly desired; so a filter time constant which is much smaller than the line width has to be used.

An ESR spectrum (Fig 3) taken at an electrolytic potential of 12 volts gives the best signal-to-noise ratio. The spectral width is over 40 gauss, and 125 out of a possible 243 lines are observed in the spectrum. Five sets of coupling constants have been assigned to the spectrum. Each coupling constant shows a 1:2:1 intensity ratio pattern; therefore, five sets of two magnetically equivalent protons are present according to the spectrum. The initial assignment is simulated by the ESR IV computer program described in Appendix 1 of Levy's thesis.[92]

A digital spectrum was recorded by the Data Logging System. After the summing and smoothing manipulations of the SUMTAP program, an intermediate output tape is produced for further data reduction. The ORGRAD least-squares fit program is used to improve the initial assignment. The inversion of a 243 by 243 matrix during each least square iteration procedure is quite time consuming even by the CDC-6600 computation. A good first order estimation of the input parameters always take less iteration steps to bring the fitting into convergence. The improved assignments

of the coupling constants and line width are listed in Table 1 along with the initial assignments for comparison. The least squares adjusted fitted spectrum is shown in Fig. 3.

Although this spectrum is well resolved and the coupling constant assignment is unambiguous, some uncertainties still exist in the position assignment of the coupling constants. Since neither Huckel nor McLachlan SCF gives a good estimation for methylene proton coupling constants, simple theoretical position assignment is impossible unless the recent INDO treatment is used. The INDO method seems to be able to solve this ambiguity in position assignment. Nevertheless, a further experimental confirmation of the assignments of the methylene proton coupling constants is desireable.

B. Di-deutero-1,3,5-cyclooctatriene

d_2-cyclooctatriene may be prepared by deuteration of COT. The COT dianion is formed when COT is added to a THF potassium medium. Excess deuterium oxide of 99.8% purity from Bio-Rad Lab. is then added to react with the COT dianion. The 1,2 addition of the deuterium gives d_2-1,3,5-cyclooctatriene and the 1,4 addition of the deuterium produces the d_2-1,3,6-cyclooctatriene isometer. A large amount of ice water is then slowly added to the solution; the products are extracted and purified as in the previous case. Spectroscopic data show that 80% of the product is the 1,3,5-isomer and 20% is the 1,3,6-isomer. A close look at their conformations and stereochemistry shows that both isomers are nonplanar; hence, cis-trans deuterated isomers may result from the deuteration of COT. Furthermore, there are endo and exo types of isomers among the cis conformation of the 7,8-dideutero-1,3,5-cyclooctatriene. Within the presently

available techniques, the separation of these cis-trans or stereo-isomers is not feasilbe. An intramolecular 1,5 hydrogen shift by thermal isomerization has been observed in these compounds. This process can also shift the deuterium to replace vinyl hydrogen in the molecule; therefore, the products can get even more complex.

The radical anion of the deuterated 1,3,5-cyclooctatriene has been generated by the procedure described in the last section. The ESR spectrum is poorly resolved and has a comparatively smaller spectral width than the undeuterated spectrum. The small magnetogyric ratio and large nuclear spin give more ESR lines in a smaller spectral width region. Nevertheless, the main cause of the unresolved spectrum lies in the many kinds of possible isomers. Fortunately, the contraction of the ESR spectral width after deuteration still gives a qualitative picture of the methylene proton coupling constants. In order to compare the spectrum before and after the deuterium substitution, a d_2-1,3,5-cyclooctatriene radical anion ESR spectrum is presented in Fig. 4.

1,3,5-cyclooctatriene has a tub conformation (see Fig.17). The compound undergoes intramolecular 1,5 shift of hydrogen[66-110] and thermally equilibrates to bicyclo(4,2,0) octa 2,4,-diene valence tautomer.[103-106] Since the eight-membered ring is not in the planar conformation, the ring may interconvert between the two possible tub forms by a ring inversion process. The energy barrier for the ring inversion is, in general, low. Hence, the ring flipping process at room temperature is fast and easy. Under this circumstance two identical atoms or groups, which are attached to a common atom, are often assumed to be indistinguishable. As we lower the experimental temperature and shorten the detection interval,

these two atoms may be magnetically distingushable. No exact energy barrier for the ring flipping has been determined for 1,3,5 cyclooctatriene; but it is expected that the barrier is about the same order of magnitude as for COT, that is, about 7 kcal/mole. This is a reasonable estimation according to two determining factors in stereochemistry, i.e. angle strain and non-bond interaction.

The ESR experiment is ideal for revealing information about the ring conformation of the radical species. The spectrum of the anion radical of 1,3,5-cyclooctatriene obtained at -60°C shows no quintet pattern of intensity ratio 1:4:6:4:1 existing anywhere in the spectrum. This result rules out the existence of four equivalent methylene protons in the radical. This gives a strong evidence that the radical anion in solution does have the nonplanar ring conformation. It also shows that the rate of inversion at -60°C is slow compared with the frequency separation between the multiplets in the ESR spectrum, since the modulation of the methylene proton hyperfine coupling constants by the ring inversion process is not observable from the spectrum.

Another interesting feature of the radical is its ESR spectral width. The spectrum has a width of 46.7 gauss, which is much larger than the width of cyclooctatetraiene radical anion (25.6 Gauss). The possible existence of the negative spin density and the hyperconjugation from the methylene groups contribute to the width of the triene radical spectrum considerably. The main contribution to the extraordinarily large spectral width comes from the presence of the methylene groups. The contribution from the possible existence of negative spin density in this alternant system is, in general, small; whereas the methylene group coulping constants depend upon the

radical conformation. This radical appears to have large methylene proton coupling constants than that of cycloheptatriene. In the cyclooctatriene radical anion, the nodal plane of the odd electron wave function is between the two methylene groups while in cycloheptatriene it is coincident with its single methylene group. Hence, the hyperconjugation effect may play an important role in cyclooctatriene radical anion. The difference between the spectral width of the cyclooctatriene and that of cycloheptatriene radical anion should be mainly due to hyperconjugation.

The angular dependence of the beta proton coupling constant is another results of the hyperconjugation effect. In 1,3, 5-cyclooctatriene radical anion, the endo- and exo protons give significantly different coupling constants. The endo- proton is believed to have a larger coupling constant than the exomethylene proton. If the hyperconjugation of the methylene groups comes mainly from the p_z orbitals of the alpha carbons, Eq. 24 or Eq. 25 should give a reasonable estimation of the dihedral angles between the C_1 and hydrogen atoms on C_8. An order of magnitude calculation can be carried out from Eq. 24, if the spin polarization parameter Q is equal to 24.9 Gauss and the coupling constants are assigned according to Table I. The dihedral angles calculated from the above assumption are 74°, for the exomethylene proton and 33.5° for the endo proton. From Fig. 5 the projection of the bond angle (∠ HCH) of the methylene group to the plane perpendicular to the C_8-C_1 bond should be 120°, but the above calculation gives the angle 108°. Hence, there must be some important contribution to the beta hyperfine splitting elsewhere which has been neglected. One possible contribution is the transannular interaction between the methylene protons and their nonadjacent carbon p_z

orbitals. The tub conformation of the radical leads to a large interaction from the p_z orbitals of C_3 and C_4. This type of interaction does not commonly occur in most of the aliphatic chain molecules, but it has been observed in many of the ring compounds. A similar ESR result has been reported for the nine membered ring compound. The radical anion of lithium or potassium monohomocyclooctatetriene or that of cyclononatetraene has an ESR spectral width well over 40 gauss; and the coupling constant for the endo methylene proton is distinctly different from that of the exo methylene proton is distinctly different from that of the exo methylene proton, with a ratio of 2.6 between them. It is also reported that the temperature variation from -90°C to -30°C gives only slight change in the coupling constants of the methylene protons. The total splitting from the olefinic protons is ca. 26 gauss which is about the same splitting as we observed in the ESR spectrum of the radical anion of cyclootatriene. The spin polarization contribution to the methylene proton hyperfine splitting is estimated to be 0.25 gauss according to Eq. 23; but a value of 0.77 gauss is obtained from the sigma-pi interaction parameter of -2.78 gauss, which was experimentally evaluated from the radical anion spectrum of cycloheptatriene.[51] The above calculation shows that spin polarization plays only a minor role in the total hyperfine splittings of the methylene protons.

Deuteration is, in general, not a stereospecific reaction. Alkali metal reduction of cyclooctatetraene followed by addition of the deuterium oxide gives a mixture of d_2-1,3,5 cyclooctatrienes.[104,110,111] Both cis- and trans-7,8-dideuterated isomers are present in the solution. Thermal isomerization can further shift the labile deuterium to the vinyl positions.

When the rate of inversion is slow at low temperatures, the endo and exo positions of the methylene groups are magnetically nonequivalent. This fact has been found in the NMR experiment on C_8H_8D and COT-metal carbonyl. A strikingly large chemical shift between the endo and exo-methylene protons is observed. The ESR spectrum of the radical anions in the mixture gives little detailed information about the coupling constants. Fortunately, the total spectral width can still be accurately measured from the two outermost lines. Careful selection of the high purity of the deuterium oxide can minimize the presence of the C_8H_{10}. Low temperature prearation and purification can reduce the rate of the 1,5-deuterium shift by thermal isomerization. The 7,8-dideutero-1,3,5-cyclooctatrienes consist of three species which are designated according to the deuterium location: trans, endo-cis, and exo-cis isomers. The ESR spectrum of the trans-7,8-dideuterated radical anion should give five sets of proton coupling constants, whereas each of the endo-cis and exo-cis species should give four proton coupling constants and one deuterium coupling constant. The overlap of these three spectra give the total observed spectrum. The measurement of the total width of the spectrum shows the extent of the shrinkage of the hyperfine splittings due to the substitution of protons by deuteriums. If either of the cis forms gives the predominate spectrum, the shrinkage can be employed to assing one of the coupling constants to the methylene groups. On the other hand, both of the methylene proton coupling constants can be assigned, if the trans conformation is the major component in the mixture. The chemical reduction by potassium, in fact, favors the transl,2-addition of the deuteriums. Hence, both of the proton coupling constants of the methylene groups can be assigned.

The deuterated 1,3,5-cyclooctatriene radical anion has an ESR spectrum with a width of about 34 gauss; therefore, the position assignment based on the known information from the cycloheptatriene agrees with the deuteration experiment very well. The methylene protons have two coupling constants of 9.6 gauss and 1.0 gauss. The noneqivalence of the methylene proton coupling constants can not be explained by Huckel MO method; and the angular dependence relation alone is still unable to explain the splittings quantitatively. A refined quantitative all-valence-electron calculation is needed to further confirm the assignment. Pople's INDO computation has successfully predicted many hyperfine splittings in various kinds of radicals; therefore, it is a worthwhile effort to examine the INDO calculation for this particularly interesting ring compound. The result should be a crucial test for the validity of this computational method.

In the INDO approximation of the HF-SCF-LCAO-MO calculation the proton hyperfine coupling constants are accounted for in terms of spin densities. The calculated results by Pople and his coworkers agree very well with the experimental ESR data in most of the planar aromatic radicals. In their calculations the sigma-pi interaction parameter of the McConnell relation could be examined from the spin densities at the proton and at its adjacent carbon. The relation is observed to hold remarkably well in most of the planar aromatic radicals; and the Q value is found to be -22 Gauss. In order to apply the INDO method to the system 1,3,5-cyclooctatriene anion radical, a geometrical model of the radical must be assumed. The uncertainties in the equilibrium conformation can greatly diminish the significance of the theoretical calculation. Never-

theless, it is reasonable to assume that the radical possesses the same conformation as its parent molecule for the INDO calculation. The INDO calculation of the radical anion of 1,3,5-cyclooctatriene is based on the model of the neutral molecule (see Fig. 17). The input coordinates for the carbon atoms and the hydrogen atoms were roughly estimated from the model. In the model, the bond lengths for the carbon-carbon bond between the sp^2 carbon atoms are 1.40A, and the bond length between two sp^3 carbon atoms or between the sp^2 and sp^3 carbon atoms is about 1.44 A. All the C-H bonds are assumed to have the bond length 1.08 A. The calculated proton coupling constants by INDO method are listed in Table along with the experimental coupling constants for comparison. Based on the assumed model, the INDO calculation overestimates both the total spectrum width and the coupling constants at protons H(2) and H(5). It also predicts a large coupling constant at H(3) or H(4) which is negative in sign. However, the calculation indicates quite different values for coupling constants of the exo and endo methylene protons. It predicts a small negative coupling constant for the exo methylene protons and a relatively large and positive coupling constant for the endo methylene protons. The INDO method clearly points out the role of the hyperconjugation mechanism for the hyperfine splitting of the endo methylene protons, whereas only a small spin polarization effect causes the splitting of the exo methylene protons. However, the calculated splittings for the methylene protons are still smaller than the experimentally observed ones. The failure of the INDO calculation to predict the correct coupling constants for the vinyl type protons does not necessarily reflect the shortcoming of the INDO approximation, since the actual conformation of the radical anion

may be quite different from the model used in our calculation. Nevertheless, it does indicate that where the spin densities calculation by INDO method is very sensitive to the geometrical model of the radical species. Any slight error in estimating the conformation for the INDO calculation may lead to the false hybridization of the carbon orbitals and, therefore, a large deivation in the spin density. Pople's result in some of the non-planar or nonbenzenoid olefinic radicals reflects the importance of the radical geometry. The calculated methylene protons coupling constants of cyclohexadienyl radical is much larger than the observed one; and the protons at the alpha carbons have a coupling constant and opposite in sign. It is believed that a better agreement between the observed coupling constants and the INDO calculated ones may be obtained, if a more precise model can be selected for the calculation. The geometrical difficulties associated with this calculations is discussed in Appendix.

Since the INDO calculation of a planar cyclooctatetraene radical anion gives a reasonable coupling constant for its protons, one may be interested in evaluating the coupling constants for the protons in 1,3,5-cycloctatriene radical anion with the assumption of a planar conformation of the ring. The bond lengths of C-C bonds were all assumed to be equal to 1.40 A as the Pople's Model B and in this planar model the coupling constants evaluated from the INDO method are equivalent for the endo and exo protons. This model als predicts large coupling constants for the protons at C-3 and C-4. All the vinyl protons except the protons at C-2 and C-5 have negative coupling constants, whereas the methylene protons have positive coupling constants. Although the agreement with observed coupling constants if fairly poor for the planar model the INDO method

TABLE I. Proton Hyperfine Coupling Constants of 1,3,5-Cyclooctatriene Radical Anion

Position	HMO	McLachlan	INDO[b]	INDO[c]	Exp.[a]
H(1,6)	-5.61	-7.14	4.4	-6.2	6.875
H(2,5)	-1.53	0.	24.6	2.0	1.302
H(3,4)	-4.59	-4.59	-8.2	-7.8	4.547
H(7,8)	+0.77[d]	+1.02[d]	3.5	3.5	9.581
H(7',8')	+0.77[d]	+1.02[d]	-0.1	3.5	1.042

[a]Experimental Assignment of the coupling constants based on the 7,8-dideuterated 1,3,5-cyclooctatriene and the assignment for the spectrum of 1,3,5-cycloheptatriene. The magnitudes of all coupling constants are in Gauss.

[b]INDO calculation based on the Model of the neutral molecule (see Fig.17).

[c]INDO calculation for the radical assumed to be in its planar conformation.

[d]Using Levy's method for hyperconjugation.

does give a close prediction of the total spectral width. The INDO method based on the planar model with a C-C bond length of 1.40 A gives 44.0 gauss for the total spectral width, which is very close to the experimental total width.

The basic Huckel MO calculation gives no information about the spin densities at the methylene groups. Levy's formula incorporated with the HMO method yields some information about the spin densities at vinyl protons as well as at methylene protons. Unlike the INDO method, the Huckel scheme does not consider the geometrical factors explicitly; it also possesses numerous adjustable input parameters. Hence, it gives good agreement to the observed coupling constants of olefinic protons, if the variation of the β value is from 0.8 to 0.9. Since the β value can be related to the overlap intergral, which is a function of the bond distance and a function of the twisted angle of the p-orbitals from their coplanarity, the approximate geometry can be estimated from the calculation. The values of 0.8 or 0.9 for β imply that there is about 30° twist between the p_z orbitals at the C_2 and C_3 atoms. Levy's formula is less useful in our case, because the formula is based on the concept of group orbitals for the methylene group. In our case the radical possesses nonequivalent protons at the methylene positions, but Levy's formula can predict only the equivalent coupling constants for the endo and exo methylene protons. The calculated result shows that Levy's formula gives a close prediction for the coupling constant of exo protons but much too small a prediction for the hyperfine splittings at endo protons. Levy's formula incorporated with the McLachlan approximation gives an improved results for the methylene protons at exo positions; it also gives better

agreement for the coupling constant at the C-1 and C-6 positions.

C. Carbon-13 Satellites in Cyclooctatetraene

A cyclooctatetraene radical anion spectrum has been recorded by Katz and Strauss. The radical anion spectrum in DME or in THF using lithium as the reducing agent exhibits some satellites.[98] Strauss and Fraenkel concluded that they arise from C-13 splittings. No satellite has been observed in liquid ammonia.[92] In the liquid ammonia system the exchange the exchange and line broadening effects increase the line width considerably; hence, these broad proton lines obscure the C-13 information completely in the analog spectrum. However, the least-squares adjusted fitting program can be used to extract satellite information from the predominate proton signals, underneath which C-13 satellites are buried.

The cyclootatetraene radical anion is generated in liquid ammonia or the THF. In a THF solution, the satellites appear on the shoulders of the main proton lines in the analog spectrum. The proper parameters are found for the simulated plot by least-squares iteration procedures. The simulated spectrum contains only the information for the protons according to the spin Hamiltoniam of protons. Hence, the difference of the simulated from the experimental digital spectrum contains the information abour the C-13 satellites and any other discrepancies which exist between the experimental results and the theoretical computations. For the COT radical anion in THF the application of the ORGRAD program reveals the center location of the satellite without height and width corrections. On the other hand, the ORGRAD program applied to the system in ammonia gives more fruitful results. The existence of the C-13 satellites appears only after the substraction of the theoretical proton absorption signals.

Nevertheless, the technique has its limitations due to the existence of discrepancies in the least-squares fitting. These discrepancies result from the presence of a dispersion signal as well as the absorption signal. Their minimum intensites of the dispersion signals were about 5% of the absorption signal intensities when the magic tee bridge network in the previous spectrometer setup was used. After the modifications of the bridge network and introduction of the PAR phase detector, the tuning of the spectometer became simple. The dispersion signals are suppressed to the limit of 1 to 2% of the absorption signals. The inclusion of the dispersive components of the Lorentzian lines into the least-squares fit procedures has a slight but noticeable improvement. This seems to be one of the shortcomings of the present spectrometer. Part of the discrepancy may also be from the NMR tracking error. This maybe a major source of error; the reduction of the scan speed may very well eliminate this tracking erro considerably. For comparison purposes, COT radical anion spectra in THF and ammonia are shown in Fig. 6 and Fig. 7 respectively. From either Fig. 6 or Fig. 7 one may notice that the discrepancies between the theoretical and experimental spectrum are more pronounced underneath the strong derivative signals. This noise seems to be dependent on the field and also the singla intensity. One may also notice that the noise becomes large where the slope of the first derivative signal is steepest. The noise which superimposes on the strong ESR signals may result from the uncertainty in the field measurement by NMR tracking unit or it could be from the presence of the dispersive component of the ESR signal. The dispersion signals can be suppressed to 2% of the absorption signals, if the present microwave network of

our spectrometer is well balanced. The noise shown in the error curve of the least-squares adjusted fitting spectrum are at least a factor of two stronger than what the dispersive components may contribute. On the other hand, if the NMR tracking system has a uncertainty of 15 mG, it can generate enough noise at the locations of the centers of the lines to smear out any significant information at those location of the spectrum. The uncertainty of 15 mG in the NMR unit considerably 1 limits the usefulness of our digital data acquisition system, although the NMR oscillator alone can have very accurate frequency stability.

D. P-cyano-pyridine-N-oxide

The sample of 4-cyano-pyridine-N-oxide was obtained from Reilly Tar and Chemical Corp. and used without further purification. A 10mg. sample was used for electrolysis in liquid ammonia at -60 C. No ESR signals can be observed until the applied electrolysis voltage is gradually increased and reaches 120 volts. At this voltage setting, the ESR signals increase in intensity rapidly and then begin to decrease. At the mean time, a single ESR signal appears and gradually increases in intensity. This single ESR signal resembles the signal observed in metal-ammonia systems and is identified as a solvated electron signal. When the applied voltage is lowered gradually, the electron signal stops growing, but the radical anion spectrum does not begin to recover its intensity until the voltage is lowered below 50 volts. The best radical anion spectrum is obtained in the presence of a solvated electron signal at 30 volts of the applied electrolytic potential. The spectrum has a width of about 30 gauss and consists of three equally intense groups. Each group has a large 1:1:1 triplet which is further split into a multiplet structure by two 1:2:1

TABLE II. P-cyano-pyridine N-oxide Radical Anion in Liquid Ammonia

Position	Coupling Constants (Gauss)			
	Experimental[b]	HMO[c]	McLachlan[c,d]	INDO
N(ring)	9.31	5.0	9.4	10.26
H(2,6)	0.85	2.7	3.41	0.60
H(3,5)	2.47	0.72	0.77	1.94
N(C=N)	1.84	1.30	1.64	1.97

[a] g factor of the radical anion 2.0034±0.0001.

[b] position assignment based on INDO calculation.

[c] N(ring) coupling constant calculation based on Ayscough and Sargent, J. Chem. Soc. (B), 903, 907 (1966).

[d] Lambda value for McLachlan calculation is set to 1.

triplet patterns. With the above observation the analysis and the assignment of the spectrum becomes simple. Four coupling constants have been assigned to the spectrum. The triplet splittings with the 1:1:1 intensity pattern come from the hyperfine interactions of the nitrogen nuclei with the unpaired electron; the 1:2:1 triplets are assigned to the proton hyperfine couplings with the odd electron. The digital data can be handled by SUMTAP program and then the spectrum parameter can be fitted by ORGRAD program. The fitted spectrum is shown in Fig. 8 and the coupling constants are listed in Table II along with the initial assignments made without the use of the data acquisition system.

Since the cyano group lies in the symmetric plane of the ring, no inequality of the ortho or meta protons is expected; this has been confirmed from our experimental observation. On the other hand, one also expects that there is a nodal plane of the first antibonding orbital of the pi electron which coincides with the symmetric plane across C-1 and C.4. Hence a small hyperfine splittings are expected for two nitrogen atoms. However, it is found that heterocyclic nitrogen nucleus gives a large coupling constant. This may be qualitatively explained by the strong electron withdrawing effect of the nitrogen due to the N-oxide bonding; the nitrogen donates its lone pair electron to the oxygen and, therefore, both its conjugation and its inductive abilities are increased considerably. Hence, a large portion of the spin density is located at NO fragment of the radical. The spin polarization parameter, Q_N^N, of nitrogen may also increase considerably. This fact has been observed by Talcott in the Q_N^N of pyrindine N-oxide comparing to that of pyridine.

In the theoretical evaluation of the spin densities by the HMO and McLachlan methods, the Q values derived by Ayscough and Sargent were used. The McLachlan method gives good coupling constants. The Huckel MO method evaluates smaller coupling constants than the experimental values. Alternatively, Q values derived by Talcott are used in the calculations. Since these Q values are considerably larger than the Q values derived by Ayscough's method. A smaller spin density at nitrogen or oxygen atom than the value calculated from the McLachlan method is needed to match with the experimental nitrogen coupling constant. The HMO method with Talcott's Q parameters gives an A(N) of about 14 Gauss, which is not too far from the experimental coupling constant. According to either the HMO or McLachlan method, in the experimental assignment of the coupling constants of the ring protons A(2,6) should be greater than A(3,5) rather than the present assignment. However, the highly approximate nature of the HMO and McLachlan method makes us believe the more quantitative INDO method. The INDO method gives suprisingly good agreement with the experimental coupling constants, but it disagrees with the HMO and McLachlan methods in the position assignment of the ring proton coupling constants. Using those bond lengths in Model B of Pople's calculation and a planar geometric model for the radical. The calculations were performed with the assumption of standard sp^2 and sp^1 bond angles. INDO can differentiate between the two protons at the 2,6 position and also the protons at the 3,5 position in the ring. Experimentally, the line width of 0.144 gauss smears out any possible difference between the proton coupling constants at 2,6 position (and at 3,5 position). This is an evidence of

the usefulness of the unrestricted MO-SCF calculation with INDO approximations in predicting and assigning the ESR spectrum.

E. Pyrazine

ESR spectra of the pyrazine radical anion have been previously reported in THF and DME with potassium reduction,[95-96] in acetonitrile with electrochemical reduction,[96] in DMSO,[97] and also in liquid ammonia.[93] Stone and Maki observed the carbon-13 isotope signals in natural abundance. They use the conventional method of the detection of the isotope satellites: boosting the gain setting of the spectrometer. The measurement of the satellite coupling constant should involve height and width corrections because ofthe presence of the strong proton hyperfine signals.[98] It should be easy to extract the satellite information directly from the digital spectrum by using the digital data acquisition system and sophisticated computer programs.

The anion radical is generated in liquid ammonia (or DMSO) by electrolytic reduction, using 0.001M pyrazine with added tetramethylammonium iodide (or tetrabutylammonium perchlorate) as the supporting electrolyte. ESR signals start to appear and begin to build up in intensity shortly after 1 volt is applied across the sample cell. The digitial spectrum obtained at 10 volts has a good signal-to-noise ratio and is shown in Fig. 9 (and Fig. 10). The weak C-13 lines are observed at bothsides of the proton signal. With 1.1% natural abundance, C-13 has a magnetic moment of 0.7021 nuclear magnetons and a spin of 1/2. The study of the C-13 satellites becomes intersting but quite simple because all four carbon atoms are equivalent.

The spectrum of the radical in liquid ammonia (Fig. 9) shows that only one of the two carbon-13 signals is observed and it lies midway

between each of the two main proton hyperfine lines. The C-13 has a coupling constant of 2.82 gauss with a line width parameter of 0.292 gauss. The proton coupling constant found in the spectrum of the radical in ammonia has a value of 2.709 gauss. The closeness of the proton and C-13 coupling constants and the large line width contribute to the accidental line overlapping of the two C-13 satellites.

When the experiments are carried out in diemthylsulfoxide, tetrabutylammonium perchlorate is used as the supporting electrolyte. A detachable side-arm tube is designed to serve the purposes of condensing and mixing of the sample and the solvent. It also serves as a switch between the electrolysis cell and the vacuum system to avoid any exposure of the solution to the atmosphere during the entire experiment. The DMSO used for ESR purposes must be purified by bulb to bulb distillation from $LiAlH_4$. During the transfer of the simple or the solvent, the side-arm tube is cooled by liquid nitrogen. The condensed sample and the solvent are then allowed to warm up for mixing purposes prior to the transfer into the cell. The cell containing the solution is then ready for electrolysis. The remaining procedures are the same as in the liquid ammonia experiment.

In the solution of DMSO, the line widths of both the proton and C-13 hyperfine signals are narrower; moreover, the proton coupling constants is reduced to 2.639 gauss. The combined factors of the line width and coupling constant yield resolved C-13 satellites with little overlap. The perturbation of the coupling constants and line widths by the solvent causes the interesting observation of the change in spectral patterns. A variation in sigma-pi interaction parameter Q is also observed

because of the solvent perturbation.

In Maki's experiment, the coupling constant of C-13 satellites can be roughly measured by interpolation of the magnetic field measurement; the intensity of the satellites, thus, can be estimated from the line width of the satellites. A large uncertainty may occur in the intensity measurement of the C-13 signals because of the rough measurement in the line width. Since the present data acquisition system and data reduction methods give a reliable field measurement and the intensity measurement becomes much accurate with the accurate field indication and expanded error curve in the least-squared-adjusted fitting spectrum (Fig. 10). Although Maki et al. give the C-13 satellite coupling constants 2.88 gauss with an error 0.02 gauss, our result indicates the C-13 coupling constant is 2.80G in DMSO and 2.81G in liquid ammonia system with an error less than one percent. Digital data acquistion system and off-line computer for data reduction assist experimental chemist to extract information out of a complicated spectrum; the data acquisition system or the computer assisted ESR spectrometer will certainly be a necessary and convenient tool for data reduction and analysis.

F. 4,5-methylene-phenanthrene

The substituted phenathrane sample was obtained from Aldrich Chemical Co. A 10^{-2}M solution of the methylene phenathrane in liquid ammonia is electrolyzed at -60°C. Some weak signals start to appear at 2 volts; and they grow in intensity as the applied voltage is increased. Electrolysis at 11 volts for up to 6 hours gives a partially resolved spectrum. An ESR spectrum of better resolution is obtained after another 15 hours of continuous electrolysis ; also, the observed line width is drastically

TABLE III. Coupling Constants of Pyrazine Radical Anion[a]

Solvent	A(N)	A(H)	A(C^{13})
THF*	7.22	2.66	
DMSO	7.213	2.639	2.88
Ammonia	7.2286	2.7105	2.81
DMSO	7.1738	2.6239	2.80

[a]All the coupling constants are measured in Gauss.

reduced. Nevertheless, the solvated electron signal still appears in the spectrum. The optimum spectrum consists of more than 70 resolved lines with a solvated electron signal superimposed on the spectrum. Five coupling constants should be assigned to the protons, as one expected from the molecular structure. The experimental spectrum recorded after continuous electrolysis for 20 hours is shown in Fig. 11. The experimental spectrum is very complex. The solvated electron signal appears in the spectrum, and it overlaps with a portion of the radical spectrum. By judging from the spectrum, one finds that the radical possesses a slightly larger g value than the solvated electron. In Fig. 11, the portion of the spectrum containing the solvated electron signal is omitted. The assignments of the coupling constants from the spectrum is not trivial. Only the septet patterns at both ends of the spectrum can be recognized. However, the septet results from two different coupling constants of 1.12G and 0.52G. The A'=2A relation gives the septet a intensity ratio: 1:2:3:4:3:2:1. The large 1:2:1 triplet splitting at the center of the spectrum can be assigned a coupling constant of 8.0G. A triplet splitting at each end of the spectrum is assigned a coupling constant of 2,6G. Using the relation that total spectral width should be equal to the summation over the hyperfine splittings, the fifth coupling constants is 6.5G. The assignment was checked through the simulation plot by varying each coupling constant slightly. The simulated plot using the final set of coupling constants is shown in Fig. 12 and the constants are listed in Table IV.

The assignment of the ring proton coupling constants shown in Table IV are based on the McLachlan MO calculation along with the hyperconju-

gation formulas derived by Levy gives a small negative hyperfine coupling constant for the methylene protons. The β value for the bond C9-C10 was assumed to have a value which is 0.6 of that of the C12-C13 bond, and a value which is 0.75 of the β value of any other bond in the polycyclic rings. This set of parameters gives a good prediction of the coupling constants, if the Q value is 36.8 Gauss. This radical has a much larger spectra width than the unsubstituted phenanthrene radical anion. Since the MO calculation gives no negative spin density at any atom in the rings and a small hyperfine splitting for the methylene protons, the large spectral width must be attributed to a large Q value. The large spin polarization parameter may be due to the change of the molecular geometry by the constraint of the methylene substituent. Our McLachlan MO calculation indicates good agreement between the experimental and theoretical data, if the β values for C12-C13 and C9-C10 are varied slightly from the standard value of 1.0. The result implies that the bond length of C12-C13 is shorter and that of C9-C10 is longer than the normal aromatic C-C bond length; hence, the overlap between the orbitals at C12 and C13 increases and the overlap between the orbitals at C9 and C10 decreases. The change in the bond length or bond angle requires a change in the hybridization of the carbon atoms, so the Q value differs considerably from the normal 25 Gauss.

In the anion radical of 4,5-methylene phenanthrene, the odd electron occupies the first antibonding orbital which possesses seven nodal planes, and one of these nodes lies across the methylene group and bisects the C9-C10 bond. The coupling constant for the methylene protons is of the same order of magnitude as that of 1,3,5-cycloheptatriene. The MO method

TABLE IV. Coupling Constants for 4,5-methylene Phenanthrene Radical Anion and Related Radical Anions[a]

	4,5-methylene phenanthrene		Phenanthrene[d]	4,5-phenanthry[e] -lene
	Calculated[b]	Exp.		
H(1,8)	5.46	6.5	3.6	3.06
H(2,7)	1.18	1.12	0.72	0.03
H(3,6)	3.79	2.6	2.88	2.12
H(9,10)	9.08	8.15	4.32	0.10
H(Methylene)[c]		0.52	-	-

a) all the coupling constants are in Gauss

b) McLachlan calculation is used, Huckel MO gives similar results. assumed $\beta(9,10)=0.75\beta$, $\beta(12,13)=1.25\beta$.

c) Levy's formula is used to estimated the hyperconjugation contribution: 0.2 Gauss.

d) S. H. Glarm and L. S. Synder, J. Chem. Phys. 36 2989 (1962).

e) R. Dehl and G. K. Fraenkel, J. Chem. Phys. 39, 1793 (1963).

predicts that the spin density at C4 or C5 is 0.05. If one uses a Q value of -3.09G[128] the observed coupling constant for the methylene protons estimated from the equation A(observed)=A(Hyperconjugation)+A (spin polarization), is equal to -0.4 Gauss, with an A(hyperconjugation) Of -0.25 Gauss estimated from the McLachlan MO calculation. If Q=+4.33G is used, the estimated A(observed) is -0.04Gauss. From the experimental result, the methylene proton coupling constant is assigned as 0.52G. Hence, our experimental data favors a Q value of -3.09 Gauss, despite the fact that Morton's data[129] support the +4.33 Gauss value.

G. 1,4 phenylene diamine

The amine sample from Eastman Kodak Co. was used without further purification. The radical was generated by in-situ electrolysis in liquid ammonia, but only a single broad ESR signal was observed in the cathode region at 15 volts. This single ESR line is believed to consist of contributions from the unresolved solvated electron and radical ion signals. About five minutes after the applied electrolytic potential is shut off, the single line broadens out and a complicated spectrum begins to appear. The supectrum gradually grows in the next ten minutes, and then the signals start to decay. The estimate of the radical concentration from the ESR intensity measurement gives the half-life of the radical as about fifteen minutes, provided that the signal decay due to diffusion is insignificant.

The recorded spectrum has more than 63 resolved first-derivative lines. Three coupling constants can be obtained by inspection. The spectrum consists of only quintet patterns with an intensity ratio of either 1:2:3:2:1 or 1:4:6:4:1. These observations imply that the radical has

two magnetically equivalent nitrogen-14 nuclei and two sets of four magnetically equivalent protons. The ESR IV computer program was used for spectrum simulation; and the ORGRAD program was used for the least-squares adjusted fitting. The assignment is listed in Table V, and the digital spectrum is shown in Fig. 13.

Numerous radical ions of benzene derivatives have been reported. The amine-substituted benzene derivative radicals which have been reported are the cation radicals of p-phenylene diamine and its substituted derivatives and some anion radicals of polynitro-substituted amines. Using the technique of electrolysis, Maki et al. first reported the cation radical spectrum of p-phenylene diamine and made a reasonable assignment of the coupling constants. However, no radical anion spectrum of p-phenylene diamine has been previously reported. The continuous electrolysis technique in liquid ammonia is excellent for generating the radical anion of p-phenylene diamine.

The observation of the ESR spectra of both anion and cation radicals is significant for the theoretical understanding of the hyperfine splittings of the radicals. A comparison of the coupling constants of cation and anion radicals is desired for further understanding of the mechanism of the spin distribution.[24-32] The MO pairing theorem demands the inclusion of a charge therm in the McConnell Equation in order to explain the differences in the observed coupling constants of the anion and cation radicals. On the other hand, most valence bond calculations predict different spin densities for cation and anion radicals even without any extra charge term. The measurement of the ESR spectra of both cation and anion radicals provides a test of the importance of the excess charge term in the McConnell Equation.

In this experiment the radical anion is successfully generated in a liquid ammonia medium by electrolysis at the cathode region of the electrolytic cell. The radical ESR spectrum has a width of about 50 gauss and can be assigned by using three coupling constants. The simulated spectrum based on a single line width parameter (Fig. 14) and the experimental one (Fig. 13) have fair agreement, although there are some noticeable discrepancies in their hyperfine components. The least-squares-adjusted fitting program, ORGRAD, gives little improvement to the predicted input parameters. Using four or even five sets of coupling constants, one does not get any great improvement in the agreement between the theoretically predicted and the experimental spectra. An obvious difference is two missing hyperfine components near the upper and lower ends of the experimental spectrum. Also, our assignment with a single line width parameter predicts stronger intensities for some hyperfine components than the experimental spectrum does. The intensities of the theoretical hyperfine lines are proportional to the degeneracies of their corresponding nuclear spin state and inversely proportional to the square of the line width in a derivative spectrum. These discrepancies between the experimental and theoretical spectra can be explained by the effect of line width variations. The change of line width can be measured by the quantity $(I/D)^{1/2}$ where I is the absorption intensity of the hyperfine line and D is the degeneracy of the corresponding line. The least squares adjusted curve fitting computer program, ORGRAD, uses a single parameter for the line widths of all the hyperfine components. Hence the program is not suitable for handling the spectrum with variable line widths.

The line width variation effect greatly influences the intensity pattern of the radical anion spectrum of p-phenylene diamine. Furthermore, the ring proton and amino proton hyperfine splittings may be modulated, if the spin density throughout the molecule is redistributed by the modulation of the nitrogen hyperfine couplings in amino groups. This phenomenon in turn causes the hyperfine splitting of the ring protons to fluctuate with time, as one observed in 1,4-dinitrobenzene anion radical. The anomalous intensity pattern of the ESR spectrum of p-phenylene diamine can be explained by the line width variations of the hyperfine lines of protons.

The line widths of the hyperfine components of radicals in solution follow the general equation of M_I dependence:

$$\Delta H = \alpha + \beta M_I + \gamma M_I^2 + \ldots \qquad (49)$$

where H is the line width parameter, M_I is the resultant spin quantum number projected along the direction of the magnetic field H_o for nuclei I, and α, β, γ etc. are parameters which depend upon the radical and its various environmental factors. For many radicals the first term is dominant and there is little or no noticeable line width variation with M_I. A common circumstance is to have the first two terms dominant so that the high field or low field lines are broadened. A less common circumstance is for the first and third term to be dominant so that both the high and low field lines are equally broadened.

For radicals with more than one hyperfine interaction one can either have a series of terms for each nucleus like Eq. 49 or other types of equations are possible. Freed and Fraenkel, for example, have examined the case of alternating line widths; they have shown that for some radicals with two equivalent N-14 nuclei that every other N-14 hyperfine

components appears to be broadened. This has been explained by them as being due to an in-phase correlation of the relaxation of the two N-14 nuclei, and the lines in which $M_I(1)$ $M_I(2)$ are broadened. This does not seem to be the case for p-phenylene diamine radical anion, since the hyperfine broadening is best explained by two series like Eq.49 for two different kinds of nuclei but both with $|\gamma| \ll |\beta|$.

A computer program, IMITATE, was written by J. J. Chang to simulate ESR spectra with variable line widths. Each hyperfine component can be assigned a different line width in the simulated spectrum by IMITATE. The comparison between the experimental spectrum and the simulated spectrum from the IMITATE program can be very useful in designating the M_I values corresponding to each hyperfine splittings. The simulated spectrum with a single line width parameter for all the hyperfine components does not give accurate agreement in the intensity patterns of the spectrum, especially for the hyperfine components near the high and low field limits of the spectrum. The following simulation efforts have been done to study the effect of line width variation: (1) One of the possible factors which could influence the line width would be that the two nitrogen nuclei could have slightly different coupling constants. The apparent line widths of the outer hyperfine components are influenced more than the line widths of the hyperfine components at the center of the spectrum, if the nitrogen coupling were different. However, a simulation based on difference in coupling constants gives little improvement to the agreement with the experimental results. It indicates that the factor of two slightly different nitrogen coupling constants is not a dominant effect for the line width variation of the radical anion spectrum of p-phenylene diamine.

(2) A common phenomenon in the line width variation is that the line width varys linearly with the designated M_I values:

$$\Delta H = \text{constant} \times M_I + \alpha \qquad (50)$$

where ΔH is the increment of the line width, and is equal to $\alpha+\beta$ when M_I is unity. Our simulation effort based on this relation gives some improvements both in the center of the spectrum and at the ends of the spectrum. However some intensity discrepancies still exist in the spectrum. When the line widths of the hyperfine components with the coupling constants of 1.966 G or 7.446G in the simulated spectrum are allowed to vary from 0.18G for the narrowest hyperfine components with $M_I = (0,0,0)$ to 0.24G or 0.36G for the line with $M_I = (2,2,2)$, the corresponding lines with M_I=1, or 2 for the splittings of 1.966G or 7.446G in the simulated spectrum decrease their intensities considerably in accordance with the experimental spectrum. When the 5.167G components are allowed to vary, the simulation plot does not give any better agreement than the single line width plot. These facts imply that the 5.167G hyperfine components have a less pronounced effect in the line width variation than either the hyperfine components of 1.966G or 7.446G, the spectra are simulated with the line width variation:

Line Width = 0.18G + C $(M_I + M_{I'})$; where I and I' designate the nuclei with 1.966G and 7.446G hyperfine splittings respectively, and C=0.04G. The simulated plot based on this line width variation equation varies too rapidly for the center lines and, therefore, broadens many resolvable hyperfine components. Hence, the linear dependence of the line width variation is too much for the center of spectrum and too little for the lines at the ends of the spectrum.

(3) We intend to simulate a variable line width spectrum with moderate line width variation in the center of the spectrum and more drastic line width variation at the ends of the spectrum. A possible relation is the M_I^2 dependent form. If the relation has the form: Line width = $0.18G + CM_I^2 + CM_{I'}^2$ where C=0.03G, we can obtain the proper line width variation for lines at the center and the ends of the spectrum. The outer lines of simulated spectrum appear weaker than the experimental ones; however, the lines which are missing in the experimental spectrum appear much weaker in the simulated spectrum. Other than these discrepancies, there is general agreement between the theoretical and the experimental spectrum. Any more refined treatment may involves rather complicated mathematical expressions for the line width variation equation.

Since all of the hyperfine splittings in the experimental spectrum are formed in the qunitet pattern. It is especially diffiuclt to distinguish the intensity pattern with 2:4:6:4:2 or 1:4:6:4:1. Hence, it is uncertain to assign the 5.167G coupling constant as the splitting from the nitrogen nuclei. Nevertheless our position assignment of the coupling constants is based on that of the cation radical spectrum. In addition, our simulation plot with the line width variation gives better agreement to the experimental spectrum and much of the predicted hyperfine structure agrees with the experimental patterns, if the nitrogen nuclei are assigned the 5.167G coupling constants. Our final assignment for the coupling constants are listed in Table V . The simulated variable line width spectrum is shown in Fig. 15.

The INDO calculations for the two radical species of p-phenylene diamine are very sensitive to the relative orientation of the ring and the NH_2 groups. Table V shows that the agreement with the observed hyperfine splittings for the radical cation is very satisfactory, if an ordinary planar D_{2h} geometry is assumed. If a nonplanar D_{2h} geometry, with the NH_2 groups perpendicular to the plane of the benzene ring, is assumed the coupling constant for the H(ring) is much too large. The prediction, in this case, is that the cation would be a sigma radical with electron removed from the lone pair instead of the pi system of the benzene ring. According to the INDO calculations and the experimental data, the cation radical of p-phenylene diamine should be in a D_{2h} geometry with the NH_2 groups coplanar with the benzene ring. Furthermore, it indicates the nitrogen atoms of the amino groups are sp^2 hybridized with the bond angle (H-N-H) 120°.

For the radical anion, Table V shows that the hyperfine splittings calculated from the INDO method are not in good agreement with the experimental ones for an assumed planar D_{2h} geometry. Both the calculated splittings for $H(NH_2)$ and $N(NH_2)$ are much too small in the planar model, whereas the coupling constant for the ring protons is too large. If either a D_{2h} or C_{2v} nonplanar geometry is assumed, the INDO values for these NH_2 splittings care greatly increased as shown in Table V. The small splittings for the NH_2 groups in the radical anion are also predicted by a modified Huckel calculation. In this case the nitrogens lie in the nodal plane of the odd electron and thus one expects very small NH_2 splittings. The INDO calculations indicates that the different geometries of the amino groups pertrubs the two degenerate energy levels of the

pi-electrons of the benzene quite differently. The coplanar configuration of the amino groups perturbs the pi-electron energy levels so that the state with nodal plane across the C-1 and C-4 has the lower energy level. On the other hand, the nonplanar configuration of the anion radical of p-phenylene diamine favors the state without the nodal plane passing through the C-1 and C-4. This seems quite reasonable according to the conjugation effect and the weak electron with drawing ability of the NH_2 groups. The planar model allows the nitrogen lone pairs to conjugate with the pi-system of the ring, so that it increases the electron density in the ring. The nonplanar model destroys the conjugation between the lone pairs of the nitrogen atoms and the ring, but it allows protons in the amino groups to hyperconjugate with the pi-system of the ring.

Consequently, the radical cation of p-phenylene diamine tends to have its planar geometry, whereas the anion radical tends to have its nonplanar geometry. The actual geometry of the radical anion of p-phenylene diamine should be somewhere between the planar D_{2h} geometry and nonplanar D_{2h} or C_{2v} configuration, according to the experimental coupling constants for the amino groups and the INDO calculated results.

Table VI illustrates the effect of variations in the C-N distances for nonplanar geometries of the radical anion of p-phenylene diamine. In the calculations, the nonplanar D_{2h} geometry requires the nitrogen valence orbitals to the sp^2 trigonal hybridized, and the nonplanar C_{2v} geometry was assumed to have sp^3 tetrahedral hybridized valence orbitals for the nitrogen atoms. In most cases, the hyperfine splittings for the ring protons and nitrogen atoms have no significant changes,

TABLE V. Hyperfine splittings for the Radical Anion and Cation of p-Phenylene Diamine[d]

	Radical Cation			Radical Anion		
	H(ring)	$N(NH_2)$	$H(NH_2)$	H(ring)	$N(NH_2)$	$H(NH_2)$
Experimental[a]	2.13	5.29	5.88			
b	2.10	5.12	5.67	c -1.966±0.003	5.167±0.002	7.446±0.003
Planar D_{2h}	-1.41	5.42	-6.13	-6.57	-0.24	0.01
Nonplanar D_{2h}	18.0	7.16	-9.83	-1.04	-4.03	32.5
Nonplanar C_{2v}	--	---	--	-1.32 and -0.46	-3.47	50.4

a) Maki's result.

b) Piette's result.

c) this work

d) calculations based on a C-N bond length of 1.37A or 1.3A and N-H bond length of 1.00A or 1.08A all the values are in the unit of Gauss.

TABLE VI. Intermediate Neglect of Differential Overlap Approximation Calculation for P-Phenylene Diamine Radical Anion

Hyperfine Splittings[a]	H(ring)	$N(NH_2)$	$H(NH_2)$
Experimental	2.00	5.17	7.45
D_{2h} Nonplanar			
C-N 1.3A[b]	-0.99	-4.70	39.0
1.37A	-1.04	-4.03	32.5
1.40A	-1.05	-3.74	28.5
1.50A	-1.05	-2.99	18.0
1.55A	-1.04	-2.76	14.2
1.60A	-1.04	-2.60	11.1
C_{2v} Nonplanar			
C-N 1.37A	-1.31 and -0.46	-3.48	50.4
1.45A	-1.41 and -0.49	-3.00	35.5
1.65A	-0.45 and -1.45	-2.42	13.7

a) all the values in Gauss

b) C-N bond lengths are all in the unit of Angstron

while that of the amino protons changes quite rapidly. This is not suprising at all, since conjugation or the inductive effect should decrease when the substituent is moved further away from the ring. However, these calculation do indicate C-N bond length affects the coupling constant of amino proton relatively more than does the H-N-H bond angle.

H. Aniline

In contrast to phenylene diamine, aniline is not easily reduced into a radical species. The ACS reagent grade aniline sample from Matheson was fractionally distilled once before use. The sample can be further purified by a distillation from Zn dust to remove any oxidized impurity. Four drops of purified aniline from a disposable pipette were then transfered intothe electrolytic cell. The electrolysis was carried out in liquid ammonia in the presence of TMAI and a slight amount of sodamide. The cell was placed in the vacuum system, and was cooled to -80°C before evacuating the air from the cell. Maintenance of the cell at this low temperature minimizes the loss of the sample due to evaporation during the evacuation. Liquid ammonia is subsequently condensed intothe cell, and the contents were well mixed before the electrolysis was started.

No ESR signal was observed at low electrolytic voltages. When the applied voltage was increased to 90 volts, a single broad line appeared and gradually grew. Further increase in voltage may cause the appearance of the sovlated electron line. The solvated electron signal disappears when the voltage is reset to 90 volts. However, there are no other observable signals besides the broad single line for the next few hours of electrolysis. After 14 hours of electrolysis at 90 volts

and 0.2 milliamperes, a complex spectrum begins to show up. The spectra were taken 17 hours after the electrolysis began. Electrolysis without using sodamide requires a longer period of time to obtain a spectrum of similar quality. The obtained spectrum has only a fiar signal to noise ratio; thismay increase the difficulty of recognizing the outermost lines of the spectrum and, therefore, cause much amibuity in the assignment of the spectrum.

Solvated electron signal was observed in some of the experimental spectra, when the electrolysis voltage was higher than 90 volts. The radical possesses a higher g value than the solvated electron. Hence, the electron signal appears at slightly higher field than the center of the radical spectrum. By lowering the applied electrolytic voltage down below 90 volts, one obtains a spectrum without the presence of the solvated electron signal. Figure 16 shows the observed spectrum of the radical species; The low field end of the spectrum appears more complex than the high field end of the spectrum. Some extra hyperfine signals are apparently observed in the low field end of the spectrum, and are absent in the high field end. This would indicate that the spectrum should be a superimposed spectrum of more than one radical species. The radical species with the weak wV signals has the smaller g value. The center of the spectrum was first assigned to be at 3235.63 Gauss, since the hyperfine component at this field has the strongest signal in the entire spectrum and it appears to be symmetric to the hyperfine components at high and low fields. Based on this observation four coupling constants corresponding to triplets can be assigned to the spectrum to predict most the hyperfine components at the high field side of the spectrum. However a number of lines at both the high field and low field

could not be predicted. Their assignment was believed to be incorrect, since the aniline should possesses at least four coupling constants of triplet pattern and a coupling of doublet pattern. An additional coupling constant of doublet 1:1 intensity pattern is obtained by measuring the difference between hyperfine components in the spectrum at high field side. The simulation plot (Fig. 19) gives a good prediction of the hyperfine components at higher field side. Interestingly enough, the center of the spectrum now appears to be at a slightly lower field of 3233.32 Gauss. There is a doublet which appears at the center of the spectrum. This doublet also appears at the high field end of the experimental spectrum. Owing to the accidental overlap by the coincidences of the coupling constant, the doublet of intensity 1:1 does not appear anywhere else in the spectrum. In the low field side of the spectrum hyperfine components are not easily recognized because their intensities are much weaker than those of the high field side. It is not known whether the decay of the radical or the line width broadening effect is the main contribution for this observation. We are also unable to identify the spectrum of the radical of low concentration except a few hyperfine components. Our present assignment of the spectrum of the radical with high concentration can explain most of the low field lines by the symmetric criteria of the spectrum.

The position assignment of the coupling constant is not trivial in this case. Four coupling constants corresponding to triplet patterns must be assigned to three sets of two equivalent protons and one nitrogen atom in the radical anion. The doublet pattern of the splitting

0.65 Gauss, is assigned to the para proton. The nitrogen atom coupling constant can be selected from the simulation plot, since it has the 1:1:1 intensity pattern. The position assignment of the rest of the three coupling constants are based upon MO theory. If the NH_2 group is coplanar to the benzene ring, the INDO calculation predicts large coupling constants for the ring protons, especially for the metal and ortho protons. The proton at the para position has a sign opposite to that of the others. This implies that the INDO method predicts a large negative spin density at the para position. In this model, the INDO calculation gives very small coupling constants for NH_2 group. It predicts that a node lies fairly close to the amino group. If the radical anion has a nonplanar configuration such that the NH_2 group is perpendicular to the benzene ring, the INDO calculation predicts a very large coupling constant for the protons of the amino group. The INDO calculations of both the planar and nonplanar radical geometries indicate the meta protons should have slightly bigger coupling constant than the ortho portons. In addition the coupling constant assignment of the radical anion of the phenylene diamine indicates the $H(NH_2)$ and $N(NH_2)$ should have comparable magnitudes of the coupling constant. Hence, we assigned the $H(NH_2)$ coupling constant to be 2.96 Gauss. The coupling constant for the meta protons was assigned to be 7.89 Gauss, which is slightly larger than the coupling constant of the ortho protons, (5.01 Gauss). The INDO calculations as well as the HMO calculation overestimate the splitting for the para proton, and all these calculation do not closely predict the splitting for the amino group. The study of the radical anion of per-deuterate ani-

TABLE VII. Coupling Constants of the Radical Anion of Aniline

	Exp.[a]	Huckel MO	INDO	
			planar	nonplanar
$N(NH_2)$	2.140	-	-0.22	-3.0
$H(NH_2)$	2.956	-	-0.04	26.0
H(meta)	7.900	0.93	-6.8	-2.9
H(Ortho)	4.811	2.2	-6.0	-0.7
H(para)	0.650	5.3	2.4	-8.6

line can further confirm the present position assignment of the coupling constants. The equilibrium configuration of the NH_2 group may be neither coplanar nor perpendicular to the benzene ring. The INDO calculations show that the NH_2 coupling constants correlate to the equilibrium configuration of the NH_2 groups (s) in the radical anions of aniline and p-phenylene diamine.

I. Radical Anion of Tetrasulfur Tetranitride

Sulfur-nitrogen Chemistry is an interesting topic in inorganic chemistry. The structure of the S_4N_4 molecule has been proved to be an eight membered ring with a coplanar nitrogen structure and with D_{2d} symmetry as shown in Fig. 26. S_4N_4 may be regarded to possess some aromatic character. Hence, the electronic structure of the S_4N_4 molecule can be qualitatively explained by its resonant hybrids. A cyclic delocalization model for the S_4N_4 molecule was proposed by Craig.[114,115] In this model the sulfur 3d orbitals effectively overlap with the nitrogen 2p orbitals in the pi-electron system. The Huckel MO and extended HMO calculations have been performed by Braterman[116] and Turner and Martimer[117] respectively. The calculation of the extended HMO approximation confirmed the coplanar nitrogen structure.

The pi radical anion of S_4N_4 should be fairly stable because of the moderate conjugation of its pi-electrons. The ESR spectrum of the S_4N_4 radical anion should give some insight into its electronic structure. Chapman and Massey[118] observed a nine line spectrum after the chemical reduction at room temperature. The intensity ratio for the hyperfine components is 1:4:10:16:19:16:10:4:1 and its g value is 2.006. Their observed A value for nitrogen nuclei is 3.22 gauss. Meinzer

et al.[119] obtained a nine line spectrum with different characteristics at -30°C. The g value is 2.0006 and the A value is 1.185 gauss. Based on the g value predicted from ESR theory and the observed chemistry, Meinzer, Pratt and Myers[120] identified the spectrum recorded at low temperature as the spectrum from S_4N_4 radical anion.

Since the S_4N_4 molecule has a D_{2d} symmetry, it possesses several alternative but strictly equivalent resonance structures. The fundamental resonance theory requires a molecule adopting a configuration which is intermediate between several alternative but equivalent canonical structures. However, Jahn and Teller[113] have shown that in a nonlinear molecule with degenerate wave functions there is always at least one nontotally symmetric normal coordinate that causes a splitting of the potential function such that "the potential minima are not in the symmetrical position." Although Jahn Teller distortions have been predicted for a number of conjugated systems, very little experimental evidence has been observed that clearly points to a Jahn-Teller distortion. If the energy increase in the Jahn-Teller distortion is of the same order of magnitude as the zero-point energy of a normal mode vibration, the familiar Born-Oppenheimer approximation will break down. The electronic motion may couple with the normal mode of vibration, which can distort the molecule. The relative magnitude of the zero-point energy of the lowest vibrational mode with respect to the static distortion energy determines whether a static or a dynamic process of distortion will occur.

The S_4N_4 radical anion possesses a degenerate ground electronic state in the Huckel picture, but it is not trully degenerate if the electronic repulsion is completely taken into account. As in the open shell $C_{4n}H_{4n}$ cyclic compounds[121] distortions may still occur in S_4N_4

radical anion, which has a very low lying excited electronic state instead of an orbitally degenerate ground state. These distortions are sometimes referred as pseudo Jahn-Teller effects, and the Jahn-Teller case may be regarded as a special case with the low-lying excited electronic state. Information about the Jahn-Teller distortion sometimes can be obtained from the ESR spectrum. The ESR spectrum of the S_4N_4 radical anion should give indirect evidence of the Jahn-Teller distortion. The observation of the distortion last a sufficiently long time compared with the ESR measurement time. The observed S_4N_4 radical anion spectrum (see Fig. 1), shows a uniform spin density at nitrogen nuclei but with large ESR line widths. If the static electron distortion energy of tetrasulfur tetranitride radical anion is much smaller than the zero-point energy of the lowest vibrational mode which causes the distortion, the large line width of the nitrogen hyperfine lines indicates the probability of a dynamic distortion. However, this fact is true only if the spin lattice relaxation is primarily causes by the dynamic Jahn-Teller distortion. In this case, the rapid time-dependent fluctuations of the spin density[124] average out the possible nonuniofmr spin density and broaden the hyperfine lines. The large line width may be also caused by the spin orbital interaction between the spin and the orbital motion of the unpaired electron around the ring.[126,127] If the distortion does occur from the rapid dynamic process, the observation of the distortion from the ESR spectrum of S_4N_4 radical anion requires a temperature dependence of the line widths at low temperatures.

On the other hand, it is possible that the static electronic distortion of the anion radical of S_4N_4 is lower than or just about the same order of magnitude as the lowest zero-point vibrational energy.

The distortion may exist as a static process, or a slow dynamic process compared with the time scale of the ESR measurement. In this case the possibility of the observation of the distortion depends upon the geometry of the distorted S_4N_4 radical anion. Since the S_4N_4 molecule possesses D_{2d} symmetry, the radical anion of S_4N_4 has a degenerate ground state in the first approximation. The four sulfur atoms occupy the corners of a tetrahedrom and the four nitrogen atoms are located at the corners of a square plane. In a displaced position of the antisymmetric vibration, the degeneracy of the E state is split into B_1 and B_2. This can deduced by the correlation table of the group theory. Since the undistorted S_4N_4 has two nonbonding orbitals with e symmetry, each orbital possesses a nodal plane perpendicular to the N_4 square plane. The distorted radical anion has C_{2v} symmetry. Hence, the E state goes into B_2 symmetry, the ESR spectrum should possess the characteristic of four equivalent nitrogen and four equivalent sulfur atoms. On the other hand, a B_1 distortion may give an ESR spectrum which is characteristic of two sets of two equivalent nitrogen nuclei.[122] Unfortunately, the sulfur in its natural abundance contents primarily the S-32 isotope which possesses no magnetic moment. Hence, no hyperfine splittings of sulfur are observed in the spectrum of the S_4N_4 radical anion. Since the S-33 isotope has a nuclear spin of 3/2 and only 0.7% natural abundance, the S-33 satellites in the ESR spectrum of S_4N_4 radical anion should have an intensity of 0.7% of the N-14 hyperfine components. With such a weak intensity, the S-33 signal cannot be easily detected vy ESR, especially since the coupling constant(s) of S-33 nuclei may be small compared with the N-14 hyperfine splittings. Although our present data acquisition system and the summing,

smoothing, and lest squares adjusted assignment computer programs should be ideal to apply to the extraction of the weak isotopic ESR satellites from the predominate N-14 signals. The limitation of the signal extraction is the accuracy of the field reading from our NMR field tracking unit and the dispersive components of the ESR signals. At present, the accuracy of the magnetic field measurement is limited to the order of magnitude about 10 milligauss. This tracking noise is field dependent and has the intensity of approximately 1/20 ofeach N-14 signal. This tracking noise can be averaged out by summing enough spectra. It is the dispersion signal which prohibits any successful extraction of S-33 signals from the natural abundance S-33 sample of tetrasulfur tetranitride anion radical. In order to study the S-33 ESR signals. The improvement of the sensitivity and the accuracy of the NMR tracking system should be needed: a better bridge network and sample cavity lock-in scheme are also recommended to suppress any residual dispersive components of the ESR signals. In the present set-up, an enriched S-33 sample of tetrasulfur tetranitride with the abundance of 15% or greater is needed to be able to detect the hyperfine splittings of the sulfur-33 nuclei.

According to Jahn-Teller theorem, the S_4N_4 radical anion should be distorted intothe form with either B_1 or B_2 symmetry. However, no calculation of the zero point energies of the distortions has been made; and the static electronic stabilization energy has not been reported. Nevertheless, an order of magnitude estimation can be quite useful to determine the possibility of the observation of the Jahn-Teller distortion. It is assumed that the S_4N_4 anion radical is similar to the eight-membered ring compound of cyclooctatetraene anion radical. Hence,

the B_1 distortion should have a zero point energy around 650 cm^{-1}. This estimation rules out the possibility of the static distortion of the Jahn-Teller effect. Synder uses a bond orderbond length curve to calculate the stable equilibrium configuration. The calculation requires the bond lengths for the symmetric configuration. During each calculation a new set of atomic orbital coefficients and bond orders are obtained by solving the secular requations with knowledge of the resonance integrals. The bond lengths are then estimated from the Morse curve function and a new cycle of calculation starts. The cycles continued until self-consistency is attained in the bond lengths, or until the total energy reaches its minimum. In the calculation of C_8H_8-, the total energy for pi-electrons is -4.5 kcal/mole and the total sigma electron energy is 2.69 kcal/mole, if the angular strain is neglected during the calculation the energy difference for the distorted and undistorted configuration is -7.2 kcal/mole C_8H_8 anion radical. However, the stabilization energy is decreased to -1 kcal/mole, if the electronic repulsion is taken into consideration during the calculation.

If the tetrasulfur tetranitride radical anion has a stabilization energy close to -1 kcal/mole, the observation of the distortion by ESR techniques should be likely only at liquid nitrogen or liquid helium temperature. Additional complications exist in the S_4N_4 system, because the d orbitals in the sulfur atoms have the greater tendencies to overlap with one another across the ring that the p_z orbitals in C_8H_8 system. If the stabilization energy of the S_4N_4 radical anion does not change considerably with the consideration of the d orbital overlapping, the polycrystalline spectra may give some information about the distortion

only from the g value. Single crystal work is necessary for the analyzing a resolvable hyperfine structure. However, the experimental work is difficult because it involves the doping of the radical anion of enriched S-33 S_4N_4 into the hosts. The instability of the S_4N_4 radical anion prohibits any such attempts. A new method in generating the anion radical of S_4N_4 in the single crystal is needed in order to solve the interesting Jahn-Teller distortion problem in this system.

APPENDIX

MOLECULAR ORBITAL CALCULATION BY THE INDO APPROXIMATION

The INDO computer program was written by P.A. Dobosh and it was obtained from the Quantum Chemistry Program Exchange at the Indiana University. The program can perform wither the Intermediate Neglect of Differential Overlap calculations or the Complete Negelect of Differential Overlap MO calculation. There are two versions of the program available in the Quantum Chemistry Program Exchange. One version is written in FORTRAN 63 language and designed for the use on a CDC 1604 digital computer; the other version is written in FORTRAN IV language and designed for the use on an IDM 360 computer.

The FORTRAN 63 version of the program consists pf several overlays and segments. Each segment of the program is loaded and linked as a unit; a group of subprogram may be delinked and removed as a unit later, upon request. The program generates overlays out to a specific file in absolute format and loads these overlays by a smaller but faster version of the loader. The purpose of segmentation of the program is to use much smaller field length during compilation and execution by allowing the programer to add programs as they are required and to eliminate those no longer required during the execution of the job. The loader provides the facility of subdividing a large task into portions called overlays, and writing them out in absolute form. These overlays can then be loaded at execution time without a relocatable loading operation. In the IBM 360/65 version, no overlay or segmentation structure is used. But most of the floating point variable are assigned as double precision variables.

The problem with applying the INDO method of 1,3,5-cyclooctatriene s mainly the evaluation of accurate input parameters for a nonplanar ring system. There are many constraints to the geometrical parameters. Several sets of bond distances and bond angles were assumed and great difficulties arose when the final input parameters were evaluated. Table A lists our final input parameters for our best nonplanar model; Table B lists similar input parameters; and the results indicates how sensitive the coupling constants are towards the slight variation in geometry of the radical according to the INDO calculations. Table C lists the input parameters for our planar model.

Since the CDC 6600 computers used a the Lawrence Radiation Laboratory have 60 bits perword and a large memory of 340k octal locations available to the users, a simpler version of the program has been used. The version for CDC 6600 computer was converted from the FORTRAN 63 version, and has been extensively tested by using the available test ouput supplied by QCPE. The multiplet annihilation subprogram, which is not included in the IBM 360 FORTRAN IV version, is included in the CDC version as an option; it is called the Density subroutine as in FORTEAN 63 version.

Most of our INDO calculations were based on Pople's crude scheme of evaluating the geometrical model 'B', in which the interatomic distance chosen depends entirely upon the two kinds of atoms involved. This crude model works suprisingly well for the aromatic planar radicals. Nevertheless, Pople et al. reported that a number of exceptions to this standard model were necessary in evaluating the coordinates from the bond lengths and bond angles

TABLE A. Input Parameters for the Coordinates for Nonplanar Model of 1,3,5-Cyclooctatriene[a]

C(1)	0.70000	-1.41945	0.0
C(2)	-0.70000	-1.41945	0.0
C(3)	-1.37222	-0.70972	1.00
C(4)	-1.37222	0.70972	1.00
C(5)	-0.700	1.41945	0.0
C(6)	0.700	1.41945	0.0
C(7)	1.59445	0.71945	0.91389
C(8)	1.59445	-0.71945	0.91389
H(1)	1.20945	-1.83167	-0.8594
H(2)	-1.20945	-1.83167	-0.8594
H(3)	-1.7805	-1.20556	1.86917
H(4)	-1.7805	1.20556	1.86917
H(5)	-1.20945	1.83167	-0.8594
H(6)	1.20945	1.83167	1.93472
H(7)	1.26389	0.83611	1.93472
H(7)	2.56667	1.05	0.58333
H(8)	1.26389	-0.83611	1.93472
H(8)	2.56667	-1.05	0.58333

a) Calculated coupling constants are listed in column b of Table I.

TABLE B

Input parameters for the coordinates of 1,3,5-cyclooctatriene

C(1)	0.70	-1.40	0.0
C(2)	-0.70	-1.40	0.0
C(3)	-1.30	0.70	0.50
C(4)	-1.30	-0.70	0.50
C(5)	0.70	1.40	0.0
C(6)	-0.70	1.40	0.0
C(7)	1.30	-0.70	0.5
C(8)	1.30	0.70	0.50
H(1)	1.24	-2.34	0.0
H(2)	-1.24	-2.34	0.0
H(3)	-1.85	0.87	0.40
H(4)	-1.85	-0.87	0.40
H(5)	1.24	2.34	0.0
H(6)	1.24	2.34	0.0
H(7)	0.70	-0.90	0.90
H(7)	1.70	-0.90	1.40
H(8)	0.70	0.90	0.90
H(8)	1.70	0.90	1.40

Calculated Hyperfine Coupling constants in Gauss

H(1)	37.6
H(2)	8.60
H(3)	1.49
H(7)	63.6
H(7)	10.0

TABLE C. Input parameters for the coordinates for the planar model of 1,3,5-Cyclooctatriene[a]

Atoms	X	Y	Z
C(1)	0.70	-1.91	0.0
C(2)	-0.70	-1.91	0.0
C(3)	-1.91	-0.70	0.0
C(4)	-1.91	0.70	0.0
C(5)	0.70	1.91	0.0
C(6)	-0.70	1.91	0.0
C(7)	1.91	0.70	0.0
C(8)	1.91	-0.70	0.0
H(1)	1.24	-2.84	0.0
H(2)	-1.24	-2.84	0.0
H(3)	-2.45	-1.63	0.0
H(4)	-2.45	-1.63	0.0
H(5)	1.24	2.84	0.0
H(6)	-1.24	2.84	0.0
H(7)	2.10	1.10	0.80
H(7)	2.10	1.10	-0.80
H(8)	2.10	-1.10	0.80
H(8)	2.10	-1.10	-0.80

a) Calculated coupling constants are listed in Column C of Table I.

ACKNOWLEDGEMENTS

I wish to express my gratitude to Professor Rollie Myers for his constant encouragement and suggestions during the course of this research. Many thanks to my colleagues: Mr. Jim Chang for his valuable assistance in instrumentation and data handling techniques; Mr. Akira Jindo for his discussion in Jahn-Teller distortion problem; Dr. Alfred Bauder for his summing and least squares curve fitting computer programs; Dr. Dick Meinzer and Mr. Mike Coggiolla for their construction of the NMR field tracking units; and Miss Joyce Tevebaugh for her special assistance in editing the manuscript.

I would like to express my appreciation to my wife for her assistance in preparing the manuscript. I also gratefully acknowledge the Science Fellowship awarded by the University of California in 1967.

Finally, I would like to thank Jane Ball for her efficient work in typing this thesis.

This work was conducted under the auspices of the United States Atomic Energy Commission.

REFERENCES

1. B. Bleaney and K. W. H. Stevens, Report Prog. Phys. 16 108 (1953).
W. A. Nierenberg, Ann. Rev. Nucl. Sci. 7 349 (1957).
2. E. Fermi, Z. Phisik 60 320 (1930).
3. F. J. Milford, Am. J. Phys. 28, 521 (1960).
4. H. Bethe and E. E. Salpeter, Quantum Mechanics of One and Two Electrons System
5. R. A. Farrell, Am. J. Phys. 28, 484 (1960).
6. R. Fessenden and R. H. Schuler, J. Chem. Phys. 39, 2147 (1963).
7. F. J. Adrian, F. L. Cochran and V. A. Bowers, J. Chem. Phys. 36, 1661 (1962).
E. L. Cochran, F. J. Adrian and V. A. Bowers, ibid. 40, 213 (1964) ibid. 43, 462 (1965), ibid. 44 4626 (1966).
8. K. D. J. Root, M.C. R. Symons and B. C. Weatherley, Mol. Phys. 11, 161 (1966).
K. D. J. Root, M. C. R. Symons and D. J. A. Tinling, J. Chem. Phys. (1967).
J. R. Morton, Cand. J. Chem. 43, 1948 (1965).
9. J. E. Bennett, B Mile, and A. Thomas, Proc. R. Soc. A293, 246 (1966).
10. B. C. Gilbert and R.O. C. Morman, J. Chem. Soc. B, 86 (1966), ibid. B, 422 (1966).
11. M. McMillan and W. A. Waters, J. A. C. S. 90 , 7155 (1968).
12. D. J. Krusic, and J. K. Kochi, J. A. C. S. 91, 3940 (1969).
13. F. J. Adrian and M. Karpulus, J. Chem. Phys. 41, 56 (1964).
14. G. A. Peterson and A. D. McLachlan, J. Chem. Phys. 45 628 (1966).

15. W. T. Dixon, Mol. Phys. 9, 201 (1965).

16. R. Hoffmann, J. Chem. Phys. 39, 1397 (1963).

17. N. M. Atherton and A. Hichliffe, Mol. Phys. 12, 349 (1967).

18. H. M. McConnell, J. Chem. Phys. 24, 633 764 (1956).

H. M. McConnell and H. H. Dearman ibid 28, 51 (1958).

H. M. McConnell and B. D. Chesnut, ibid. 28, 107 (1958).

19. R. Bersohn, J. Chem. Phys. 1066, 24, (1956).

20. S. I. Weissman, J. Chem. Phys. 25, 890 (1956).

D. B. Chesnut, J. Chem. Phys. 29, 43 (1958).

21. H. S. Jarrett, J. Chem. Phys. 26, 1289 (1957).

22. J. R. Bolton and G. K. Fraenkel, J. Chem. Phys. 40, 3307 (1964).

23. T. H. Brown and M. Karplus, J. Chem. Phys. 46, 870 (1967).

24. J. P. Colpa and J. R. Bolton Mo. Phys. 273, 6 (1963).

25. J. E. Bloor and B. E. Gilson, J. Phys. Chem. 71, 3100 (1967).

26. G. Giacometti, P. L. Nordio and M. V. Pavan, Theor. Chim. Acta. 1, 404.

27. R. E. Moss and G. K. Fraenkel, J. Chem. Phys. 252, 50, (1969).

28. J. R. Bolton, J. Chem. Phys. 43, 309 (1965).

29. J. E. Bloor, B. R. Gilson and P. N. Daykin, J. Phys. Chem. 70, 1457 (1966).

30. K. G. Kay, and H. J. Silverstone, J. Chem. Phys. 46. 2854 (1967).

31. J. R. Bolton, J. Phys. Chem., 71, 3702 (1967), 3099 71, (1967).

32. I C. Lewis and L. S. Singer, J. Chem. Phys. 43. 2712 (1965).

33. L. S. Synder and T. Amos, J. Chem. Phys. 42, 3670 (1965).

34. M. Karpulus, and G. K. Fraenkel, J. Chem. Phys. 35, 1312 (1961),

G. K. Fraenkel, Pure and Applied Chem., 143, (1962).

35. C. L. Talcott, PhD Thesis University of Cal., Berkeley, UCRL-17743 (1967).

36. R. G. Lawler, J. R. Bolton, G. K. Fraenkel and T. H. Brown, JACS 86, 520 (1964).

37. M. T. Jones, A Cairnvross and D. W. Wiley, J. Chem. Phys. 43, 3403 (1965).

38. M. R. Das and G. K. Fraenkel, J. Chem. Phys. 42, 792 (1965).

39. A. Carrington, H. C. Longuett Higgins, R. E. Moss and P. F. Todd Mol. Phys. 9, 187 (1965).

40. M. Karplus, R. G. Lawler and G. K. Fraenkel, J. A. C.S. 87, 5260 (1965).

41. M. Rossi, P. L. Nordio and G. Giacometti, Theor. Chim. Acta. 10, 263 (1968).

42. M. C. R. Symons, Tetrahedron 18, 333 (1962).

43. A. S. McLachlan, Mol. Phys. 233 (1959).

44. A. Aono and J. Higuchi, Prog. Thero. Phys. 589, 28, (1962).

45. J. R. Bolton, A. D. McLachlan and A. Carrington, Mol. Phys. 5, 31 (1962).

46. J. P. Colpa and E. De Boer, Mol. Phys. 333 (1964).

47. D. H. Levy, Mol. Phys. 10, 233 (1966).

48. P. Nordio, M. V. Pavan and G. Giacometti, Theor. Chim. Acta, 1, 302 (1963).

49. R. S. Mulliken, C. A. Rieke and W. Brown, J.A.C.S. 63. 41 (1941).

50. C. A. Coulson and V. A. Crawford, J.A.C.S. 2052 (1953).

51. D. H. Levy, and R. J. Myers, J. Chem. Phys. 43. 3063 (1965).

52. C. Heller and H. M. McConnell, J. Chem. Phys. 32, 1535 (1965).

53. J. R. Morton and A. Horasfield, J. Chem. Phys. 35, 1142 (1961).

54. D. Pooley and D. H. Whiffen, Mol. Phys. 81 (1962).

55. A. Horsfield, J. E. Morton and D. H. Whiffen, 5, 425 Mol. Phys. (1962).

56. ibid. 5, 115, (1962).

57. C. Heller, J. Chem. Phys. 175 36 (1962).

58. D. H. Geske, Progress in Phys. Org. Chem., 4, 125 Interscience (1967).

59. V. A. Crawford, Quart. Rev. 3, 226 (1949).

60. Hyperconjugation Conference, Tetrahedron 5, 105-274.

61. Hyperconjugation, J. W. Baker, Clarendom Press, Oxford (1952).

62. Hyperconjugation, M.J. S. Dewar, Ronald Press Co. , New York (1962).

63. R. S. Mulliken, J. C. P. 7, 339 (1939).

64. C. A. Coulson, Quart. Rev. 1, 144 (1947).

65. M. Gloppert-Mayer and A. L. Sklar, J. Chem. Phys. 6, 645 (1938).

66. E. Huckel, Z. Physik 70, 204 (1931), ibid. 76, 628 (1932).

67. A. Streitweisser, Molecular Orbital Theory for Organic Chemists (1962).

68. R. Daudel, R. Levebvre and C. Moser, Quantum Chemistry (1959).

69. M. Goeppert-Mayer and A. L. Sklar, J. Chem. Phys. 6, 645 (1938).

70. C. C. Roothaan, Revs. Modern Phys. 23, 69 (1951).

71. R. Fariser and R. G. Parr, J. Chem. Phys. 21, 466 (1953), ibid. 21, 767 (1953).

72. J. A. Pople, Trans. Faraday Soc. 49, 1375 (1953).

73. J. E. Lennard-Jones, Proc. Roy. Soc. A198, 14 (1949).

74. R. McWeeny, ibid. A241, 239 (1957).

75. C. C. Roothaan, Rev. Modern Phys. 32, 179 (1960).

76. R. E. Watson and A. J. Freeman, Phys. Rev. 120, 1125 (1960).

77. A. D. McLachlan, Mol. Phys. 3, 233 (1960).

78. A. T. Amos and G. G. Hall, Proc. Roy. Soc. A263, 483 (1961).

79. L. C. Synder and A. T. Amos, J. A. C. S. 86, 1647 (1964).

80. H. H. Jaffe, Acc. of Chem. Research 2, 136 (1968).

81. J. A. Pople, D. P. Santry and G. A. Segal, J. Chem. Phys. 43, S129 (1965), ibid. 43, S136 (1965).

82. J. A. Pople and G. A. Segal, J. Chem. Phys. 44, 3289 (1966).

83. J.A. Pople, D. L. Beveridge and N. S. Ostlund, International J. of Quantum Chem. 1, 293 (1967).

84. R. N. Dixon, Mol. Phys. 12, 83 (1967).

85. J. A. Pople, D. C.Beveridge and P. A. Dobosh, J. Chem. Phys. 47 2026 (1967).

86. J. A. Pople, D. L. Beveridge and P. A. Dobosh, J. A. C. S. 90, 4201 (1968).

87. P. A. Dobosh, Quantum Chem. Program Exchange No. 141 and No. 142.

88. H. Smith, Chemistry in Anhydrous Liquid Ammonia, Vol. I, Part 2. Organic Reactions in Liquid Ammonia (1963), also Part 1, Inorganic and General Chemistry in Liquid Ammonia (1966). Edited by G. Jander, H. Spandau and C. C. Addison (in German), C. H. Hutchison and R. C. Pastor, J. Chem. Phys. 21, 1959 (1953), R. Catterall and M. C. R. Symons, p. 277-285 in "Solutions Metal-Ammoniac, Properties Physicochimiques," (1964).

89. G. Fraenkel, S. H. Ellis and D. T. Dix, J. A. C. S. 87, 1406 (1965). E. Franta, J. Chaudhuri, A. Cserhegyi, J. Jagur-Grodzinski and M. Szwrc, J. A. C.S. 89, 7129 (1967).

90. A. H. Maki and D. H. Geske, Anal. Chem. 31, 1450 (1959); J. Chem. Phys. 30, 1356 (1959); J. A. C.S. 83, 1852 (1961).

91. D. H. Levy and R. J. Myers, J. Chem. Phys. 41, 1062 (1964).

92. D. H. Levy, Ph.D. Thesis, University of California (1965).

93. C. L. Talcott, Ph.D. Thesis, University of California (1967).

94. A. Bauder and R. J. Myers, U.C. Radiation Lab. Report (1967) UCRL-17829.

95. A. Carrington and J. Dos Santos-Veoga, Mol. Phys. 5, 21 (1962).

96. J. C. M. Henning, J. Chem. Phys. 35, 2258 (1961).

97. E. W. Stone and A. H. Maki, J. Chem. Phys. 39, 1635 (1963).

98. H. L. Strauss and G. Fraenkel, J. Chem. Phys. 35, 1738 (1961).

99. C. P. Poole, Electron Spin Resonance, Interscience (1967).

100. W. O. Jones, J. Chem. Soc., 1808 (1954). W. Sanne and O. Schlichting, Angew. Chem. 75, 156 (1963) L. E. Craig, Chem. Rev., 49, 120 (1951).

101. A. C. Cope, C. L. Stevens and F. A. Hochstein, J. A. C. S. 72, 2510 (1950).

102. L. E. Craig, R. M. Elofson and I. J. Ressa, J. A. C. S. 75, 480 (1953).

103. E. Vogel, Angew. Chem. 74, 836 (1962).

104. W. R. Roth and B. Peltzer, Liebigs Ann. Chem. 685, 56(1965).

105. A. C. Cope, A. C. Haven, F. L. Ramp and E. R. Trumbull, J. A. C. S. 74, 4867 (1952).

106. D. S. Glass, J. W. H. Wattey and S. Winstein, Tetrahedron (L) 377 (1965).

107. J. Zirner and S. Weinstein, J. Chem. Soc. Proc., 235 (1964).

108. D. S. Glass, J. Zirner and S. Winstein, J. Chem. Soc. Proc., 276 (1963).

109. A. P. Ter Borg, H. Kloosterziel, and N. Van Meurs, J. Chem. Soc. Proc., 359, (1963).

110. H. Kloosterziel and A. P. Ter Borg, Recueil 84, 1305 (1965).

111. Von W. R. Roth, Ann. Chem. 671, 25 (1964).

112. F. Smenthowski, R. Owens, and B. Daubion, J.A.C.S., 82, 1537 (1968).

113. T. J. Katz and C. Talcott, J.A.C.S. 88, 4732, (1966).

114. D. P. Craig, J.A.C.S. 997 (1959).

115. ibid, 1376 (1962).

116. Braterman, J. A. C. S., 2297 (1965).

117. Mortimer, Inorg. Chem. 5, 906 (1966).

118. Chapman and Massey Trans. Farad. Soc. 58, 1679 (1962).

119. Meinzer, Pratt, Myers, Submitted to J.A.C.S., UCRL-19007 (1969).

120. D. W. Pratt, Ph.D. Thesis University of California, UCRL-17406, (1967).

121. Salem, Molecular Orbital Theory, Chapter 8.

122. G. Herzberg, Electronic Spectra of Polyatomic Molecules, Chapt. 1, Section 2.

123. H. A. Jahn and E. Teller, Proc. Roy. Soc. (London) A161 (1937).

124. O. P. Craig, Theoretical Organic Chemistry, (Keckule Symposium) p. 20 1960 Butterworth, London.

125. H. M. McConnell and A. D. McLachlan, J. Chem. Phys. 34, 1 (1961).

126. H. M. McConnell, J. Chem. Phys. 34, 13 (1961).

127. S. Basa, J. Chem. Phys. 41. 1453 (1964).

128. D. H. Levy and R. J. Myers, J. Chem. Phys. 43, 3063 (1965).

129. J. R. Morton, J. Chem. Phys. 41, 2956 (1964).

FIGURE CAPTIONS

Fig. 1. ESR spectrum of S_4N_4 radical anion.

Fig. 2. Block diagram of ESR spectrometer.

Fig. 3. ESR spectrum of the radical anion of 1,3,5-cyclooctatriene.

Fig. 4. ESR spectra of the radical anions of di-deutero-1,3,5-cyclooctatriene.

Fig. 5. Dihedral angles between the P_z orbital of C_1 with the CH Bonds of CH_2 Group in 1,3,5-cyclooctatriene radical anion.

Fig. 6. ESR spectrum of the radical anion of cyclooctatetraene in tetrahydrofuran.

Fig. 7. ESR spectrum of the radical anion of cyclooctatetraene in liquid ammonia.

Fig. 8. ESR spectrum of the radical anion of p-cyan-pyridine-N-oxide.

Fig. 9. ESR spectrum of pyrazine radical anion in liquid ammonia.

Fig.10. ESR spectrum of pyrazine radical anion in DMSO.

Fig.11. ESR spectrum of 4,5-methylene phenanthrene radical anion.

Fig.12. Simulated spectrum of 4,5-methylene phenanthrene radical anion.

Fig.13. ESR spectrum of 1,4-phenylene diamine radical anion.

Fig.14. Simulated spectrum of 1,4-phenylene diamine radical anion.

Fig.15. Simulated spectrum of the radical anion of 1,4-phenylene diamine with variable line widths.

Fig.16. ESR spectrum of aniline radical anion.

Fig.17. Geometrical and stereo isomers of 7,8-dideutero- 1,3,5-cyclooctatriene.

Fig.18. Notations and formulae of some molecules.

Fig.19. Simulated spectrum of aniline radical anion.

Fig.20. Geometrical model of S_4N_4.

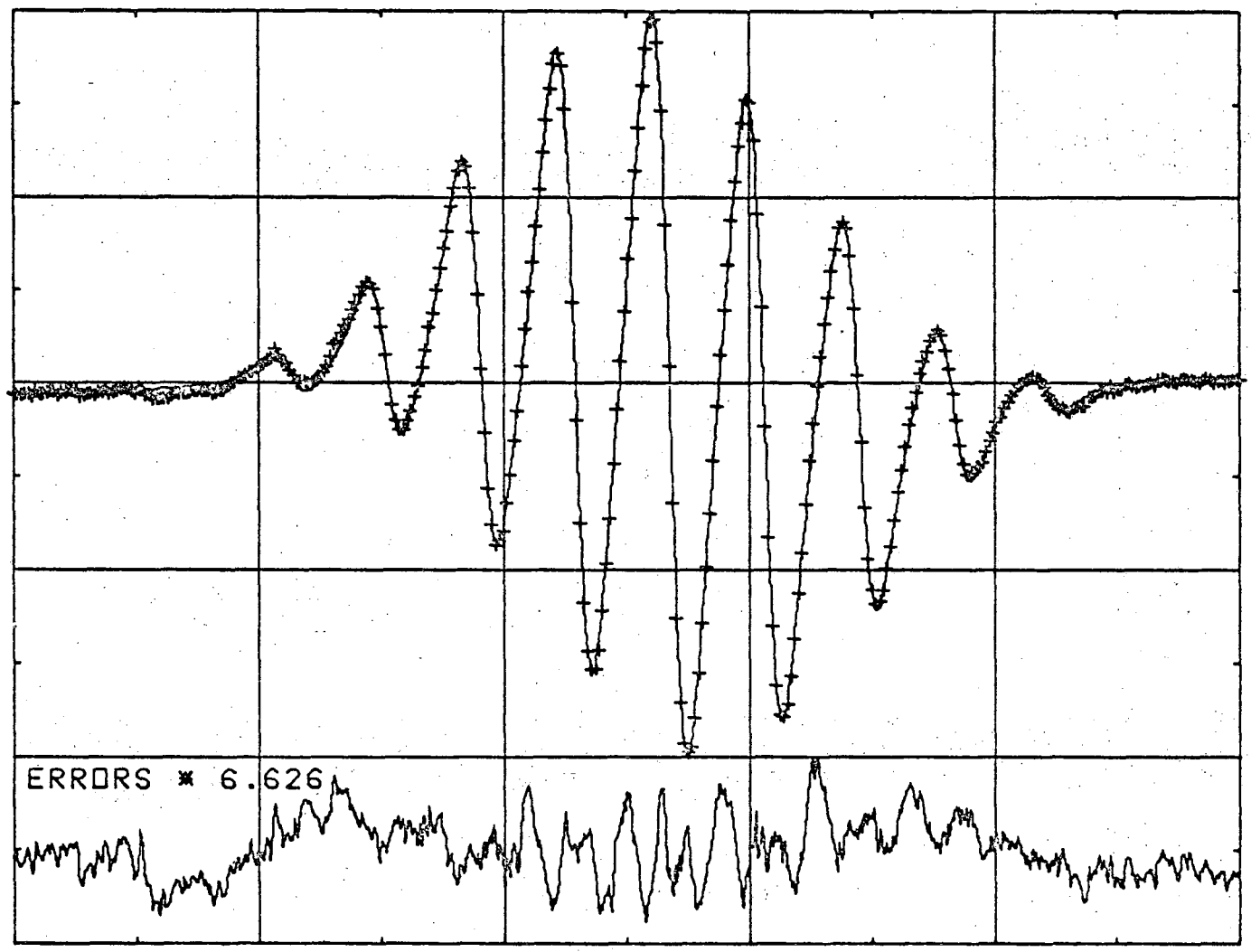

FIGURE 1 S4N4 RADICAL ANION

XBL 6912-6754

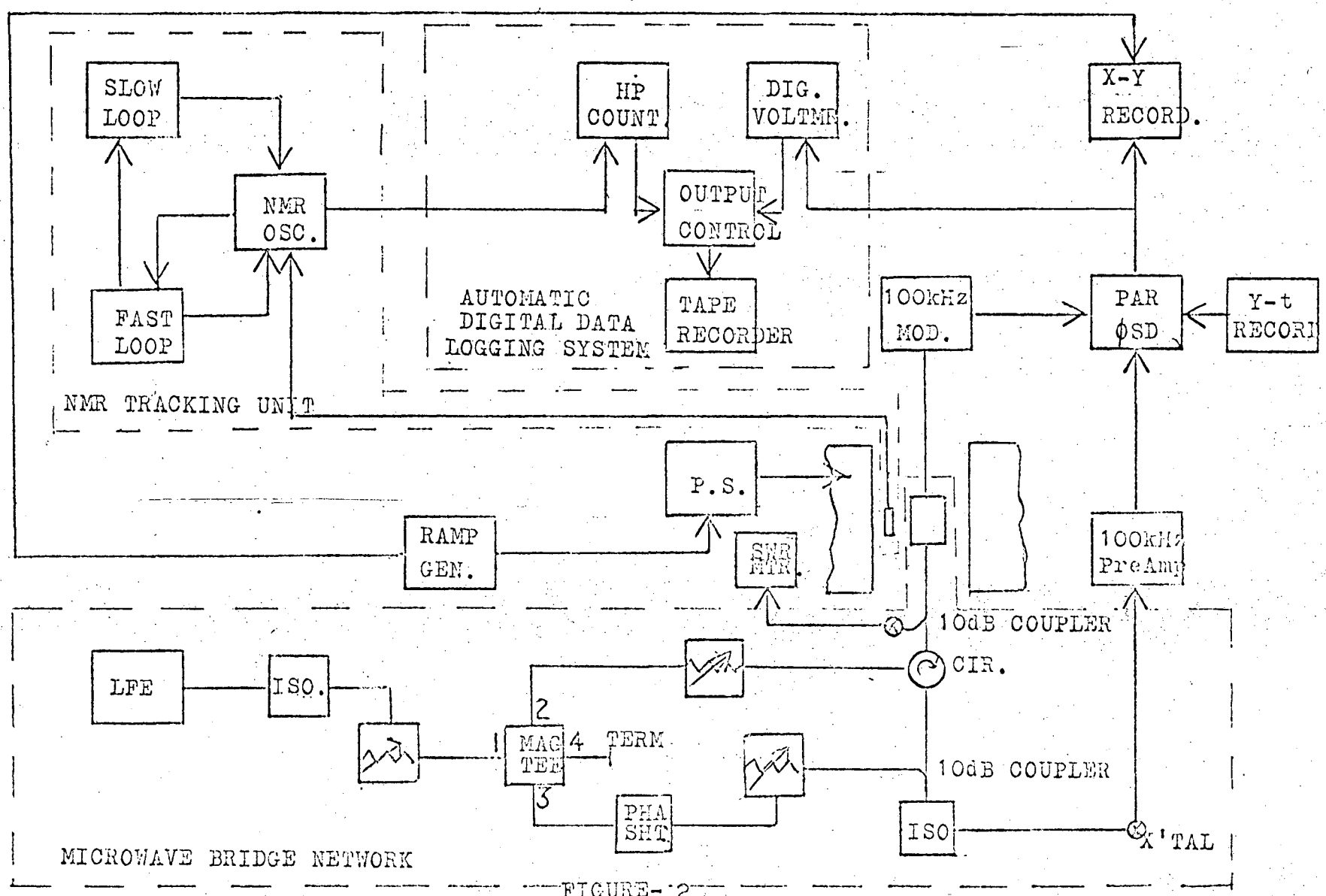

FIGURE- 2
Block Diagram of ESR Spectrometer

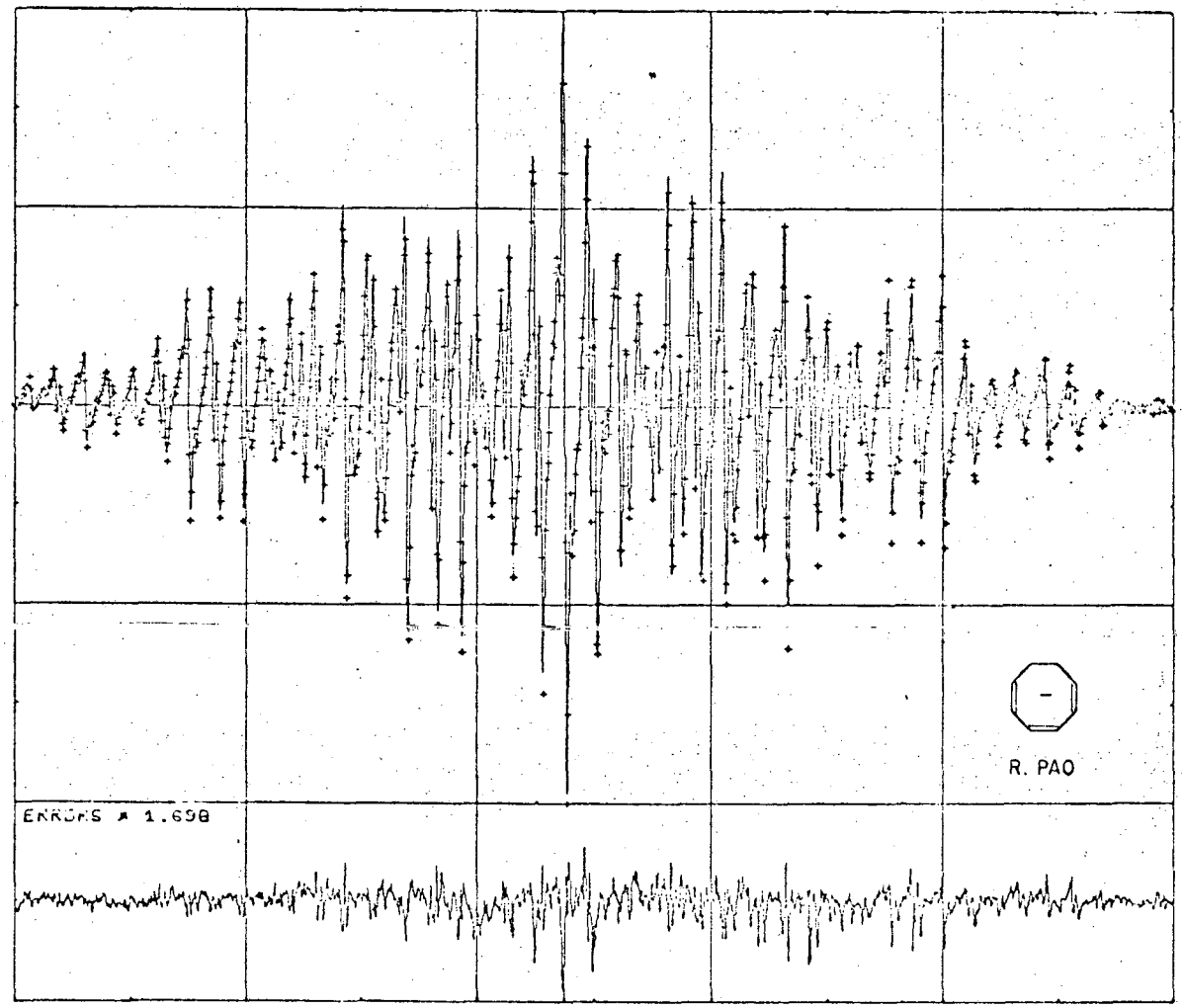

Figure-3 1,3,5-Cyclooctatriene

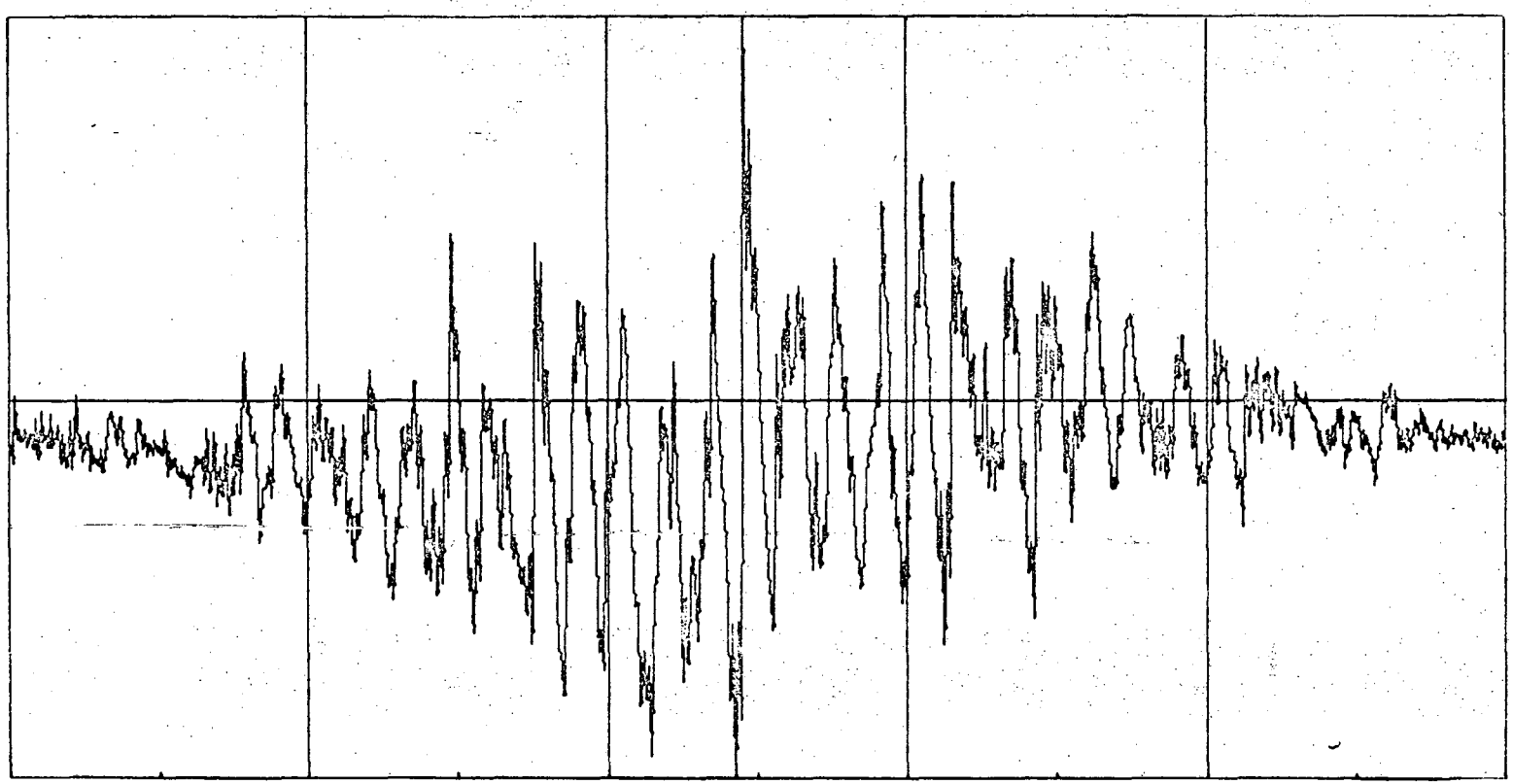

Figure-4 ESR Spectrua of the Radical Anions of di-deutero-1,3,5-cyclo-octatrienes.

XBL 6912-6755

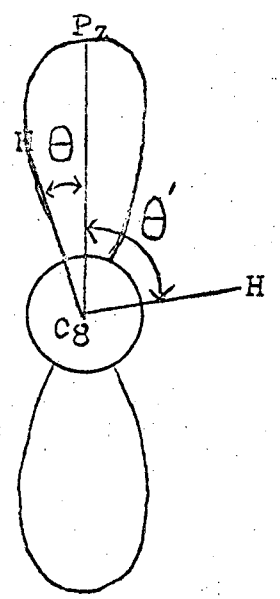

Figure-5 Dihedral Angles between P_z Orbital of C_1 with the CH Bonds of CH_2 Group in 1,3,5-Cyclooctatriene Radical Anion

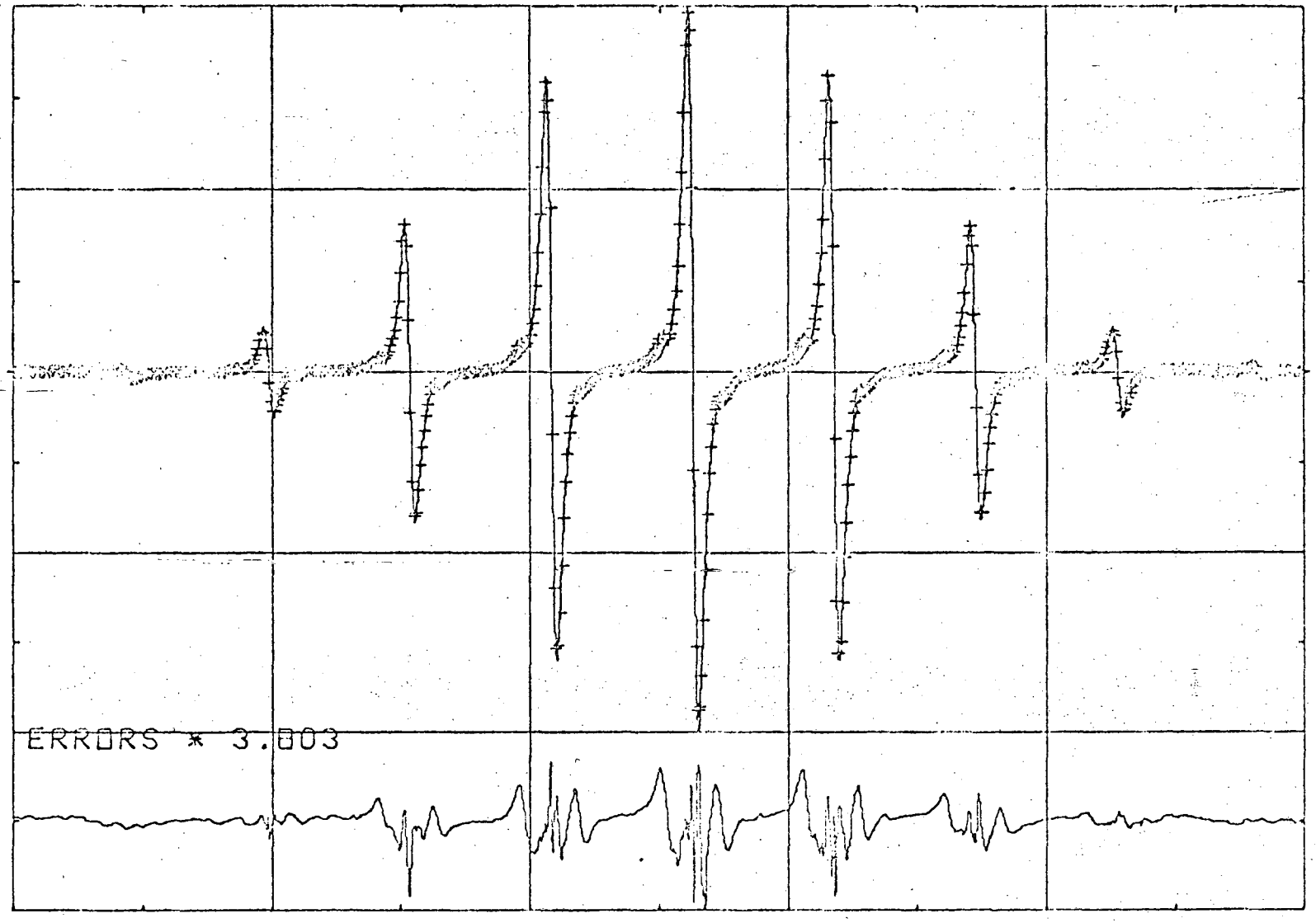

Fig.- 6 Radical Anion of Cyclooctatetraene in Tetrahydrofuran

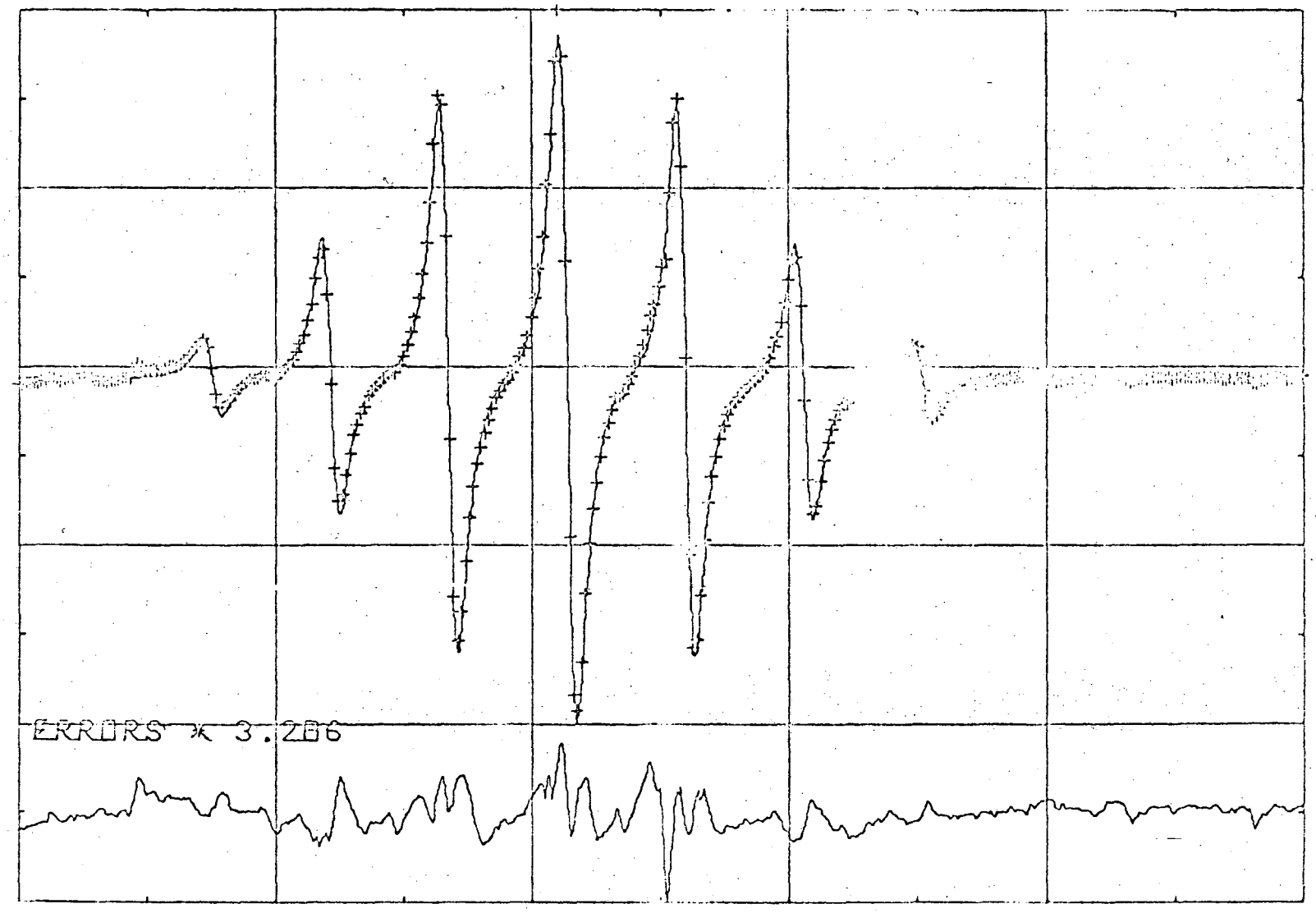

Fig.-7 Radical Anion of Cyclooctatetraene in Liquid Ammonia

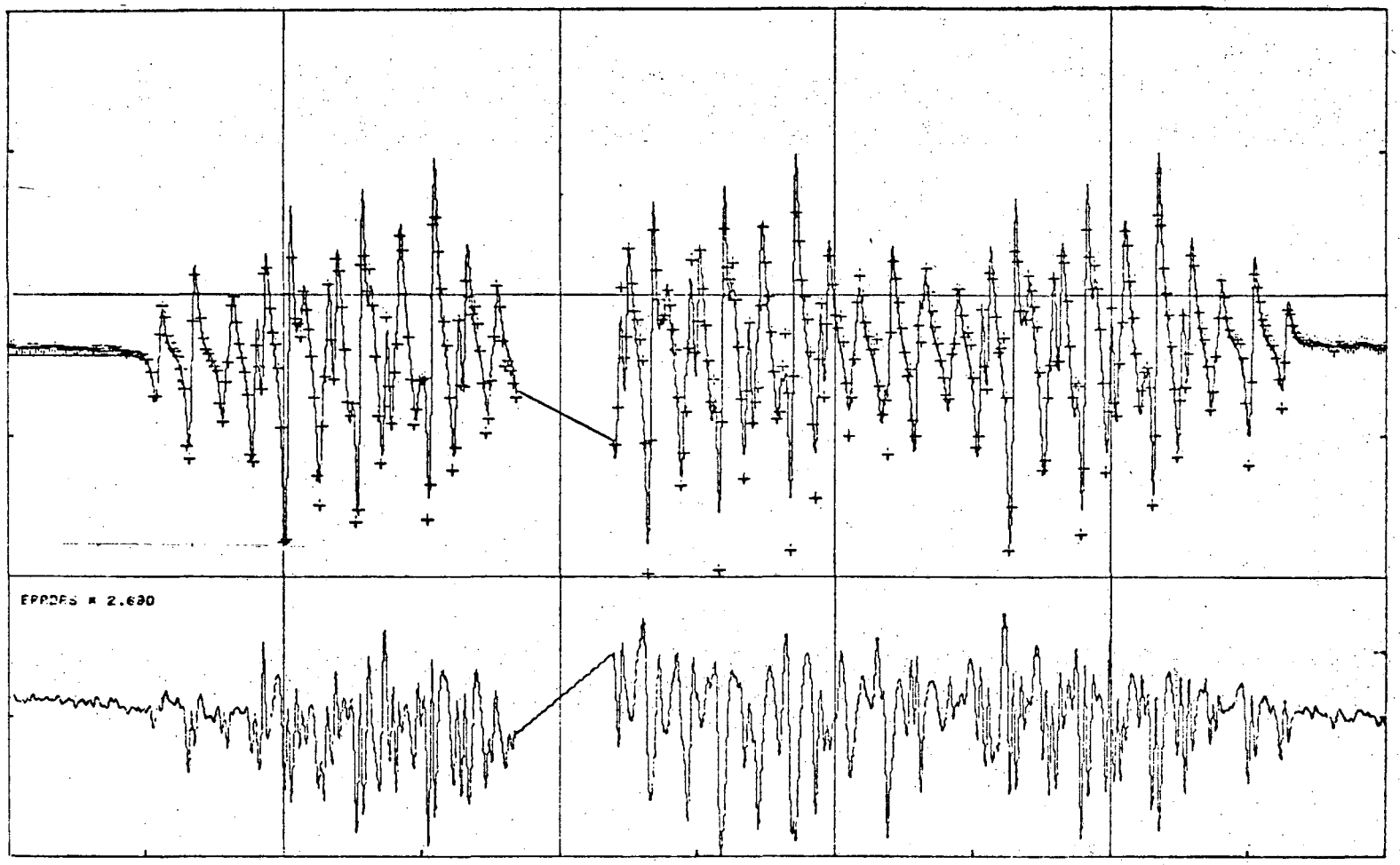

Fidure-8 ESR Spectrum of the Radical Anion of p-cyano-pyridine-N-oxide XBL 6912-6753

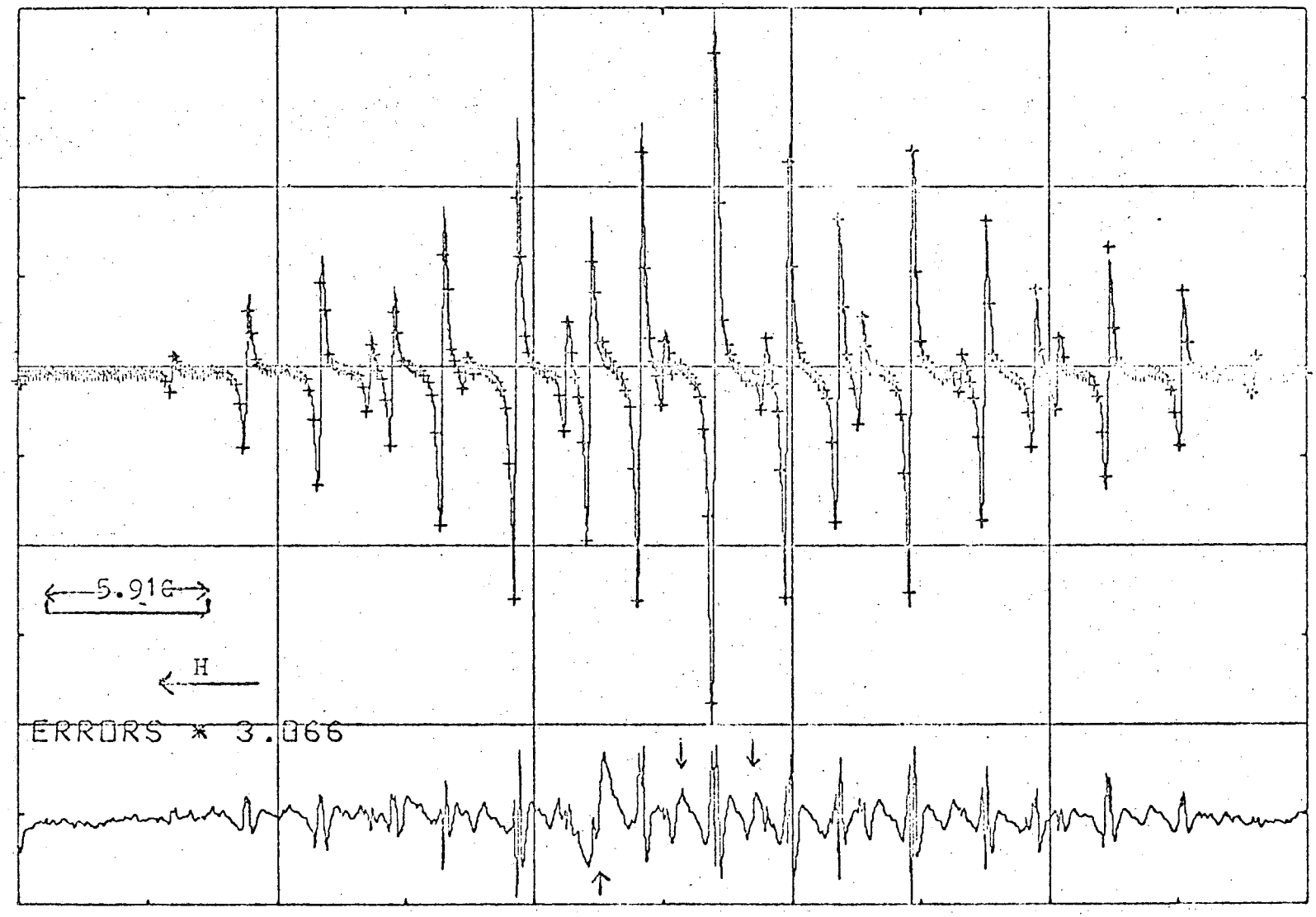

Fig.-9 Pyrazine Radical Anion in Liquid Ammonia

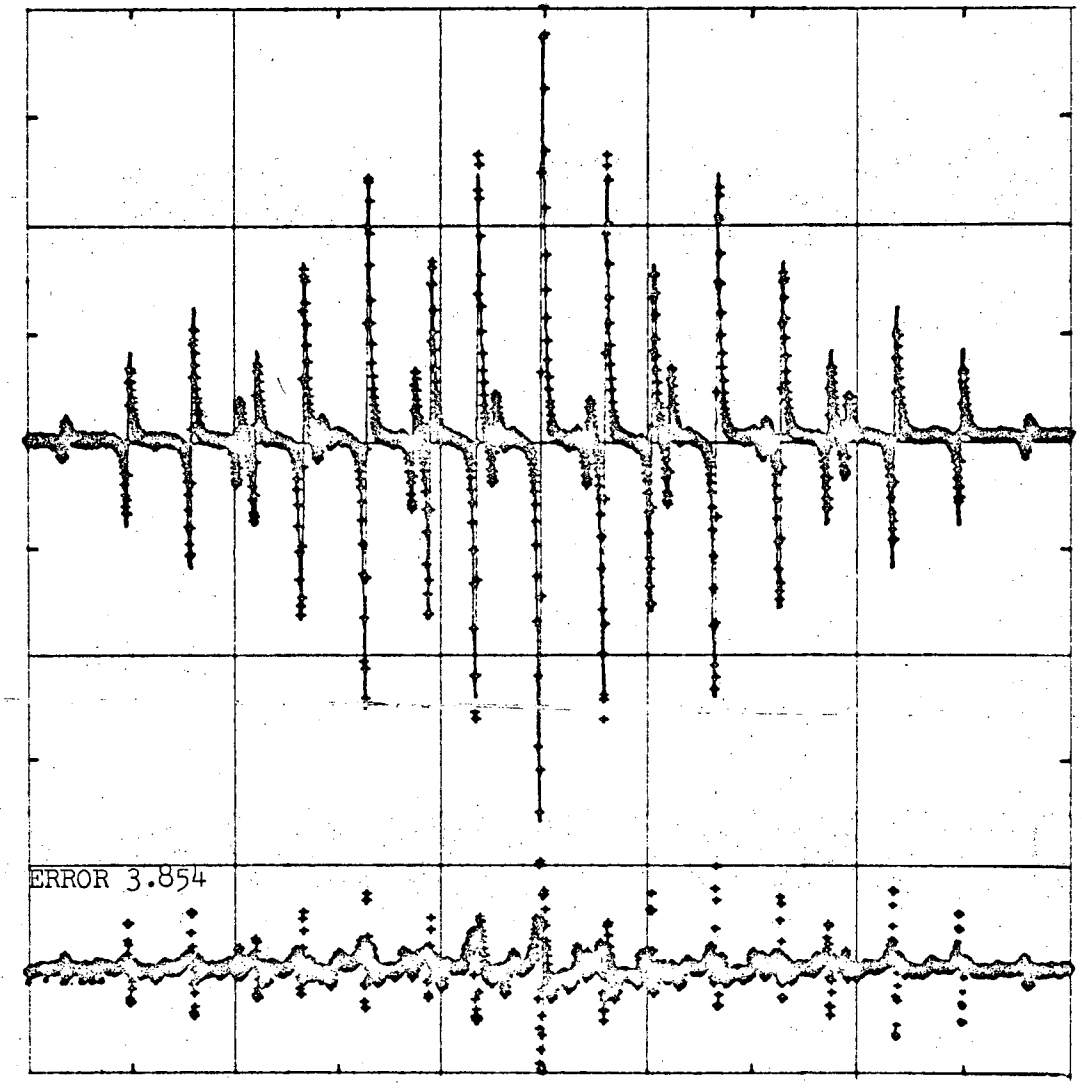

Figure-10 ESR Spectrum of pyrazine Radical Anion in DMSO

XBL 6912-6756

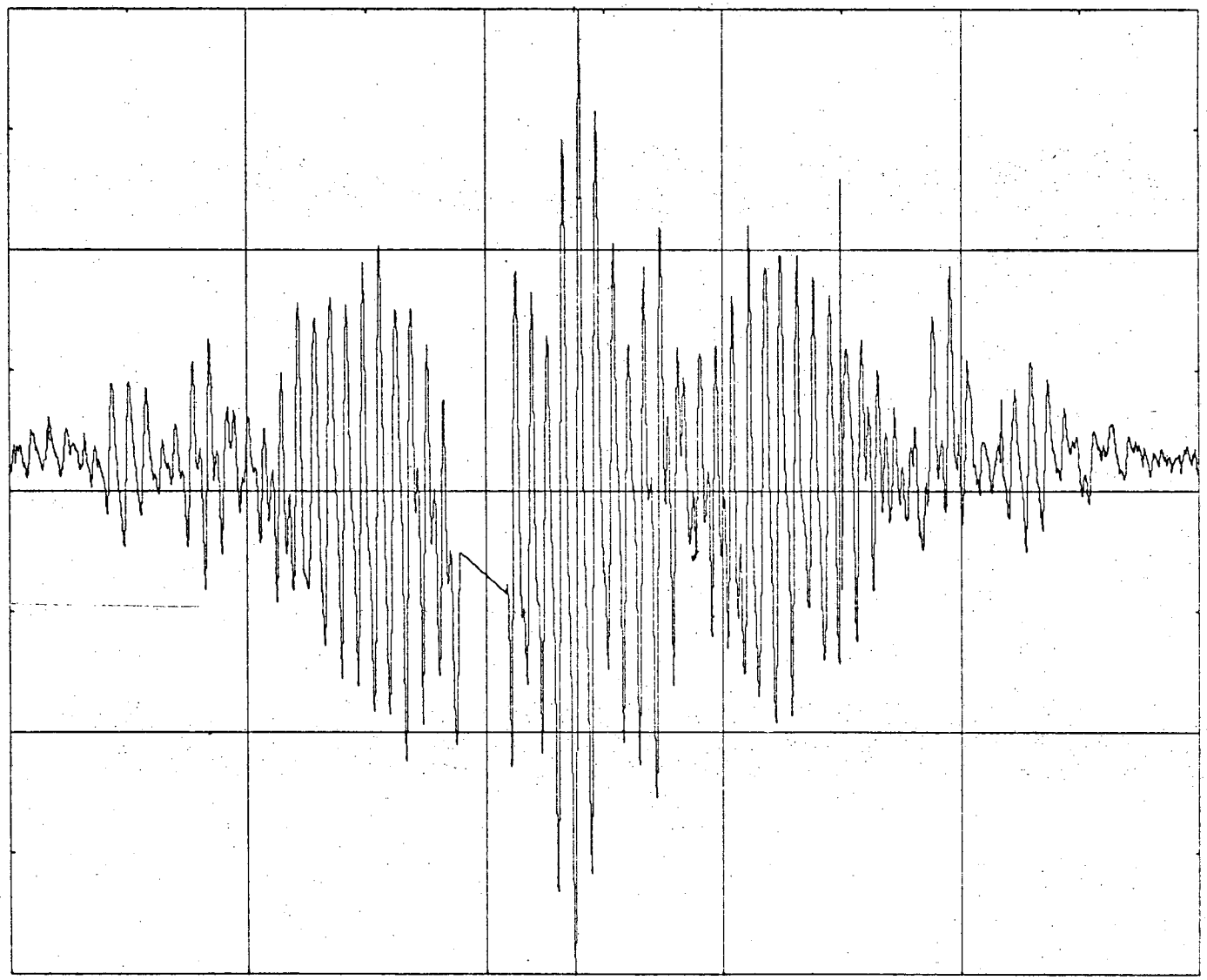

Figure-11 ESR Spectrum of 4,5-methylene phenanthrene Radical Anion XBL 6912-6750

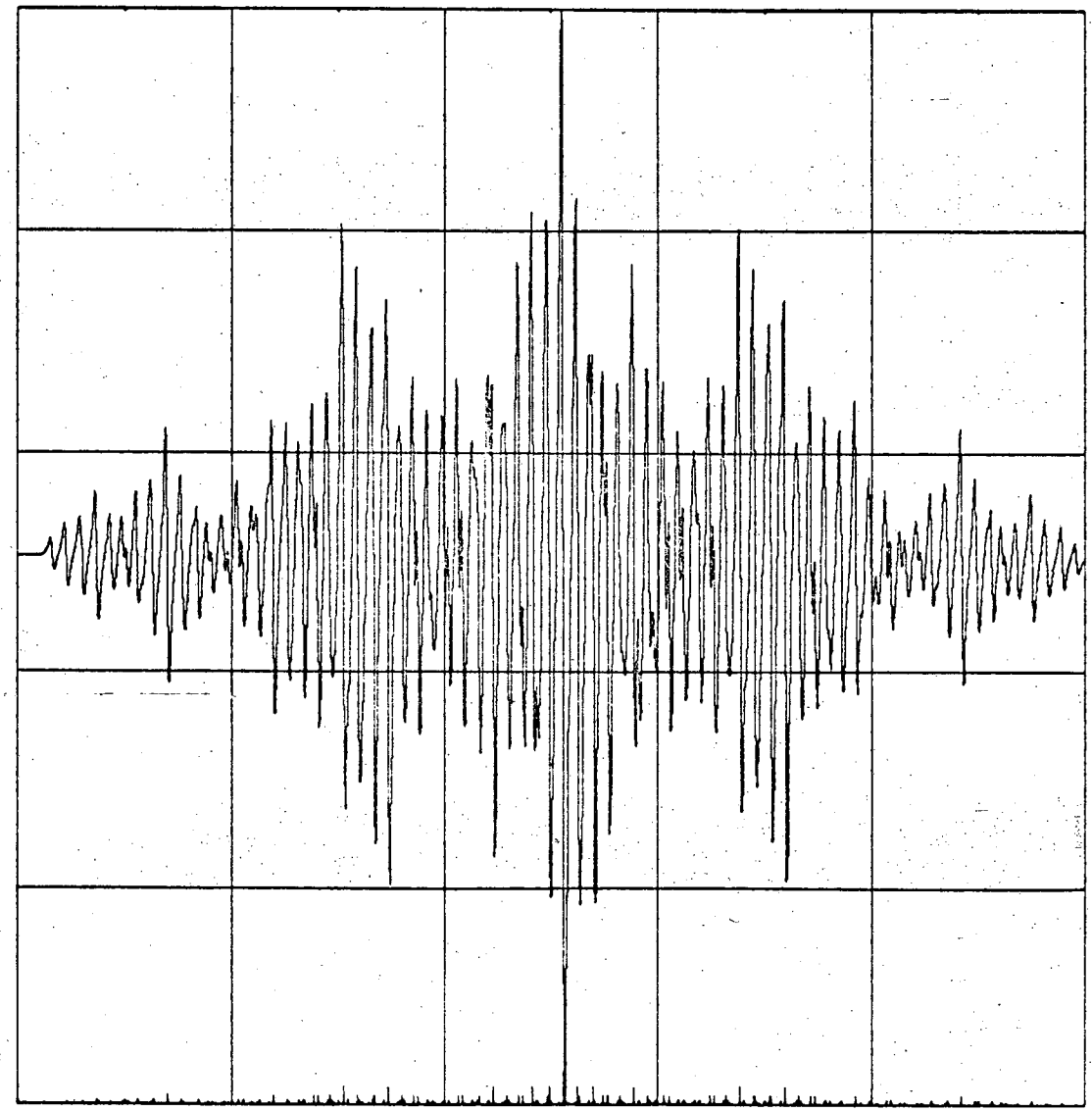

XBL 6912-6752

Figure-12 Simulated Spectrum of 4,5-methylene phenanthrene Radical Anion

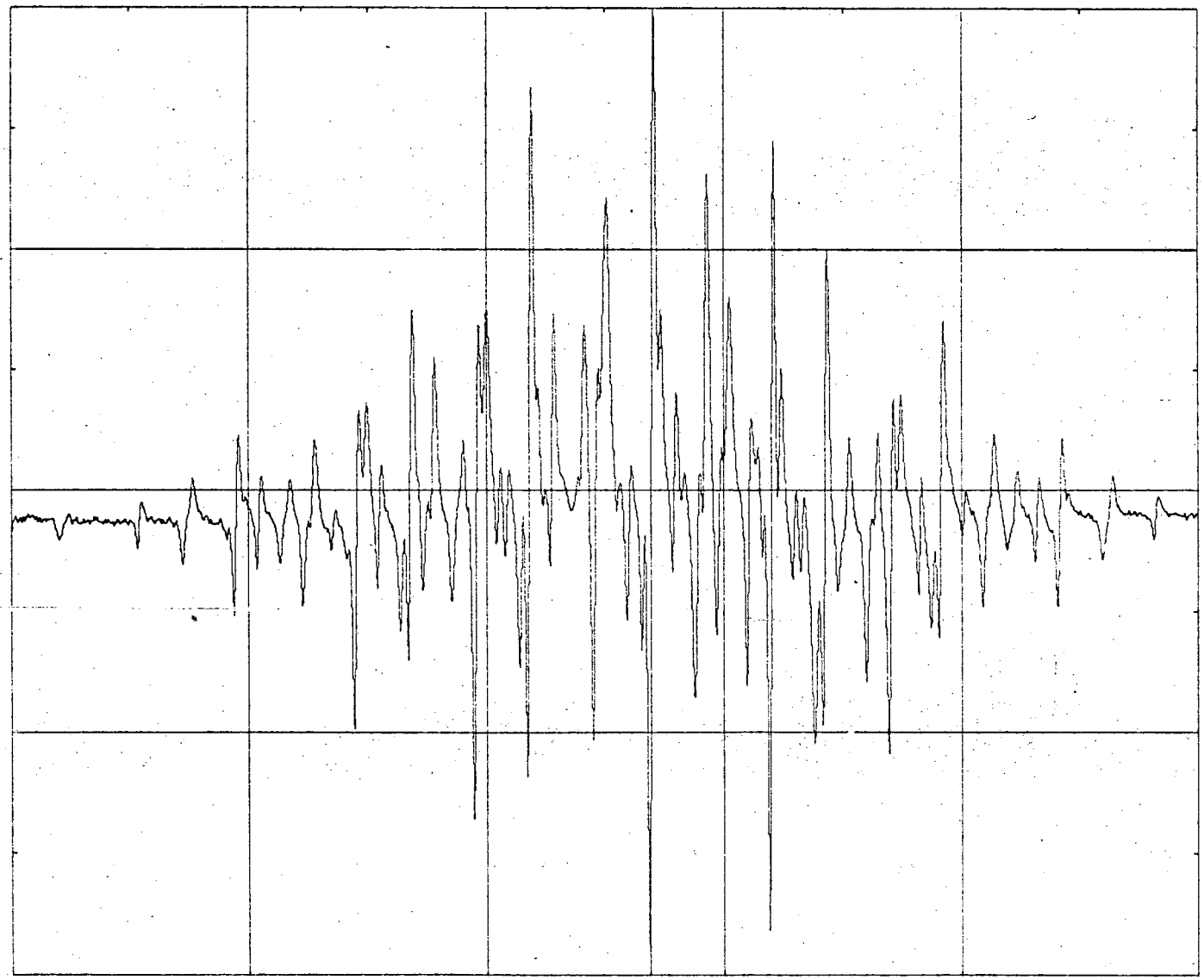

XBL 6912-6751

Figure-13 ESR Spectrum of 1,4-phenylene diamine Radical Anion

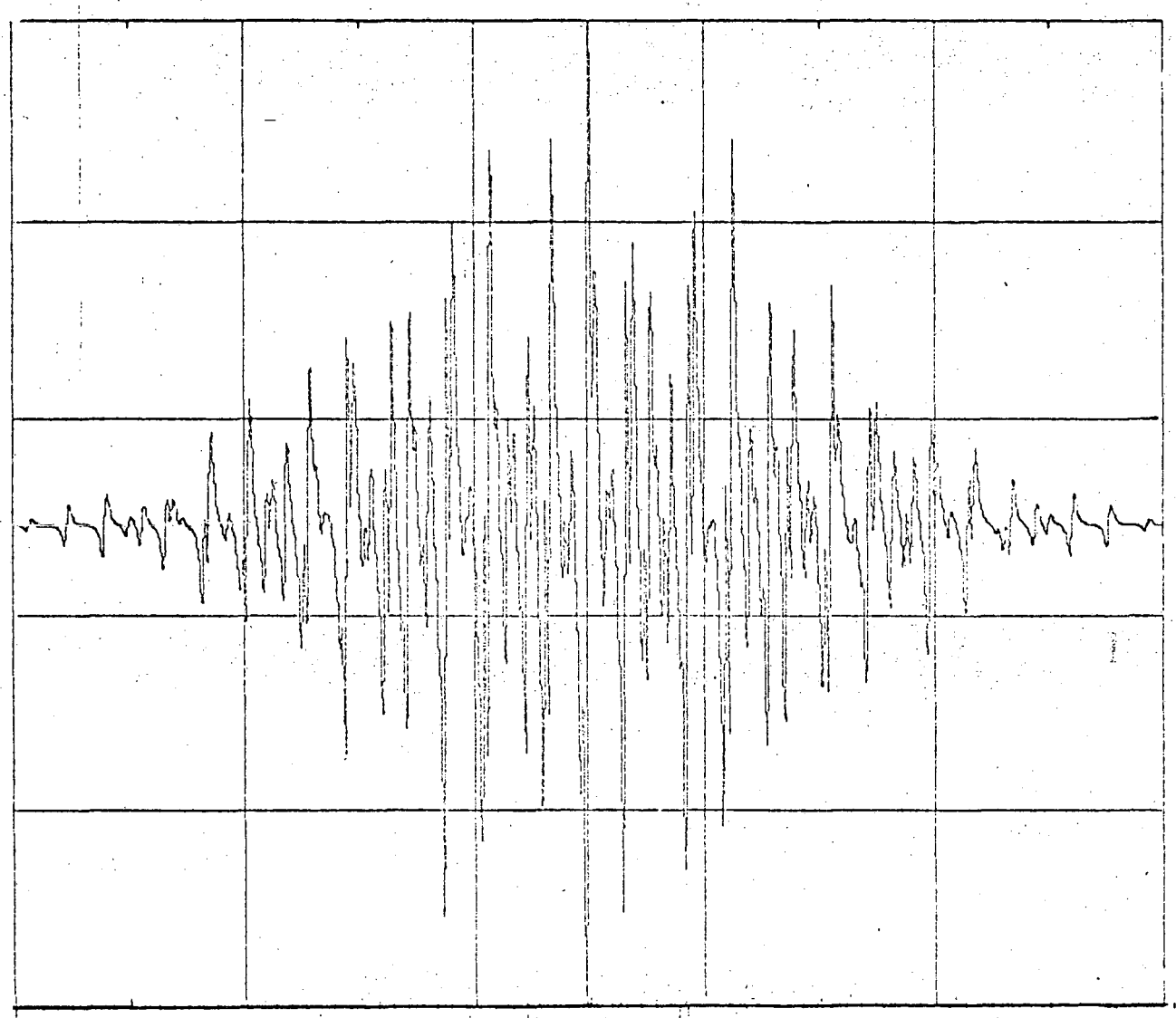

Figure-14 Simulated Spectrum of 1,4-phenylene diamine Radical Anion

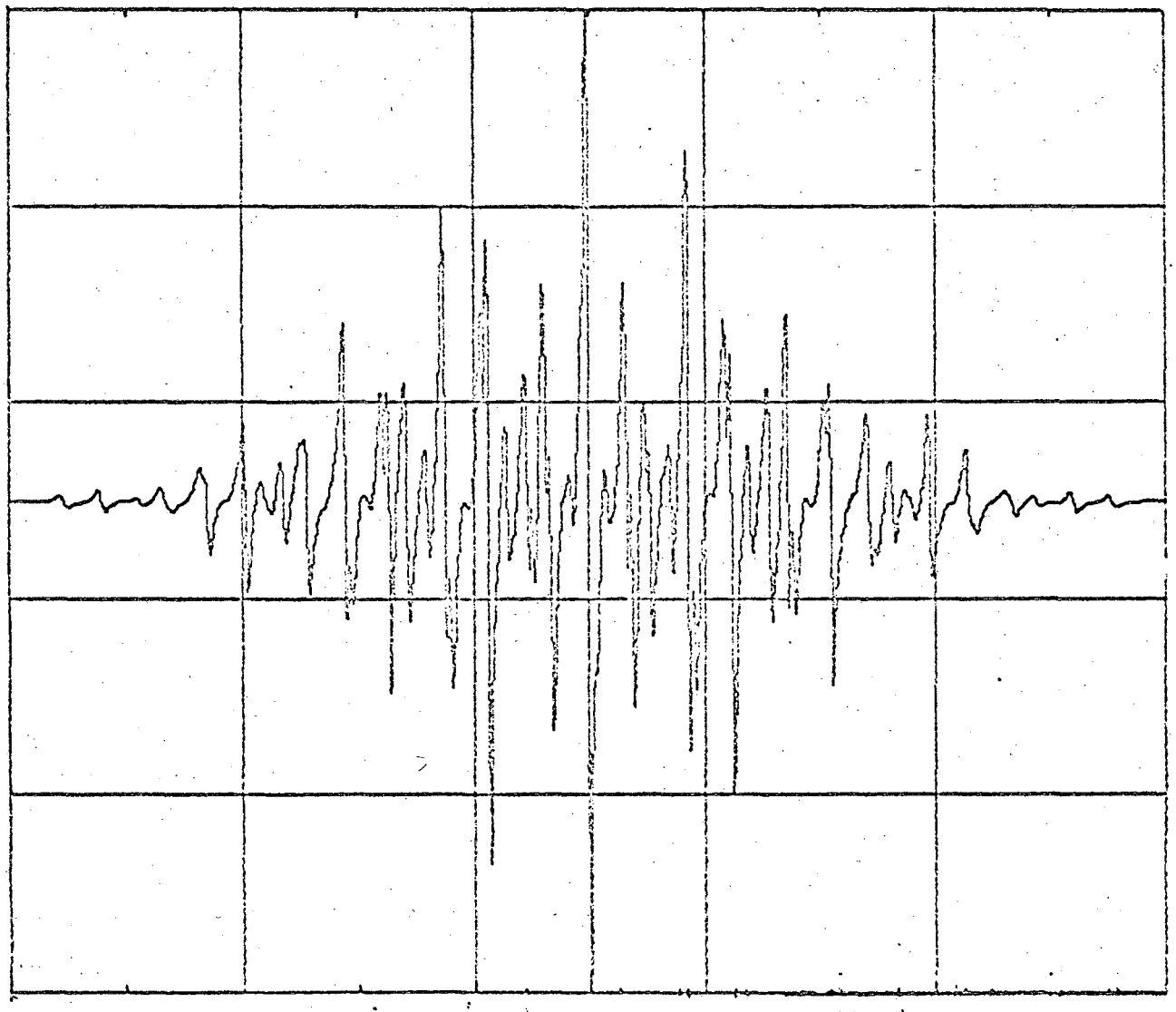

Figure-15 Simulated Spectrum of the Radical Anion of 1,4-phenylene diamine with Variable line widths.

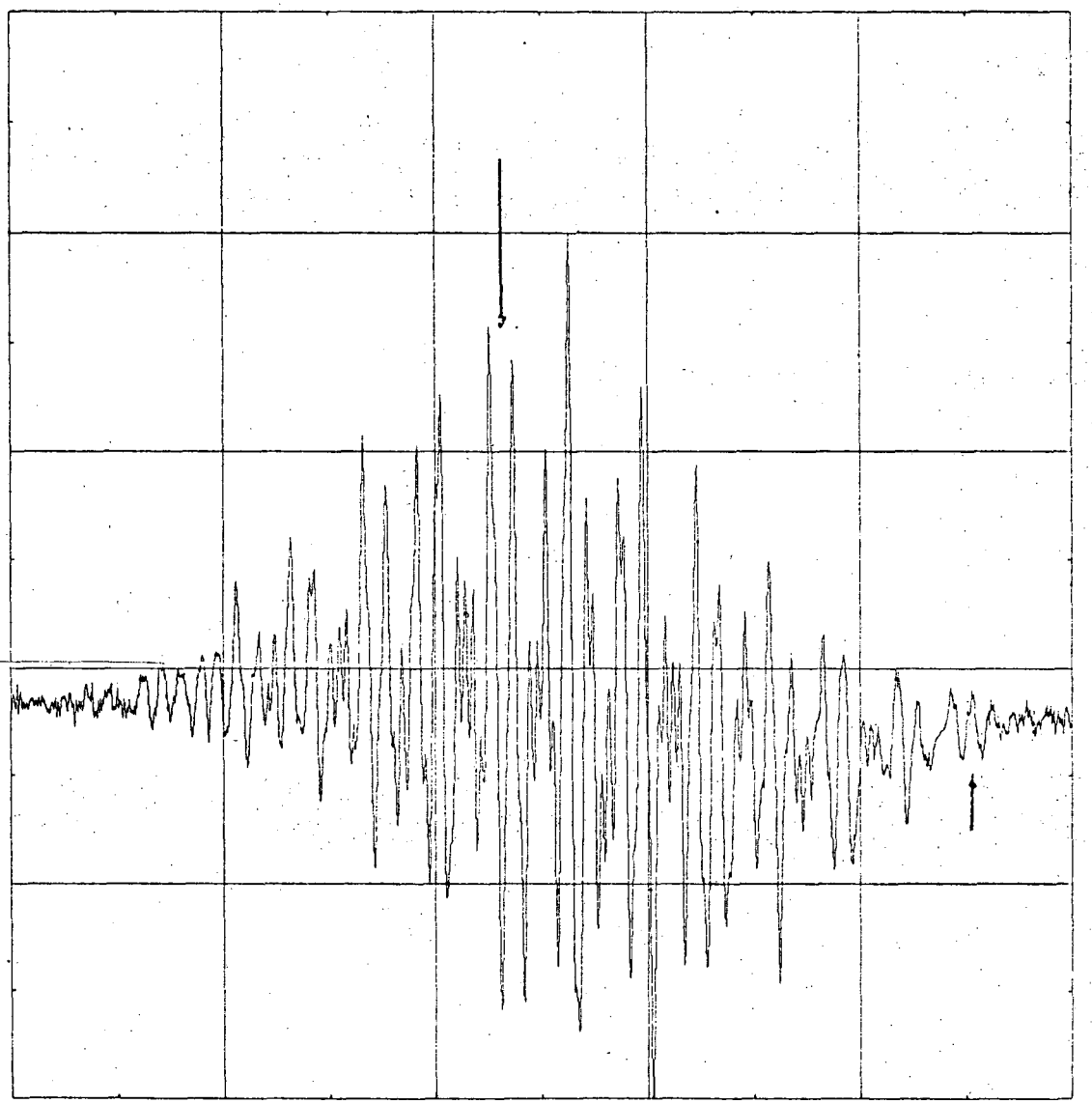

Figure-16 ESR Spectrum of Aniline Radical Anion

XBL 6912-6749

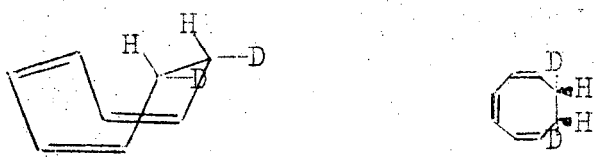

exo-cis form

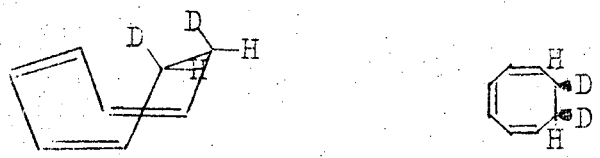

endo-cis form

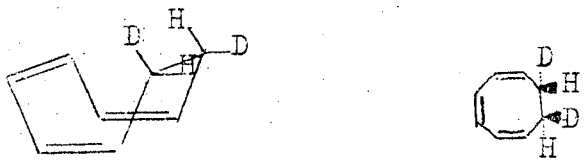

trans form

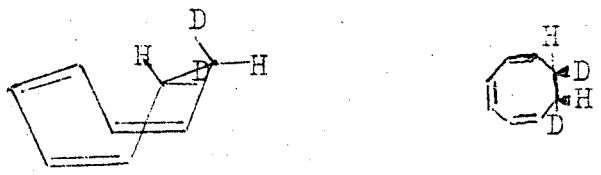

trans form

Fig-17 7,8-dideutero-1,3,5-cyclooctatriene isomers

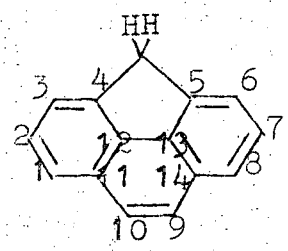

4,5-methylene phenathrane

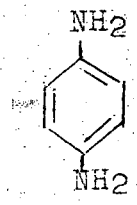

p-phenylene diamine

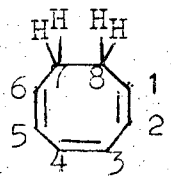

1,3,5-cyclooctatriene

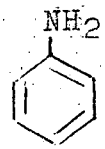

aniline

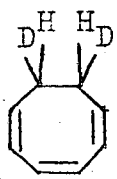

7,8-dideutero-1,3,5-cyclooctatriene

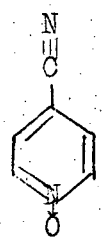

p-cyano-pyridine N-oxide

Figure-18

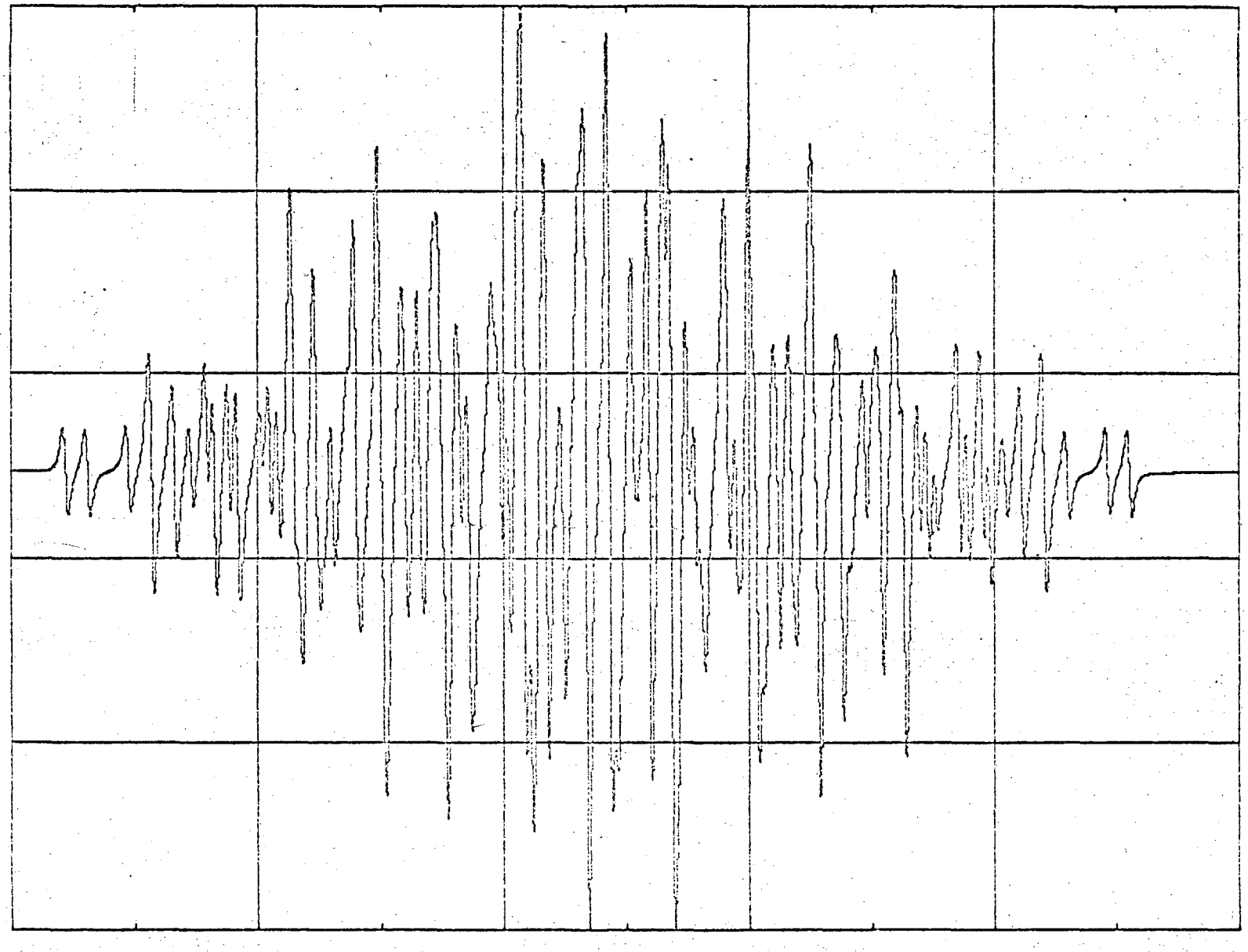

Figure-19 Simulated Spectrum of Aniline Radical Anion

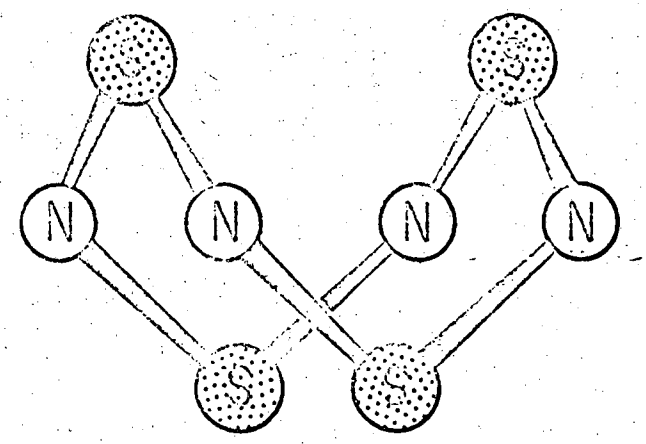

Figure-20 Geometrical Model of S_4N_4

LEGAL NOTICE

This report was prepared as an account of Government sponsored work. Neither the United States, nor the Commission, nor any person acting on behalf of the Commission:

A. Makes any warranty or representation, expressed or implied, with respect to the accuracy, completeness, or usefulness of the information contained in this report, or that the use of any information, apparatus, method, or process disclosed in this report may not infringe privately owned rights; or

B. Assumes any liabilities with respect to the use of, or for damages resulting from the use of any information, apparatus, method, or process disclosed in this report.

As used in the above, "person acting on behalf of the Commission" includes any employee or contractor of the Commission, or employee of such contractor, to the extent that such employee or contractor of the Commission, or employee of such contractor prepares, disseminates, or provides access to, any information pursuant to his employment or contract with the Commission, or his employment with such contractor.

TECHNICAL INFORMATION DIVISION
LAWRENCE RADIATION LABORATORY
UNIVERSITY OF CALIFORNIA
BERKELEY, CALIFORNIA 94720